

NASA CR-157,366

A Reproduced Copy  
OF

NASA CR-157,366

Reproduced for NASA  
*by the*  
**NASA Scientific and Technical Information Facility**

LIBRARY COPY

SEP 26 1966

LANGLEY RESEARCH CENTER  
LIBRARY NASA  
HAMPTON, VIRGINIA

FFNo 672 Aug 65

3 1176 01327 5780

~~Boeing Document~~  
~~DATE 10/22/81~~

*Final Report*

# FLAW GROWTH OF VARIOUS NERVA ENGINE MATERIALS

*By*  
*W. D. Bixler*

*Prepared For*  
**AEROJET NUCLEAR SYSTEMS COMPANY**  
March 1972  
Contract P. O. N-01499

*RECEIVED*

THE **BOEING** COMPANY

DISTRIBUTION OF THIS DOCUMENT UNLIMITED

*N78-79364*

FINAL REPORT

FLAW GROWTH OF VARIOUS  
NERVA ENGINE MATERIALS

By  
W. D. BIXLER

Prepared for  
AEROJET NUCLEAR SYSTEMS COMPANY  
March 1972  
Contract P.O. N-01499

NOTICE

This report was prepared as an account of work sponsored by the United States Government. Neither the United States nor the United States Energy Research and Development Administration, nor any of their employees, nor any of their contractors, subcontractors, or their employees, makes any warranty, express or implied, or assumes any legal liability or responsibility for the accuracy, completeness or usefulness of any information, apparatus, product or process disclosed, or represents that its use would not infringe privately owned rights.

Aerospace Group  
THE BOEING COMPANY  
Seattle, Washington

DISTRIBUTION OF THIS DOCUMENT UNLIMITED

## FLAW GROWTH OF VARIOUS NERVA ENGINE MATERIALS

By

W. D. Bixler

### ABSTRACT

Fracture and fatigue crack growth characteristics were experimentally determined using precracked compact tension specimens for the following materials:

Armco 22-13-5 Steel  
Phosphor Bronze  
A286 Steel  
Hastelloy X  
347 Stainless Steel  
9310 Carburized Steel  
5Al-2.5Sn(ELI) Titanium

The tests were conducted in low and high pressure gaseous helium, low and high pressure/high purity gaseous hydrogen, and liquid hydrogen. Test temperatures were 70° F, -160° F and -423° F. Valid plane strain fracture toughness values per ASTM E399-70T were only obtained at -423° F for the 9310 carburized steel and 5Al-2.5Sn(ELI) titanium. The static fracture test results were unaffected by high pressure gaseous hydrogen at 70° F for all materials tested except the 9310 carburized steel. Significant flaw growth occurred in the 9310 carburized steel while loading to failure. Pancake forgings of 5Al-2.5Sn(ELI) titanium were found to have higher toughness than die forgings when tested at -423° F. The fatigue crack growth rates of Armco 22-13-5, phosphor bronze and A286 steel at 70° F and 5Al-2.5Sn(ELI) titanium at -160° F were found to be insensitive to high pressure gaseous hydrogen, whereas Hastelloy X, 347 stainless steel and 9310 carburized steel were moderately to significantly affected. Low pressure gaseous hydrogen had a questionable effect on the fatigue crack rates of 5Al-2.5Sn(ELI) titanium at 70° F. The cyclic life, as well as static fracture results obtained for the titanium were very consistent between die forgings for a given test temperature. Pancake forgings of titanium were found to have longer cyclic lives than die forgings when tested at -423° F.

### KEY WORDS

Armco 22-13-5 Steel	Static Fracture
Phosphor Bronze	Fatigue Crack Growth Rates
A286 Steel	Compact Tension Specimen
Hastelloy X	Gaseous Helium
347 Stainless Steel	Gaseous Hydrogen
9310 Carburized Steel	Liquid Hydrogen
5Al-2.5Sn(ELI) Titanium	

## FOREWORD

This report describes the work performed by the Aerospace Group of The Boeing Company during the period from August 1971 to March 1972 under Aerojet Nuclear Systems Company Purchase Order N-01499. The objective of this program was to determine the fracture characteristics of various candidate materials being considered in the NERVA nuclear engine.

Boeing personnel who participated in this investigation include J. N. Masters, Program Leader and W. D. Bixler, Technical Leader. Structural test support was provided by A. A. Ottlyk and H. M. Olden.

## SUMMARY

The experimental work described herein was undertaken to investigate the fracture and flaw growth characteristics of various materials being considered for application on the NERVA nuclear engine. The materials involved include Armco 22-13-5 steel, phosphor bronze, A286 steel, Hastelloy X, 347 stainless steel, 9310 carburized steel and 5Al-2.5Sn(ELI) titanium. Static fracture test and cyclic life tests (primarily at 5 cps) were conducted using compact tension specimens. The test environments included 100 psig gaseous helium and hydrogen, 1200 psig gaseous helium and hydrogen, and liquid hydrogen; test temperatures were 70°F, -160°F and -423°F. The gaseous hydrogen used was high purity meeting the purity requirements set forth in MSFC-SPEC-356A, Table Ia. A summary of the results obtained is presented below:

MATERIAL	TEST		SIGNIFICANT OBSERVATIONS
	TEMP.	ENVIRON.	
ARMCO 22-13-5	70°F	1200 PSIG GH <sub>2</sub>	• NO VALID K <sub>IC</sub> TESTS OBTAINED. • NO EFFECT OF GH <sub>2</sub> ON STATIC FRACTURE OR CYCLIC LIFE RESULTS.
		1200 PSIG CH <sub>2</sub>	• NO VALID K <sub>IC</sub> TESTS OBTAINED. • NO EFFECT OF CH <sub>2</sub> ON STATIC FRACTURE OR CYCLIC LIFE RESULTS.
PHOSPHOR BROONZE	70°F	1200 PSIG GH <sub>2</sub>	• NO VALID K <sub>IC</sub> TESTS OBTAINED. • NO EFFECT OF GH <sub>2</sub> ON STATIC FRACTURE OR CYCLIC LIFE RESULTS.
		1200 PSIG GH <sub>2</sub>	• NO VALID K <sub>IC</sub> TESTS OBTAINED. • NO EFFECT OF GH <sub>2</sub> ON STATIC FRACTURE OR CYCLIC LIFE RESULTS.
A286 STEEL	70°F	1200 PSIG GH <sub>2</sub>	• NO VALID K <sub>IC</sub> TESTS OBTAINED. • NO EFFECT OF GH <sub>2</sub> ON STATIC FRACTURE OR CYCLIC LIFE RESULTS (AT 5 CPS)
		1200 PSIG GH <sub>2</sub>	• NO VALID K <sub>IC</sub> TESTS OBTAINED. • NO EFFECT OF GH <sub>2</sub> ON STATIC FRACTURE RESULTS. • MODERATE EFFECT OF GH <sub>2</sub> ON CYCLIC LIFE RESULTS
HASTELLOY X	70°F	1200 PSIG GH <sub>2</sub>	• NO VALID K <sub>IC</sub> TESTS OBTAINED. • NO EFFECT OF GH <sub>2</sub> ON STATIC FRACTURE RESULTS.
		1200 PSIG GH <sub>2</sub>	• NO VALID K <sub>IC</sub> TESTS OBTAINED. • NO EFFECT OF GH <sub>2</sub> ON STATIC FRACTURE RESULTS. • MODERATE EFFECT OF GH <sub>2</sub> ON CYCLIC LIFE RESULTS
347 STAINLESS STEEL	70°F	1200 PSIG GH <sub>2</sub>	• NO VALID K <sub>IC</sub> TESTS OBTAINED. • NO EFFECT OF GH <sub>2</sub> ON STATIC FRACTURE RESULTS.
		1200 PSIG GH <sub>2</sub>	• NO VALID K <sub>IC</sub> TESTS OBTAINED. • MODERATE EFFECT OF GH <sub>2</sub> ON CYCLIC LIFE RESULTS
9310 CARBURIZED STEEL	70°F	1200 PSIG GH <sub>2</sub>	• ESSENTIALLY VALID K <sub>IC</sub> TESTS OBTAINED IN GH <sub>2</sub> .
		1200 PSIG GH <sub>2</sub>	• SIGNIFICANT EFFECT OF GH <sub>2</sub> ON STATIC FRACTURE AND CYCLIC LIFE RESULTS.
5Al-2.5 Sn (ELI) TITANIUM	-423°F	LH <sub>2</sub>	• VALID K <sub>IC</sub> TESTS OBTAINED. • NO VALID K <sub>IC</sub> TESTS OBTAINED.
		100 PSIG GH <sub>2</sub>	• POSSIBLE SLIGHT EFFECT OF GH <sub>2</sub> ON CYCLIC LIFE RESULTS.
	-160°F	100 PSIG GH <sub>2</sub>	• STATIC FRACTURE AND CYCLIC LIFE RESULTS VERY CONSISTENT BETWEEN D.E. FORGINGS
		1200 PSIG GH <sub>2</sub>	• ESSENTIALLY VALID K <sub>IC</sub> TESTS OBTAINED. • NO EFFECT OF GH <sub>2</sub> ON CYCLIC LIFE RESULTS.
	-423°F	1200 PSIG GH <sub>2</sub>	• STATIC FRACTURE AND CYCLIC LIFE RESULTS VERY CONSISTENT BETWEEN D.E. FORGINGS
		LH <sub>2</sub>	• VALID K <sub>IC</sub> TESTS OBTAINED. • PANCAKE FORGINGS EXHIBITED HIGHER TOUGHNESS AND CYCLIC LIFE THAN D.E. FORGINGS TESTED. • STATIC FRACTURE AND CYCLIC LIFE RESULTS VERY CONSISTENT BETWEEN D.E. FORGINGS

## TABLE OF CONTENTS

	<u>Page</u>
SUMMARY	iv
1.0 INTRODUCTION	1
2.0 MATERIALS	3
3.0 PROCEDURES	5
3.1 Specimen Fabrication	5
3.2 Test Setup	5
3.3 Experimental Approach	7
3.4 Data Analysis	7
4.0 TEST RESULTS AND ANALYSIS	9
4.1 Hydrogen Gas Purity	9
4.2 Armco 22-13-5 Steel	9
4.3 Phosphor Bronze	10
4.4 A286 Steel	11
4.5 Hastelloy X	12
4.6 347 Stainless Steel	13
4.7 9310 Carburized Steel	14
4.7.1 RT Tests	14
4.7.2 -423° F Tests	16
4.8 5Al-2.5 Sn (ELI) Titanium	16
4.8.1 RT Tests	16
4.8.2 -160° F Tests	17
4.8.3 -423° F Tests	18
5.0 OBSERVATIONS	21
REFERENCES	25

## LIST OF ILLUSTRATIONS

<u>Figure No.</u>		<u>Page</u>
1	Specimen/Material Flaw Orientations	26
2	Compact Tension Specimen Configuration	27
3	5Al-2.5 Sn (ELI) Titanium Specimen/Forging Location	28
4	Test Setup Schematic	29
5	Test Setup	30
6	Open Test Cavity	31
7	Helium Leak Detector	32
8	Diffusion Pump	33
9	Hydrogen Gas Sample Bottle	34
10	Y Function for Stress Intensity Calculations	35
11	Analysis of Cyclic Flaw Growth Data	36
12	Cyclic Test Results of Armco 22-13-5	37
13	Growth Rate Results of Armco 22-13-5 in 1200 psig Gaseous Helium at Room Temperature	38
14	Growth Rate Results of Armco 22-13-5 in 1200 psig Gaseous Hydrogen at Room Temperature	39
15	Cyclic Test Results of Phosphor Bronze	40
16	Growth Rate Results of Phosphor Bronze in 1200 psig Gaseous Helium at Room Temperature	41
17	Growth Rate Results of Phosphor Bronze in 1200 psig Gaseous Hydrogen at Room Temperature	42
18	Cyclic Test Results of A286 Steel	43
19	Growth Rate Results of A286 Steel in 1200 psig Gaseous Helium at Room Temperature	44
20	Growth Rate Results of A286 Steel in 1200 psig Gaseous Hydrogen at Room Temperature	45
21	Cyclic Test Results of Hastelloy X	46
22	Growth Rate Results of Hastelloy X in 1200 psig Gaseous Helium at Room Temperature	47

LIST OF ILLUSTRATIONS (Cont.)

<u>Figure No.</u>		<u>Page</u>
23	Growth Rate Results of Hastelloy X in 1200 psig Gaseous Hydrogen at Room Temperature	48
24	Cyclic Test Results of 347 Stainless Steel	49
25	Growth Rate Results of 347 Stainless steel in 1200 psig Gaseous Helium at Room Temperature	50
26	Growth Rate Results of 347 Stainless Steel in 1200 psig Gaseous Hydrogen at Room Temperature	51
27	Cyclic Test Results of 9310 Carborized Steel	52
28	Growth Rate of Results of 9310 Carborized Steel in 1200 psig Gaseous Helium at Room Temperature	53
29	Growth Rate Result's of 9310 Carborized Steel in 1200 psig Gaseous Hydrogen at Room Temperature	54
30	Growth Rate Results of 9310 Carborized Steel in Liquid Hydrogen at -423°F	55
31	Cyclic Test Results of 5Al-2.5 Sn (ELI) Titanium at Room Temperature	56
32	Growth Rate Results of 5Al-2.5 Sn (ELI) Titanium in 100 psig Gaseous Helium at Room Temperature	57
33	Growth Rate Results of 5Al-2.5 Sn (ELI) Titanium in 100 psig Gaseous Hydrogen at Room Temperature	58
34	Cyclic Test Results of 5Al-2.5 Sn (ELI) Titanium at -160°F	59
35	Growth Rate Results of 5Al-2.5 Sn (ELI) Titanium in 1200 psig Gaseous Helium at -160°F	60
36	Growth Rate Results of 5Al-2.5 Sn (ELI) Titanium in 1200 psig Gaseous Hydrogen at -160°F	61
37	Cyclic Test Results of 5Al-2.5 Sn (ELI) Titanium in Liquid Hydrogen at -423°F	62
38	Growth Rate Results of 5Al-2.5 Sn (ELI) Titanium in Liquid Hydrogen at -423°F	63

## LIST OF TABLES

<u>Table No.</u>		<u>Page</u>
1	Analysis of High Purity Gaseous Hydrogen	64
2	5Al-2.5 Sn (ELI) Titanium Specimen/Forging Correlation	65
3	Static Fracture Tests of Armco 22-13-5 at Room Temperature	66
4	Cyclic Tests of Armco 22-13-5 at Room Temperature in Gaseous Helium	66
5	Cyclic Tests of Armco 22-13-5 at Room Temperature in Gaseous Hydrogen	67
6	Static Fracture Tests of Phosphor Bronze at Room Temperature	67
7	Cyclic Tests of Phosphor Bronze at Room Temperature in Gaseous Helium	68
8	Cyclic Tests of Phosphor Bronze at Room Temperature in Gaseous Hydrogen	68
9	Static Fracture Tests of A286 Steel at Room Temperature	69
10	Cyclic Tests of A286 Steel at Room Temperature in Gaseous Helium	69
11	Cyclic Tests of A286 Steel at Room Temperature in Gaseous Hydrogen	70
12	Static Fracture Tests of Hastelloy X at Room Temperature	70
13	Cyclic Tests of Hastelloy X at Room Temperature in Gaseous Helium	71
14	Cyclic Tests of Hastelloy X at Room Temperature in Gaseous Hydrogen	71
15	Static Fracture Tests of 347 Stainless Steel at Room Temperature	72
16	Cyclic Tests of 347 Stainless Steel at Room Temperature in Gaseous Helium	72
17	Cyclic Tests of 347 Stainless Steel at Room Temperature in Gaseous Hydrogen	73
18	Static Fracture Tests of 9310 Carburized Steel at Room Temperature and -423°F	73
19	Cyclic Tests of 9310 Carburized Steel at Room Temperature in Gaseous Helium	74

LIST OF TABLES (Cont.)

<u>Table No.</u>		<u>Page</u>
20	Cyclic Tests of 9310 Carburized Steel at Room Temperature in Gaseous Hydrogen	74
21	Cyclic Tests of 9310 Carburized Steel in Liquid Hydrogen	75
22	Static Fracture Tests of 5Al-2.5 Sn (ELI) Titanium at RT, -160°F and -423°F	75
23	Cyclic Tests of 5Al-2.5 Sn (ELI) Titanium at Room Temperature	76
24	Cyclic Tests of 5Al-2.5 Sn (ELI) Titanium at -160°F	77
25	Cyclic Tests of 5Al-2.5 Sn (ELI) Titanium at -423°F	77

## ABBREVIATIONS AND SYMBOLS

$a$	=	crack length
$B$	=	specimen thickness
COD	=	crack opening displacement
CT	=	compact tension
$da/dN$	=	fatigue crack growth rate
GHe	=	gaseous helium
GH <sub>2</sub>	=	gaseous hydrogen
$K_I$	=	plane strain stress intensity
$K_Q$	=	conditional plane strain fracture toughness
$(K_I)_{max}$	=	maximum apparent critical stress intensity $f(a_i, P_{max})$
$K_{Ic}$	=	plane strain fracture toughness
LH <sub>2</sub>	=	liquid hydrogen
N	=	cycles
P	=	load
RT	=	room temperature
S/N	=	serial number
W	=	specimen width
Y	=	correction factor
$\Delta$	=	peak-to-peak COD
$\sigma_{ys}$	=	material yield strength

## SUBSCRIPTS

$i$	=	initial
$f$	=	final
$max$	=	maximum

## 1.0 INTRODUCTION

The objective of this investigation was to determine the static fracture and cyclic flow growth characteristics of a variety of materials to be used on the NERVA nuclear engine. Compact tension specimens were tested in environments of gaseous helium, high purity gaseous hydrogen and liquid hydrogen. The specific materials, test conditions and quantity of specimens tested are indicated below:

MATERIAL	TEST CONDITION	TEST ENVIRONMENT					
		GHe			GH <sub>2</sub>		LH <sub>2</sub>
		RT	-160° F	RT	-160° F	-423° F	
		100 PSIG	1200 PSIG	1200 PSIG	100 PSIG	1200 PSIG	ZERO PSIG
ARMCO 22-13-5 STEEL	STATIC FRACTURE	1			1		
	CYCLIC	4			6		
PHOSPHOR BRONZE	STATIC FRACTURE	1			1		
	CYCLIC	4			6		
A286 STEEL	STATIC FRACTURE	1			1		
	CYCLIC	4			5		
HASTELLOY X	STATIC FRACTURE	1			1		
	CYCLIC	5			5		
347 STAINLESS STEEL	STATIC FRACTURE	1			2		
	CYCLIC	3			6		
9310 CARBURIZED STEEL	STATIC FRACTURE	1			1		1
	CYCLIC	3			5		3
5Al-2,5Sn (ELI) TITANIUM	STATIC FRACTURE			3		2	4
	CYCLIC	1		1	6	3	4

**BLANK PAGE**

10. TESTIMONY

The witness is the same witness as the one who gave evidence at the trial of State v. John G. Coughlin. The witness was the son of Frank Coughlin and his wife, Anna. He was born in 1910 and has three brothers and two sisters. He is a carpenter by trade and has been working at it since he left school at the age of 14.

NAME	AGE	SEX	RELATIONSHIP
John G. Coughlin	35	M	Father
Frank Coughlin	35	M	Son
Anna Coughlin	35	F	Daughter
John Coughlin	15	M	Son
Frank Coughlin	13	M	Son
Anna Coughlin	11	F	Sister
John Coughlin	9	M	Son
Frank Coughlin	7	M	Son
Anna Coughlin	5	F	Sister
John Coughlin	3	M	Son
Frank Coughlin	1	M	Son

11. TESTIMONY

The witness is the same witness as the one who gave evidence at the trial of State v. John G. Coughlin.

The witness gave evidence and the testimony was accepted by State Coughlin - State Coughlin is the son of John G. Coughlin. Party of the defense and he was present at the trial and heard the testimony during the trial of State v. John G. Coughlin. The witness can not be identified with the party which consisted in the State of West Virginia which consisted in John G. Coughlin - State Coughlin. Much of the testimony was contradicted by State Coughlin - State Coughlin.

**BLANK PAGE**

### 3.0 PROCEDURES

#### 3.1 Specimen Fabrication

The SAI-2.5Sn(ELI) titanium specimens fabricated at Boeing were identical in configuration to the specimens supplied by Aerojet. All specimens were fabricated to Aerojet drawing 1138365 and a sketch of the configuration is shown in Figure 2. Drawing 1138365 is in accordance with the requirements of ASTM E399-70T.

As indicated in Figure 1, the flaw propagation direction of the specimens was always maintained parallel to the longitudinal grain or the radial direction in the case of the dia and pancake forgings. The SAI-2.5Sn(ELI) titanium specimens were machined from various forgings as shown in Figure 3. Table 2 correlates the specimen number with the forging number for the titanium alloy. The final machined specimens supplied by Aerojet were received in the precracked condition; i.e., the flaw front had been sharpened by low load/high cycle fatigue per ASTM E399-70T. Precracking during the final stages was accomplished at a load no greater than 2700 lb. for the Aerojet supplied specimens with the exception of the 9310 steel where the load was 5500 lb. Any plastic zone created during precracking of the 9310 steel was eliminated when the specimens were carburized and effectively stress relieved. The titanium specimens fabricated at Boeing were precracked in room temperature (RT) air at a load of 4000 lb. to propagate the flaw front to within 0.05 inches of the final desired flaw length followed by final precracking at 2500 lb. Approximately 70 000 cycles were required during the first stage of precracking with about 45 000 cycles necessary to complete it. These specimens were also precracked per ASTM E399-70T.

#### 3.2 Test Setup

All specimen tests were conducted in a 80 000 lb static/60 000 lb cyclic Research Incorporated test machine located at Boeing's remote Tulalip Test Site. The system utilized for gaseous helium and hydrogen testing is illustrated in Figure 4 and shown

pictorially in Figure 5. The specimens were installed in the pressure load compensating test cavity illustrated in Figure 6 and then the system was purged and pressurized with helium. All fittings and seals that were loosen or broken during removal of the prior test specimens were then checked with a helium mass spectrometer leak detector shown in Figure 7 (CEC Model 120A). The sensitivity of the leak detector was characteristically  $4 \times 10^{-10}$  atm cc/sec of helium. For specimens tested in gaseous hydrogen, the system was purged of all helium after leak checking by alternately evacuating and pressurizing using high purity gaseous hydrogen from a standard K cylinder. The evacuation was done with a diffusion pump (Figure 8) to approximately  $3 \times 10^{-6}$  Torr, measured at the pump while pressurization was to about 200 psig. This procedure was repeated about 3 times prior to pressurizing to the required test pressure. To prevent the possibility of contamination by the diffusion pump, a liquid nitrogen cold trap was used as depicted in Figure 4. The hydrogen supply was also run through a liquid nitrogen cold trap to further ensure the removal of oxygen, water, etc., prior to the gas entering the test cavity. During the entire testing period the liquid nitrogen cold traps were maintained submerged. Periodically, hydrogen gas samples were removed from the system for analysis which required the gas to pass through the test cavity before entering the sample bottle. A typical sample bottle is shown in Figure 9.

The cryogenic temperature conditioning system used to maintain  $-160^{\circ}\text{F}$  is shown schematically in Figure 4. Gaseous nitrogen at RT and liquid nitrogen at  $-320^{\circ}\text{F}$  were mixed at a three way valve and regulated to maintain  $-160^{\circ}\text{F}$  in the test cavity. For tests conducted at RT, thermocouple controlled heating coils and fan were employed. The test cavity temperature for all tests was maintained at  $\pm 10^{\circ}\text{F}$  of the test temperature and the test cavity pressure was maintained within  $\pm 20$  psi.

For liquid hydrogen testing (which was at zero pressure), the test specimen was surrounded by a cryostat and then submerged in liquid hydrogen.

### 3.3 Experimental Approach

Static fracture tests were conducted for each material investigated per Section 1.0 using the CT specimen illustrated in Figure 2. These specimens were loaded to failure at a load rate of 8500 lb/minute. During the test, the crack opening displacement (COD) was recorded as a function of load.

Cyclic tests were conducted for each material investigated per Section 1.0 using the CT specimen. These cyclic tests were run at a sinusoidal frequency of 5 cps primarily, with a few tests conducted at a slower frequency of 1 cps. The slower frequency tests were conducted to further demonstrate the susceptibility of a given material to gaseous hydrogen. It was the objective of these tests (with the exception of the 5Al-2.5Sn(ELI) titanium) to obtain cyclic life data to a minimum of 10 000 cycles. The titanium testing objective was to obtain life data to a minimum of 1000 cycles. As with the static fracture specimens, the cyclic specimens were instrumented to determine the COD during testing. In general, the cyclic tests were terminated just prior to specimen failure (within a few cycles as indicated by the COD). After the test was terminated, the system pressure was vented and the flaw front was "marked" by low load cyclic fatigue at 5 cps for about 100 cycles. The load for the "marking" procedure was about 60% of the test load. The records of COD versus cycles for each specimen were analyzed to determine the fatigue crack growth rates ( $da/dN$ ).

### 3.4 Data Analysis

The stress intensity values for all CT specimens tested were calculated using the expression:

$$K_I = Y \frac{P a^{1/2}}{BW}$$

where  $K_I$  = plane strain stress intensity  
 $Y$  = correction factor,  $f(a/W)$   
 $P$  = load  
 $a$  = crack length measured from the point of load application to the flaw front  
 $b$  = specimen thickness  
 $W$  = specimen width

Values of  $\gamma$  are presented in Figure 10 for the specimen configuration presented in Figure 2. Background in use of the above stress intensity solution is presented in ASTM STP 410.

The analysis of the static fracture data was done in accordance with ASTM E399-70T. The cyclic data obtained was used to generate fatigue crack growth rates as described in the following paragraph.

A COD versus cycles plot was obtained for each cyclic specimen tested as schematically illustrated in Figure 11a. The flaw length at initiation and termination of the test was known from the fracture face along with the corresponding peak-to-peak COD. From this data, a compliance curve relating peak-to-peak COD versus flaw length was plotted as shown in Figure 11b. The instantaneous flaw length as a function of the number of cycles was then known and the  $da/dN$  could be determined as a function of stress intensity (see Figures 11c and 11d).

## 4.0 TEST RESULTS AND ANALYSIS

### 4.1 Hydrogen Gas Purity

A total of five hydrogen gas samples were extracted from the test system during the course of the program and analyzed using a gas chromatograph. The gas analysis was done by Union Carbide - Linde Division. The results of these analyses are tabulated in Table 1 along with the required purity levels established in MSFC SPEC 356A. As indicated by the analyses results, the hydrogen gas purity during testing was well within the requirements. The maximum oxygen content was 0.8 ppm while the total purity was consistently above 99.998 percent. As noted in paragraph 3.2, a helium leak detector was employed to leak check mechanical joints supplying hydrogen gas to the specimen prior to testing each specimen. In addition, the system was purged by evacuating the system and backfilling with hydrogen gas a minimum of three times. These procedures, along with the liquid nitrogen cold traps, resulted in a high purity system as the gas analyses indicated.

### 4.2 Armco 22-13-5 Steel

Two static fracture tests were conducted at room temperature (RT); one in 1200 psig gaseous helium and one in 1200 psig gaseous hydrogen. Conditional plane strain fracture toughness values ( $K_Q$ ) for the 2 specimens were determined to be 62.9 and 59.1 ksi  $\sqrt{\text{in}}$ , respectively. The tests did not meet the ASTM-E399-70T requirements because of limited specimen thickness. Based on the specimen thickness of 1.0 inch and material yield strength of 50 ksi,  $K_Q$  would have to have been  $\leq 31.6 \sqrt{\text{in}}$  to represent a valid plane strain fracture toughness value ( $K_{Ic}$ ). The maximum apparent critical stress intensity,  $(K_I)_{\max}$ , obtained during the test was also determined using the maximum attained load ( $P_{\max}$ ) and the initial crack length ( $a_i$ ) and found to be 124.3 and 117.8 ksi  $\sqrt{\text{in}}$  for the gaseous helium and

$$\boxed{K_Q \leq \sigma_{ys} \left( \frac{B}{2.5} \right)^{1/2}} \text{ per ASTM-E399-70T}$$

hydrogen tests, respectively. All of the detailed static fracture results are presented in Table 3. Although no valid plane strain fracture toughness values were determined for the Armco 22-13-5, the results obtained do not show any effect of high pressure gaseous hydrogen.

A total of 10 specimens were cyclic tested at RT to essentially failure; 4 in 1200 psig gaseous helium and 6 in 1200 psig gaseous hydrogen. The tests were conducted at 5 cps with the exception of one specimen tested in hydrogen at 1 cps. The results of these tests are presented in Figure 12 and Tables 4 and 5. Figure 12 indicates that a single curve adequately represents the variation of initial stress intensity ( $K_{II}$ ) with cycles to failure,  $N$ , in either environment. Instantaneous fatigue crack growth rates ( $da/dN$ ) were determined for each specimen tested and the results are presented in Figures 13 and 14 for the gaseous helium and hydrogen tests, respectively. The  $da/dN$  values were obtained from the crack opening displacement (COD) data and analyzed per paragraph 3.4. The scatter band on the  $da/dN$  data obtained for the gaseous helium encompasses the  $da/dN$  results for hydrogen tests. From these results, it appears that the cyclic life and flaw growth rates are unaffected by high pressure hydrogen compared to high pressure helium at RT for Armco 22-13-5 material.

#### 4.3 Phosphor Bronze

Two static fracture tests were conducted at RT; one in 1200 psig gaseous helium and one in 1200 psig gaseous hydrogen.  $K_Q$  values of 57.9 and 64.4  $\text{ksi}\sqrt{\text{in}}$  were obtained, respectively. The tests did not meet the ASTM-E399-70T requirements for thickness. Based on a material yield strength of 67 ksi,  $K_Q$  would have to have been  $\leq 42.4 \text{ ksi}\sqrt{\text{in}}$  to be considered a valid  $K_{Ic}$  test.  $(K_I)_{\max}$  values of 89.0 and 88.6  $\text{ksi}\sqrt{\text{in}}$  were obtained for the tests run in gaseous helium and hydrogen, respectively. All of the detailed static fracture results are presented in Table 6. Although no valid plane strain fracture toughness values were determined for the phosphor bronze, the results obtained do not show any effect of high pressure gaseous hydrogen.

A total of 10 specimens were cyclic tested at RT to failure; 4 in 1200 psig gaseous helium and 6 in 1200 psig gaseous hydrogen. The tests were conducted at 5 cps with the exception of one specimen tested in hydrogen at 1 cps. The results of these tests are presented in Figure 15 and Tables 7 and 8. Figure 15 indicates that a single curve adequately represents the variation of  $K_{Ii}$  with  $N$  in either environment. The results of the instantaneous  $da/dN$  for the specimens tested in helium and hydrogen are presented in Figure 16 and 17, respectively. The scatter band on the helium  $da/dN$  data encompasses the hydrogen  $da/dN$  results. From these results, it appears that the cyclic life and flaw growth rates are unaffected by high pressure hydrogen compared to high pressure helium at RT for phosphor bronze material.

#### 4.4 A286 Steel

Two static fracture tests were conducted at RT; one in 1200 psig gaseous helium and one in 1200 psig gaseous hydrogen. The detailed results are presented in Table 9.  $K_Q$  values of 40.5 and  $40.7 \text{ ksi} \sqrt{\text{in}}$  were obtained, respectively. The tests did meet the ASTM-E399-70T requirements for valid  $K_{Ic}$  determination. Based on a material yield strength of 123 ksi,  $K_Q$  must be  $\leq 77.9 \text{ ksi} \sqrt{\text{in}}$  for a valid test, which was the case. Deviation from linearity of the load/displacement record also met the ASTM requirement. Although the ASTM requirements were met, the investigator believes that valid  $K_{Ic}$  values were not obtained from these tests.  $(K_I)_{\max}$  values of 95.1 and  $95.9 \text{ ksi} \sqrt{\text{in}}$  for the specimens tested in helium and hydrogen, respectively, were obtained which were greater than 135% of  $K_Q$ . The load/displacement records did not indicate any pop-in behavior and if the material did have such a low  $K_{Ic}$  ( $40 \text{ ksi} \sqrt{\text{in}}$ ) the fracture face would have been extremely flat and not excessively deformed plastically as observed. All of these facts leads one to believe that the  $K_Q$  values determined were meaningless quantities. For valid  $K_{Ic}$  tests, a much greater thickness would probably be required. Although it is believed that no valid plane strain fracture toughness values were determined for the A286 steel, the results obtained do not show any effect of high pressure gaseous hydrogen.

A total of 9 specimens were cyclic tested at RT to essentially failure; 4 in 1200 psig gaseous helium and 5 in 1200 psig gaseous hydrogen. The tests were conducted at 5 cps with the exception of one specimen tested in hydrogen at 1 cps. The results of these tests are presented in Figure 18 and Tables 10 and 11.

Figure 18 indicates that a single curve adequately represents the variation of  $K_I$  with  $N$  in either environment when tested at 5 cps. The results of the instantaneous  $da/dN$  for the specimens tested in helium and hydrogen are presented in Figures 19 and 20, respectively. The scatter band on the 5 cps helium  $da/dN$  data encompasses the 5 cps hydrogen  $da/dN$  results. The one specimen tested at 1 cps in gaseous hydrogen did indicate a shorter life (Figure 18) and higher fatigue crack growth rates (Figure 20) than those tested at 5 cps. The A286 steel material might be strain rate sensitive or slightly affected by high pressure hydrogen, but additional specimens would have to be tested to verify this point. From the 5 cps cyclic results, it appears that the cyclic life and flaw growth rates are apparently unaffected by high pressure hydrogen compared to high pressure helium at RT for A286 steel material.

#### 4.5 Hastelloy X

Two static fracture tests were conducted at RT; one in 1200 psig gaseous helium and one in 1200 psig gaseous hydrogen.  $K_Q$  values of 46.4 and 44.9 ksi  $\sqrt{\text{in}}$  were obtained, respectively. The tests did not meet the ASTM-E399-70T requirements for thickness. Based on a material yield strength of 45–50 ksi,  $K_Q$  would have to have been  $\leq 30 \text{ ksi} \sqrt{\text{in}}$  to be considered a valid  $K_{Ic}$  test.  $(K_I)_{\max}$  values of 98.6 and 95.5 ksi  $\sqrt{\text{in}}$  were obtained for the tests run in gaseous helium and hydrogen, respectively. All of the detailed static fracture results are presented in Table 12. Although no valid plane strain fracture toughness values were determined for the Hastelloy X, the results obtained do not show any effect of high pressure gaseous hydrogen.

A total of 10 specimens were cyclic tested at RT to essentially failure; 5 in 1200 psig gaseous helium and 5 in 1200 psig gaseous hydrogen. The tests were conducted at 5 cps with the exception of one specimen tested in hydrogen at 1 cps. The

results of these tests are presented in Figure 21 and Tables 13 and 14. Figure 21 illustrates that the cyclic life of Hastelloy X specimens is moderately affected by high pressure hydrogen compared to high pressure helium. Further evidence of the susceptibility of Hastelloy X to hydrogen is presented with the single specimen tested at 1 cps in hydrogen. This specimen exhibited reduced cyclic life as shown in Figure 21. Based on this data, it appears that flaw growth of Hastelloy X would occur when sustained loaded in a high pressure gaseous hydrogen environment; depending upon the applied stress intensity. The lower frequency cyclic test run essentially increased the time at stress intensity levels above the sustained load threshold. The results of the instantaneous  $da/dN$  for the specimens tested in helium and hydrogen are presented in Figures 22 and 23, respectively. Figure 23 shows that the fatigue crack growth rates in hydrogen are moderately faster than those obtained in helium when the tests are conducted at 5 cps and the rates are further increased when the test frequency is reduced. From these results, it appears that the cyclic life and flaw growth rates are moderately affected by high pressure hydrogen compared to high pressure helium at RT for Hastelloy X material.

#### 4.6 347 Stainless Steel

Four static fracture tests were conducted at RT; one in 1200 psig gaseous helium and 3 in 1200 psig gaseous hydrogen. Two of the specimens tested in hydrogen had prior loading histories. The detailed results of all the tests are presented in Table 15.  $K_Q$  values of 28.7 and 33.5 ksi $\sqrt{in}$  were obtained in the helium and hydrogen environments, respectively, for the specimens not exposed to a prior load history. The tests did not meet the ASTM-E399-70T requirements for thickness. Based on a material yield strength of 40 ksi,  $K_Q$  would have to have been 25.3 ksi $\sqrt{in}$  to be considered a valid  $K_{Ic}$  test. Even though it appears on the surface that these tests were almost valid tests, the investigator believes that the same arguments presented in paragraph 4.5 for the A286 steel specimen test apply here also.  $(K_I)_{max}$  values of 79.1 and 63.3 ksi $\sqrt{in}$  were obtained for the static fracture tests run in gaseous helium and hydrogen, respectively, for specimens which did not have a prior loading history. These 2 tests indicated that a possible hydrogen effect on the  $(K_I)_{max}$  exists, so 2 other specimens were static fractured after being

exposed to a prior loading history. These 2 specimens had  $(K_I)_{max}$  values of 79.9 and 78.7 ksi  $\sqrt{\text{in}}$  when tested in hydrogen which tended to discredit the idea that high pressure hydrogen had an effect on the  $(K_I)_{max}$  value obtained. It appears that the single low  $(K_I)_{max}$  value obtained was probably due to material variability. Therefore, it appears that high pressure hydrogen does not have any effect on the static fracture tests.

A total of 9 specimens were cyclic tested at RT to failure; 3 in 1200 psig gaseous helium and 6 in 1200 psig gaseous hydrogen. The tests were conducted at 5 cps with the exception of 2 specimens tested in hydrogen at 1 cps. The results of these tests are presented in Figure 24 and Tables 16 and 17. Figure 24 illustrates that the cyclic life of 347 stainless steel specimens is moderately affected by high pressure hydrogen compared to high pressure helium when tested at 5 cps. Contrary to the cyclic results for Hastelloy X which showed a hydrogen effect at 5 cps and further substantiating evidence at 1 cps, the 347 stainless steel showed the same cyclic life at 5 cps and 1 cps when tested in hydrogen. The results of this instantaneous  $da/dN$  for the specimens tested in helium and hydrogen are presented in Figures 25 and 26, respectively. Figure 26 shows that the fatigue crack growth rates in hydrogen are moderately faster than those obtained in helium at test frequencies of 5 or 1 cps. From these results, it appears that the cyclic life and flaw growth rates are moderately affected by high pressure hydrogen compared to high pressure helium at RT for 347 stainless steel material.

#### 4.7 9310 Carburized Steel

##### 4.7.1 RT Tests

Seven static fracture tests were conducted at RT; 2 in 1200 psig gaseous helium, one in 1200 psig gaseous hydrogen and 4 in zero psig gaseous hydrogen. One of the helium and all 4 of the zero psig hydrogen test specimens had been exposed to a prior loading history. The detailed results of all the tests are presented in Table 18.  $K_Q$  values of 107.7 and 45.0 ksi  $\sqrt{\text{in}}$  were obtained in the helium and hydrogen environments, respectively, for the specimens not exposed to a prior loading history. It was apparent from the appearance of the specimen fracture face

and the load/displacement record that significant flaw growth had taken place during loading to failure of the hydrogen specimen. The crack length at unstable crack propagation was measured from the hydrogen specimen fracture face and was found to agree with that predicted using the load/displacement record. A critical stress intensity value for this specimen was calculated using the critical crack length and maximum load and found to equal  $120.4 \text{ ksi} \sqrt{\text{in}}$ . The companion specimen tested in helium indicated a pop-in at a stress intensity value of  $118.5 \text{ ksi} \sqrt{\text{in}}$  and a  $(K_I)_{\max}$  value of  $122.4 \text{ ksi} \sqrt{\text{in}}$ . The static fracture specimens which had prior loading histories exhibited  $K_Q$  values ranging from 100.0 to  $122.7 \text{ ksi} \sqrt{\text{in}}$ . The tests did not meet the ASTM-E399-70T requirements for thickness. Based on a material yield strength of 130 ksi,  $K_Q$  would have to have been  $\leq 82.3 \text{ ksi} \sqrt{\text{in}}$  to be considered a valid  $K_{Ic}$  test. Although the tests did not meet ASTM requirements, the investigator believes that a stress intensity value of about  $120 \text{ ksi} \sqrt{\text{in}}$  is close to  $K_{Ic}$  because of the pop-in behavior observed in some specimens and the extreme flatness of the fracture faces. From these static fracture results presented, it appears that the 9310 carburized steel is sensitive to high pressure hydrogen with significant flaw growth occurring during the loading to failure of the specimen. Zero pressure gaseous hydrogen does not affect the static fracture test results when compared to high pressure gaseous helium.

A total of 8 specimens were cyclic tested at RT to essentially failure; 3 in 1200 psig gaseous helium and 5 in 1200 psig gaseous hydrogen. The tests were conducted at 5 cps with the exception of one specimen tested in hydrogen at 1 cps. The results of these tests are presented in Figure 27 and Tables 19 and 20. Figure 27 illustrates that the cyclic life of 9310 carburized steel specimens is significantly affected by high pressure hydrogen. Further evidence of the susceptibility of 9310 steel to hydrogen is presented with the single specimen tested at 1 cps in hydrogen. This specimen exhibited reduced cyclic life compared to the 5 cps hydrogen data. Based on this data it appears that the 9310 steel would have a low sustained load stress intensity threshold. The results of the instantaneous  $da/dN$  for the specimens tested in helium and hydrogen are presented in Figures 28 and 29, respectively. Figure 29 shows that the fatigue crack growth rates in hydrogen are significantly faster than

those obtained in helium when the tests are conducted at 5 cps and the rates are further increased when the test frequency is reduced. It is significant to note in Figure 29 that a hydrogen effect was observed even at a stress intensity level as low as 11 ksi $\sqrt{\text{in}}$ . From these results, it appears that the cyclic life and flaw growth rates are significantly affected by high pressure hydrogen compared to high pressure helium at RT for 9310 carburized steel material.

#### 4.7.2 -423°F Tests

One static fracture test was conducted in zero psig liquid hydrogen at -423°F. The detailed results of this test is also presented in Table 18 along with the RT results. A  $K_Q$  value of 32.2 ksi $\sqrt{\text{in}}$  and a  $(K_I)_{\max}$  value of 34.1 ksi $\sqrt{\text{in}}$  was obtained. The test did meet all of the ASTM requirements. Based on an assumed material yield strength of 210 ksi at -423°F, a  $K_Q$  value of  $\leq 133.0$  ksi $\sqrt{\text{in}}$  would be necessary to be considered a valid  $K_{Ic}$  test. The load/displacement record indicated a very abrupt fracture and the specimen fracture face was very flat.

Three specimens were cyclic tested to failure in liquid hydrogen at 5 cps. The results of these tests are presented in Figure 27 and Table 21. Instantaneous da/dN results are presented in Figure 30.

### 4.8 5Al-2.5 Sn (ELI) Titanium

#### 4.8.1 RT Tests

Three static fracture tests were conducted at RT in 100 psig gaseous hydrogen; one from one die forging and two from another die forging. The detailed results of these tests are presented in Table 22.  $K_Q$  values ranged from 97.4 to 108.4 ksi $\sqrt{\text{in}}$  and  $(K_I)_{\max}$  values ranged from 116.8 to 126.8 ksi $\sqrt{\text{in}}$ . The tests did not meet the ASTM-E399-70T requirements for thickness. Based on an assumed RT yield strength of 94 ksi,  $K_Q$  would have to have been  $\leq 59.5$  ksi $\sqrt{\text{in}}$  to be considered a valid  $K_{Ic}$  test. Although no valid plane strain fracture toughness values were determined for the 5Al-2.5Sn (ELI) titanium at RT, the results obtained do show little variability of static fracture properties of the die forgings tested. The effect of 100 psig hydrogen on the static fracture properties of the titanium was not assessed since tests in helium were not conducted.

A total of 7 specimens were cyclic tested at RT to essentially failure; one in 100 psig gaseous helium and 6 in 100 psig gaseous hydrogen (one from one die forging, 2 from another die forging and 4 from yet another die forging). All of the tests were conducted at 5 cps and the results are presented in Figure 31 and Table 23. Figure 31 indicates that a single curve adequately represents the variation of  $K_{Ii}$  with  $N$  in the hydrogen environment. The single specimen tested in gaseous helium demonstrated a very slightly longer life. The results of the instantaneous da/dN for the specimens tested in helium and hydrogen are presented in Figures 32 and 33, respectively. The scatter band on the helium da/dN data lies within the scatter band of the hydrogen da/dN data but tends to the slow side. Although it appears that 100 psig hydrogen might have a very slight effect on the cyclic life and crack growth rates at 5 cps, additional tests would have to be conducted to verify this point since this observation is based on only one test specimen. Variability of material properties from die forging to die forging might account for the slight differences observed. It is a known fact that 5Al-2.5Sn (ELI) titanium forging material is susceptible to high pressure (1400 psig) gaseous hydrogen at RT as observed in Reference 1. The Reference 1 work indicated sustained load thresholds as low as 20 ksi  $\sqrt{\text{in}}$  for the high pressure hydrogen, but it is not known how the susceptibility varies with pressure for this material. In conclusion, it appears that the cyclic life and flaw growth rates at RT are only very slightly affected, if at all, by 100 psig gaseous hydrogen compared to helium for the titanium material when tested at 5 cps.

#### 4.8.2 -160°F Tests

Two static fracture tests were conducted at -160°F in 1200 psig gaseous hydrogen, each from a different die forging. The detailed results of these tests are presented in Table 22.  $K_Q$  values of 84.9 and 86.0 ksi  $\sqrt{\text{in}}$  and  $(K_I)_{\max}$  values of 84.9 and 88.5 ksi  $\sqrt{\text{in}}$  were obtained. The tests did not quite meet the ASTM-E399-70T requirement for thickness. Based on a -160°F yield strength of 128 ksi,  $K_Q$  would had to have been  $\leq 81.0$  ksi  $\sqrt{\text{in}}$  to be considered a valid  $K_{Ic}$  test per ASTM. The flat appearance of the fracture face plus the failure abruptness of the load/displacement curves, leads one to believe that the tests were valid. The results obtained

At these temperatures of about 150°K the rate of diffusion was slow and the effect of diffusion was the same as that of the hydrogen. The diffusion results for the liquid hydrogen are discussed below in the present paper while the fusion rate theories of a liquid hydrogen are given in the next section.

A study of the diffusion and fusion of deuterium in the liquid hydrogen was made by the author in 1950 at a temperature of 150°K and the results are given in Figure 20 and Table II. Figure 20 indicates that a slight increase in diffusion of deuterium in liquid hydrogen is observed at 150°K, and is in fact observed. The rate of diffusion of deuterium in liquid hydrogen is given in Figure 20 as unity. The same figure is the fusion of deuterium in liquid hydrogen at 150°K and the results of the diffusion of the hydrogen are given in Figure 20, both curves being similar. The diffusion and fusion from a very low to 150°K is the same and at a very vicinity of 150°K the crack had occurred in the form that appears upon hydrogen melting place and this occurs in the high pressure area. From these results it appears that the cyclic life and the fusion rate are influenced by high pressure hydrogen resulting in the diffusion rate as at the liquid 150°K the diffusion increased. Additional supporting evidence of the results of the diffusion of deuterium hydrogen at 150°K is presented in Figure 20 and the fusion rate of the deuterium.

### 3.3.3. Deuteron fusion

Finally, 2 steel fracture tests were conducted at -150°K in zero liquid hydrogen, one each from 1 die forging and the other from 1 pancake forging slice. The detailed results of these tests are given in Table II. For two die forging were used hot 1<sub>1</sub> values of 12.4 and 35.2 and 1<sub>2</sub> which are cyclic fracture parameter for die forging specimen resulted a value of 49.4 to 51.2. The remaining pancake forging specimen was initially important for use as a cyclic specimen, but failed without causing any damage due to the dashed cyclic load. This specimen

demonstrated a  $K_Q$  value of 50.5 ksi  $\sqrt{\text{in}}$ , considerably below the other pancake forging specimen test. All of the tests did meet the ASTM-E399-70T requirements. Based on an assumed  $-423^{\circ}\text{F}$  yield strength of 168 ksi, a  $K_Q$  value of  $\leq 106.2 \text{ ksi} \sqrt{\text{in}}$  would be considered a valid  $K_{Ic}$  test. It should be mentioned that the strain rate to failure for the specimen intended for cyclic testing was considerably higher than that of the standard static fracture test. The loading rate normally was 8500 lb/minute, whereas the low toughness specimen was loaded at almost 500 times that rate. This difference in loading rates could account for the difference in toughnesses. One other difference between the two pancake forging specimens was the appearance of the fracture faces. The low toughness specimen exhibited a smoother texture macroscopically than the other specimen. Both specimens were examined microscopically but only very minor differences were observed. Additional tests would be required to definitely establish the reason for the low toughness observed.

Four specimens were cyclic tested at  $-423^{\circ}\text{F}$  in zero psig liquid hydrogen; 2 specimens from one die forging, one specimen from another die forging and one specimen from a pancake forging. All of the tests were conducted at 5 cps and the results are presented in Figure 37 and Table 25. Grouping the results based on whether or not the specimen was made from a die forging or a pancake forging, resulted in single curves representing the variation of  $K_{Ic}$  with  $N$ . The single pancake forging specimen tested exhibited a very rough textured fracture face. Instantaneous  $da/dN$  results of these specimen tests are presented in Figure 38. The pancake forging specimen exhibited slower fatigue crack growth rates than the die forging specimens.

**BLANK PAGE**

## 5.0 OBSERVATIONS

- (1) The static fracture results were unaffected by 1200 psig high purity gaseous hydrogen compared to 1200 psig gaseous helium at RT for Armco 22-13-5 steel, phosphor bronze, A286 steel, Hastelloy X and 347 stainless steel. Valid fracture toughness values were not obtained in the above tests due to limited material thickness.
- (2) An apparent hydrogen effect was observed in the static fracture testing of 9310 carburized steel when considerable time dependent growth occurred during loading to failure in 1200 psig gaseous hydrogen at RT. The growth on this specimen was distinguishable on the fracture face as well as indicated on the load/crack opening displacement record. Using the flaw size at fracture plus the load at failure resulted in an apparent toughness equal to that observed in a helium environment. An apparent  $K_{Ic}$  equal to about 120 ksi $\sqrt{\text{in}}$  was observed at RT in helium for the 9310 steel. At -423°F in liquid hydrogen this material exhibited a  $K_{Ic}$  value of 32 ksi $\sqrt{\text{in}}$ .
- (3) The static fracture tests for 5Al-2.5 Sn (ELI) titanium in 100 psig gaseous hydrogen at RT were not valid  $K_{Ic}$  tests due to limited material thickness available. The two different die forging materials tested at RT did not indicate any significant variability in apparent fracture toughness. The static fracture tests conducted at -160°F in 1200 psig gaseous hydrogen were essentially valid  $K_{Ic}$  values. These results also demonstrated uniformity of toughness results between the two die forgings tested. The fracture tests at -423°F in liquid hydrogen involved specimens fabricated from a pancake forging as well as two die forgings. All fracture toughness tests at -423°F resulted in valid  $K_{Ic}$  results with the pancake forging demonstrating a higher toughness than the die forgings.
- (4) The cyclic life and flaw growth rates were unaffected by 1200 psig gaseous hydrogen compared to 1200 psig gaseous helium at RT for Armco 22-13-5 and phosphor bronze.

- (5) The cyclic life and flaw growth rates were apparently unaffected by 1200 psig gaseous hydrogen at RT for A286 steel tested at 5 cps. A single specimen tested at 1 cps in hydrogen had flaw growth rates slightly higher than that observed in either hydrogen or helium at 5 cps. This could either indicate a slight hydrogen effect or a strain rate sensitivity phenomenon. Additional specimens would have to be tested to establish this point.
- (6) The cyclic life and flaw growth rates were moderately affected by the 1200 psig gaseous hydrogen at RT for Hastelloy X and 347 stainless steel. For Hastelloy X, a single specimen tested at 1 cps showed significantly higher flaw growth rates than specimens tested at 5 cps in hydrogen. The 347 stainless steel did not show this dependence of flaw growth rate with test frequency.
- (7) The cyclic life and flaw growth rates were significantly affected by the 1200 psig gaseous hydrogen at RT for 9310 carburized steel. The flaw growth rate also increased when the test frequency was decreased. This hydrogen effect was observed at a stress intensity level as low as  $11 \text{ ksi}\sqrt{\text{in.}}$ .
- (8) The cyclic life and flaw growth rates were apparently slightly affected by 100 psig gaseous hydrogen at RT for 5Al-2.5 Sn (ELI) titanium as compared with gaseous helium when tested at 5 cps. The single specimen tested in gaseous helium demonstrated growth rates that fell within the gaseous hydrogen scatter band but was on the slow side which might indicate a slight hydrogen effect at 5 cps. Additional specimens would have to be tested to establish this point. The cyclic flaw growth rates obtained were very consistent between the 3 die forgings tested.
- (9) The cyclic life and flaw growth rates were unaffected by 1200 psig gaseous hydrogen at  $-160^{\circ}\text{F}$  for 5Al-2.5 Sn (ELI) titanium as compared with gaseous helium at 5 cps. The data scatter bands for both environments were essentially the same and consistent between the 2 die forgings tested.

- (10) The cyclic life and flaw growth rates at -423° F in liquid hydrogen for 9310 carburized steel and 5Al-2.5 Sn (ELI) titanium were determined. Flaw growth rates for titanium specimens fabricated from die forgings were faster than for a specimen made from a pancake forging.

**BLANK PAGE**

#### REFERENCES

1. Bixler, W. D., "Flaw Growth of Inconel 718 and 5Al-2.5 Sn (ELI) Titanium in a High Purity Gaseous Hydrogen Environment", Boeing Document D180-10142-I, September 1970.

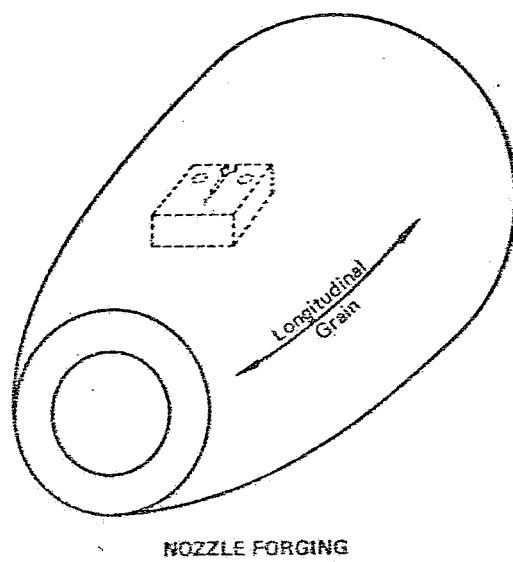
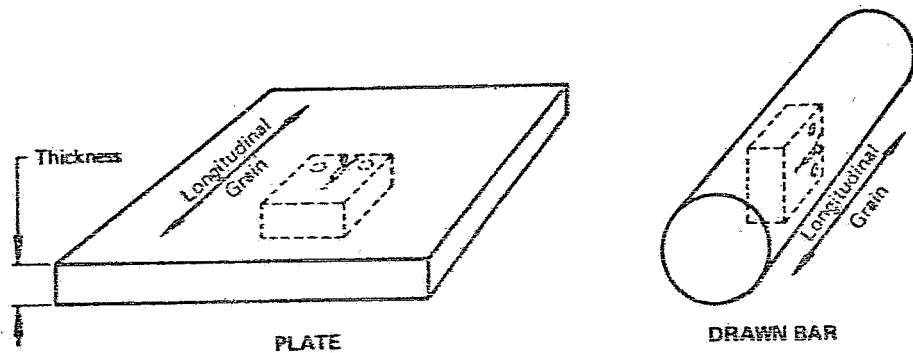
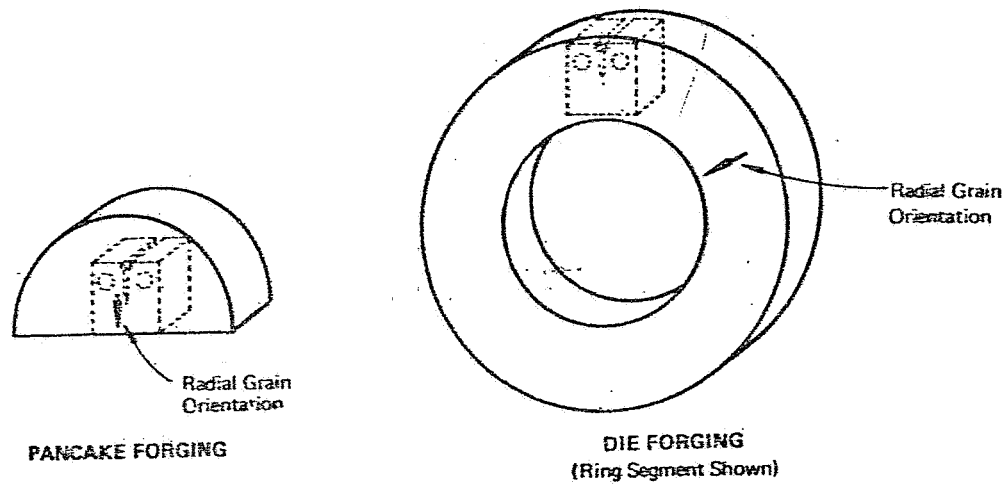


Figure 1: Specimen/Material Flow Orientations

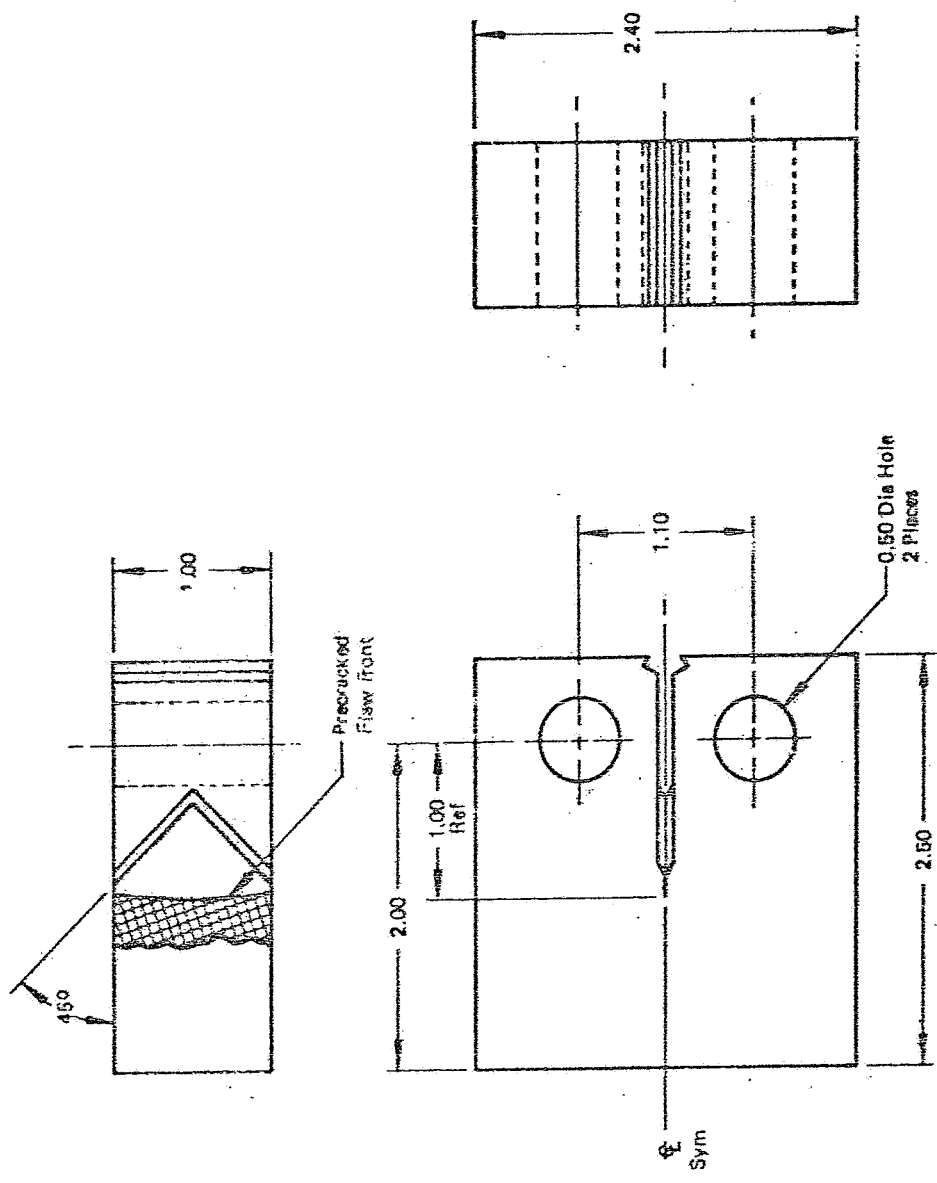
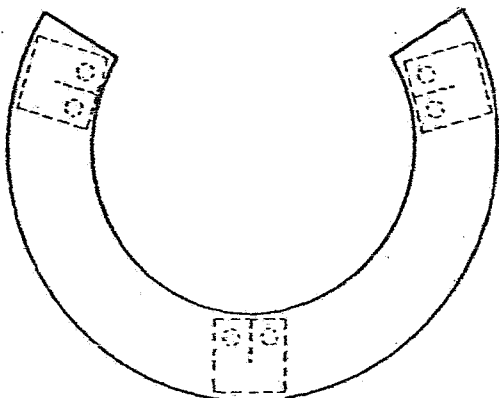
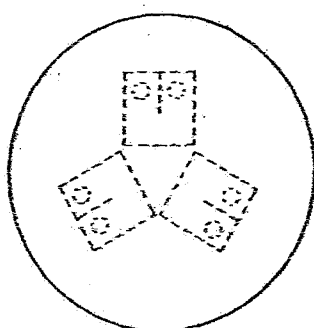


Figure 2: Compact Tension Specimen Specimen Configuration



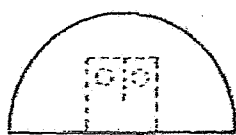
DIE
FORGING
RING
SEGMENTS

P/N 1138575  
1138576  
1138577  
1138578



WHOLE
DIE
FORGING

P/N 1138578



HALF
PANCAKE
FORGING

P/N 1138579

Figure 3: 5Al-2.5Sn (EEL) Titanium Specimen/Forging Location

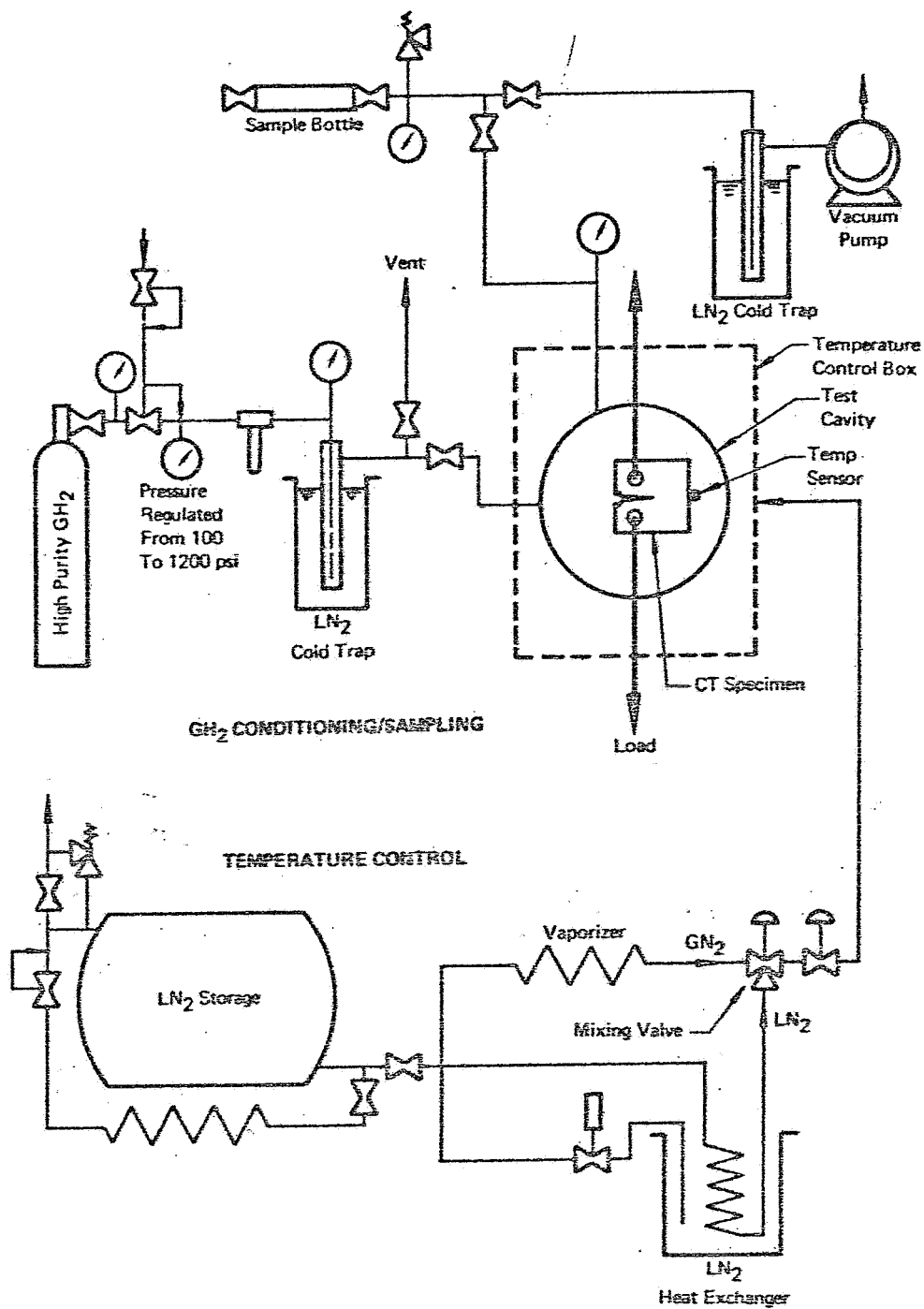


Figure 4: Test Setup Schematic



*Figure 5: Test Setup*

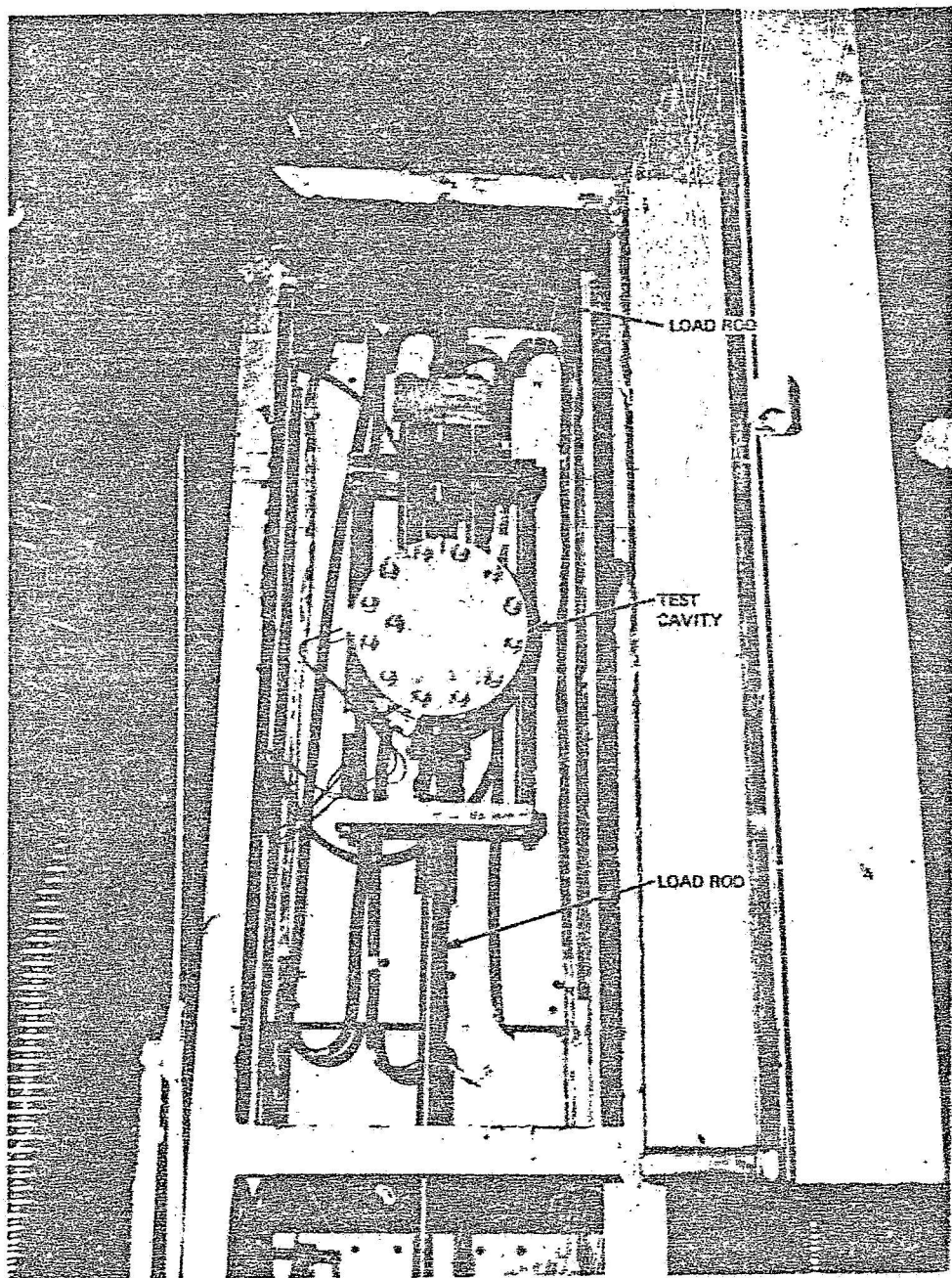


Figure 6: Open Test Cavity

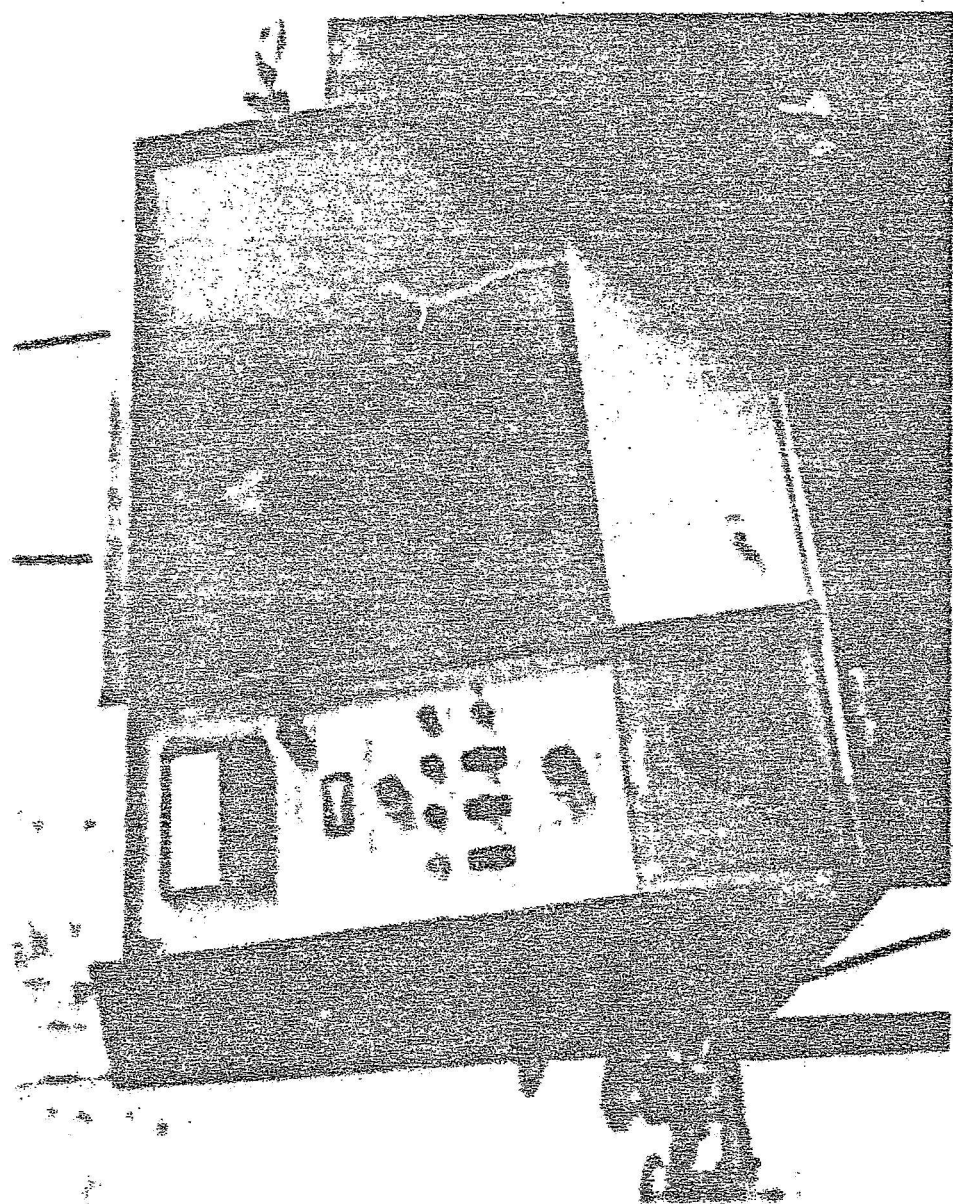
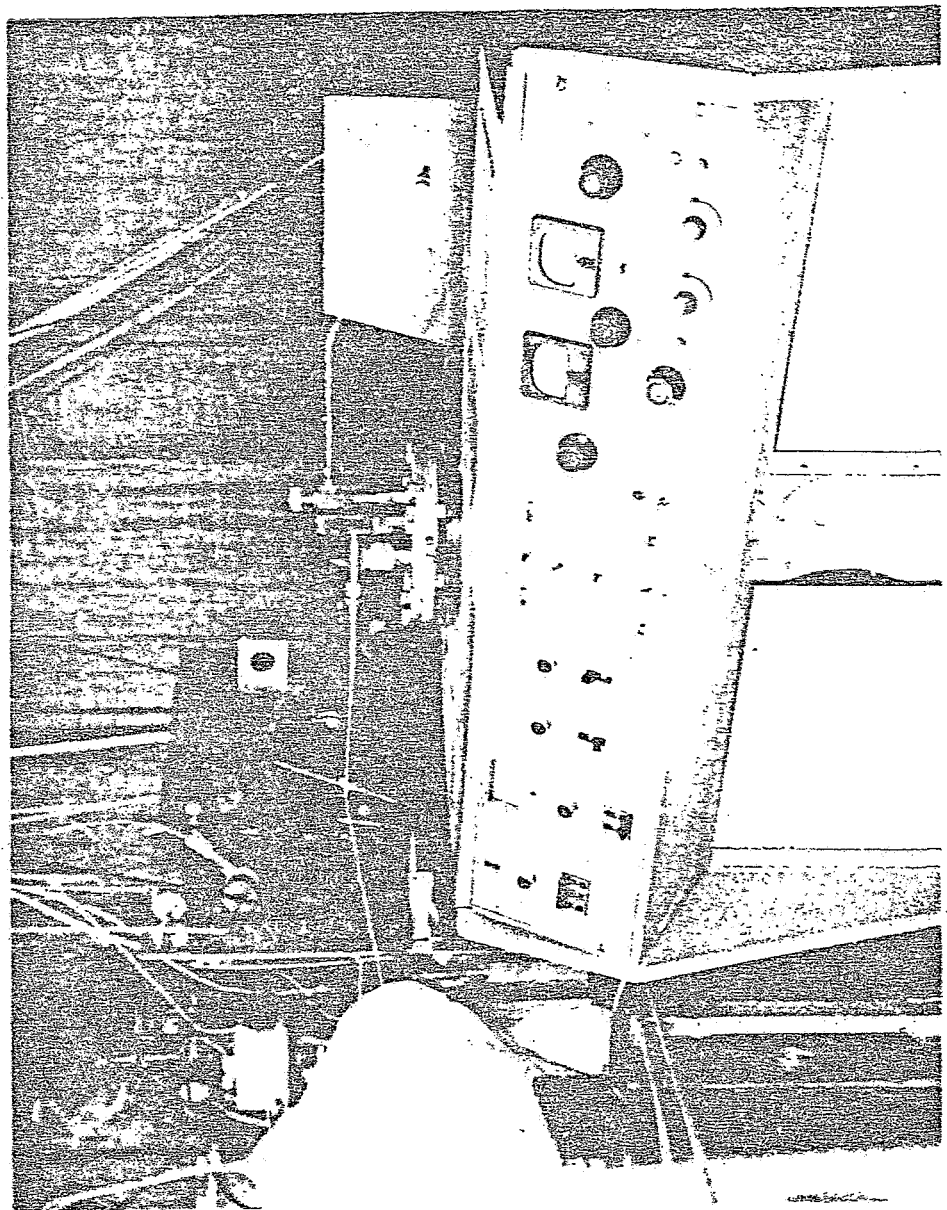


Figure 8. - Results of the experiments

*Figure 8: Diffusion Pump*



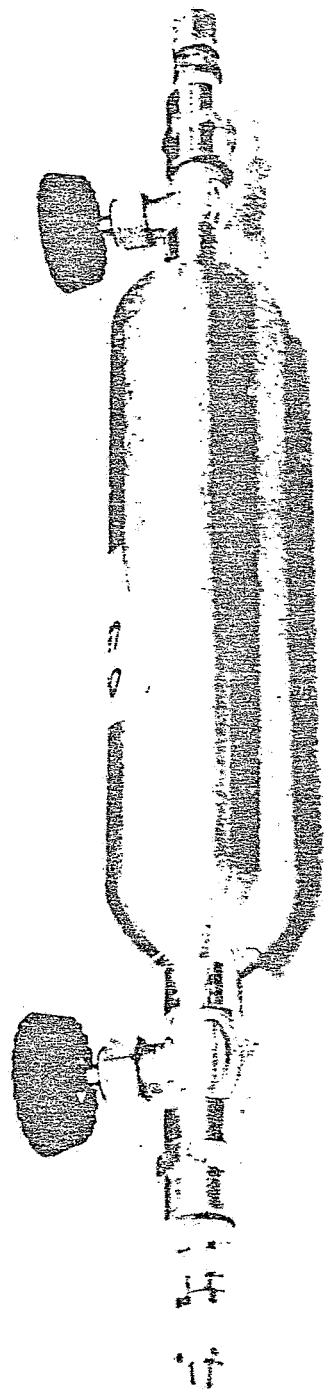


Figure 9: Hydrogen Gas Sample Bottle

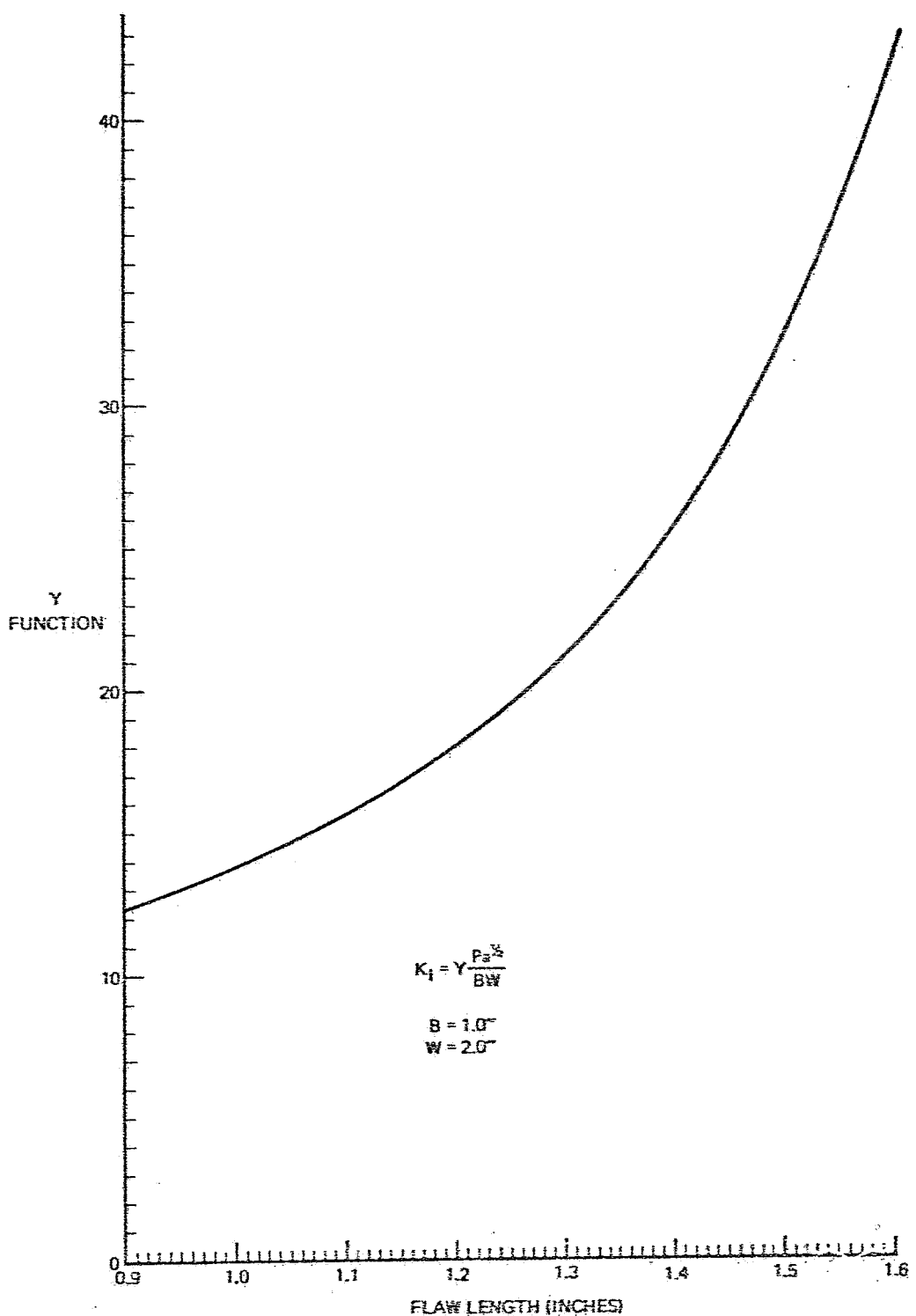


Figure 10: Y Function for Stress Intensity Calculations

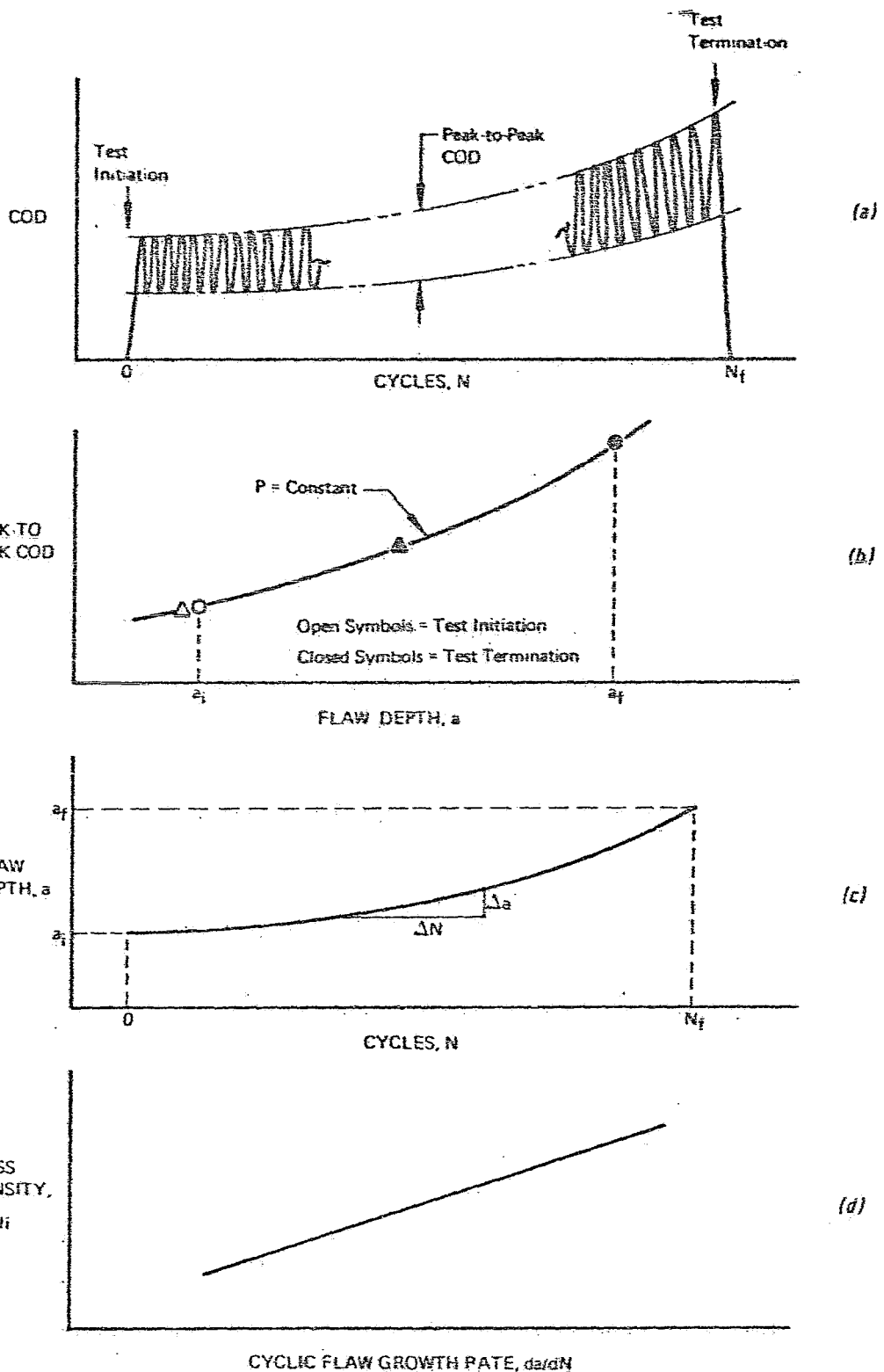


Figure 11: Analysis of Cyclic Flaw Growth Data

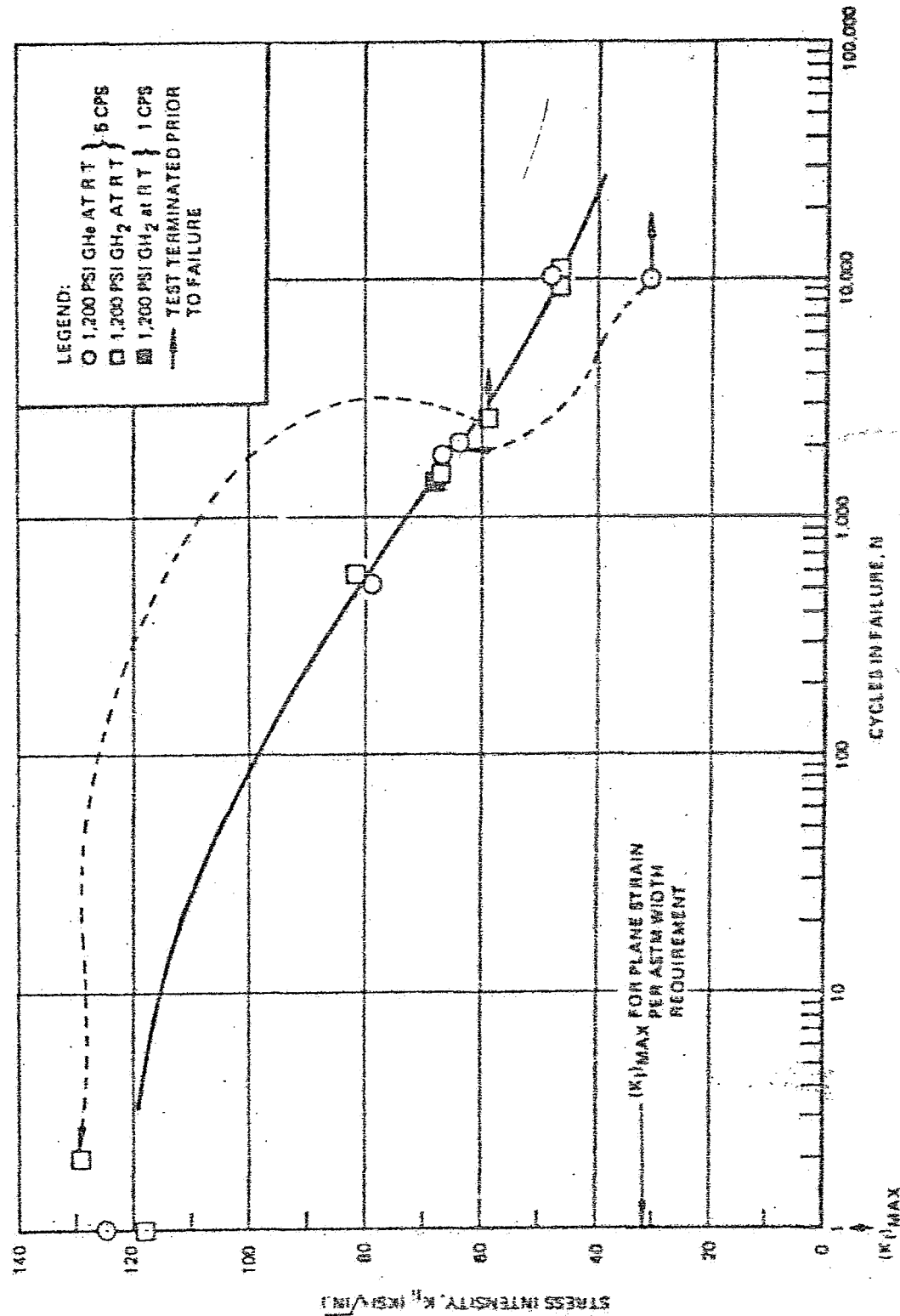


Figure 12: Circle Test Results of Annex Z2.115

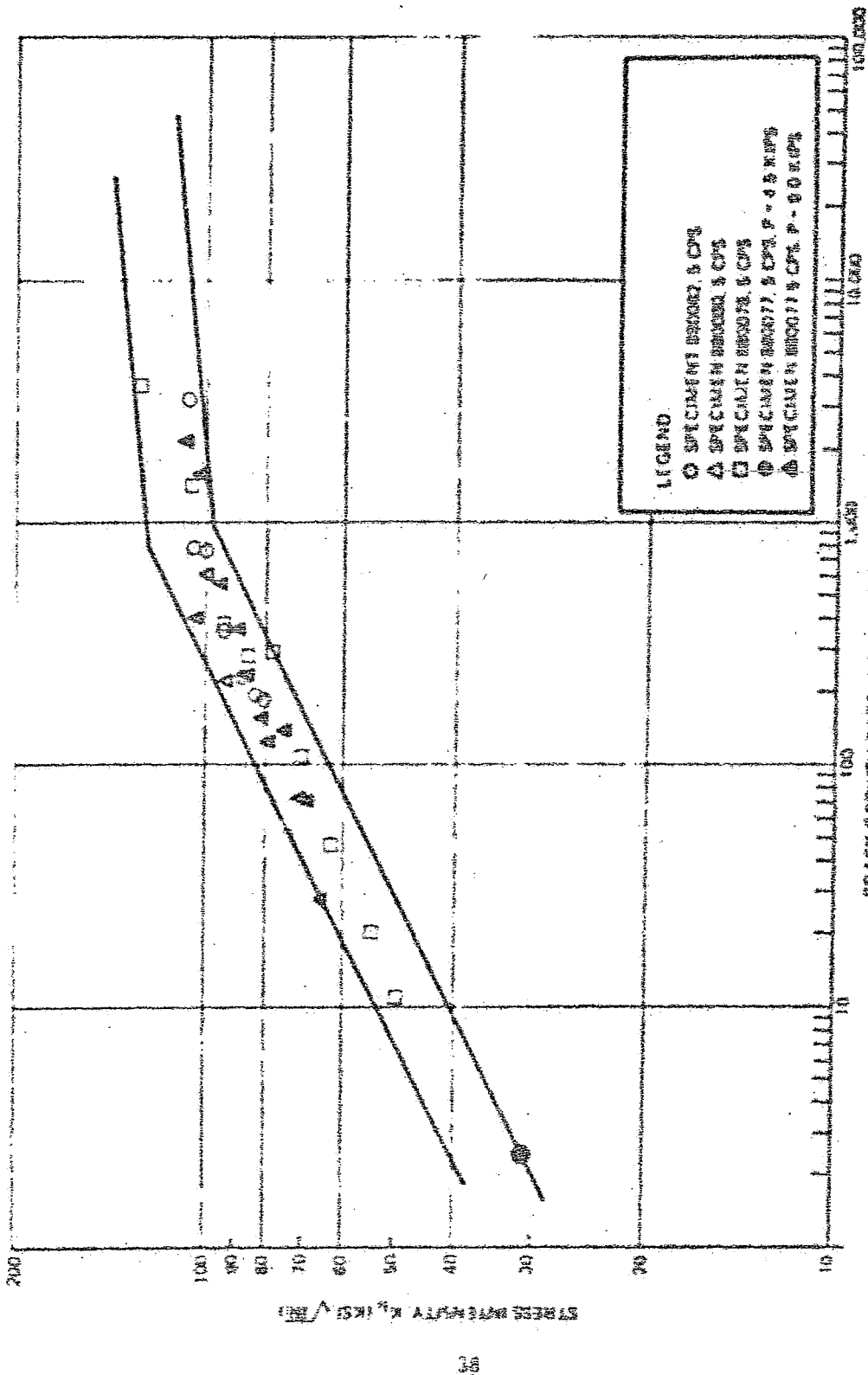


Figure 17. Growth Rate (Rate of Increase %) of Various Microorganisms during Various Phases of Microbial Fermentation

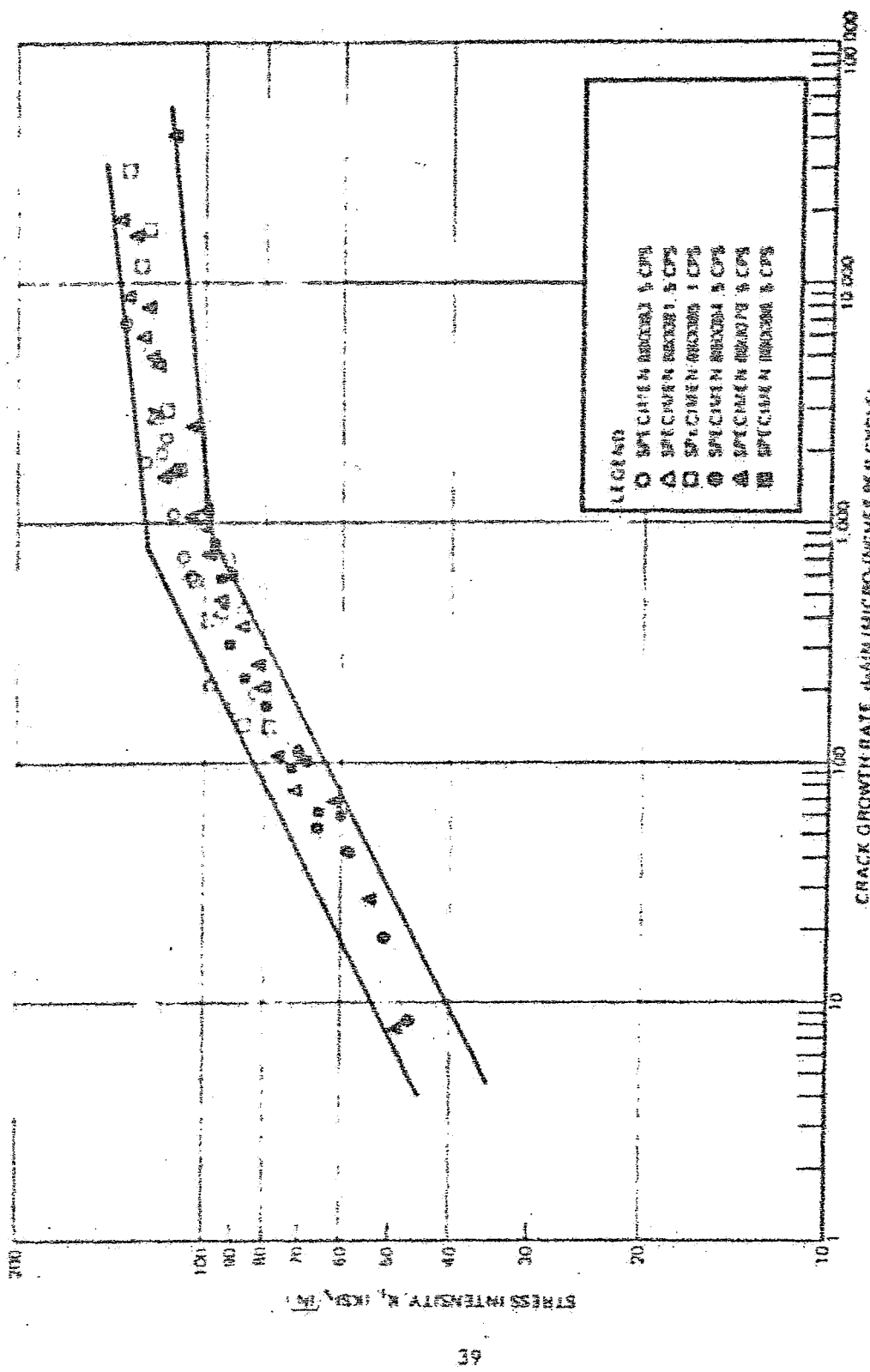


Figure 14 : Growth Rate Results of Almed 27-13-S in 1700 psig of repeat Hydrogen at Room Temperature.

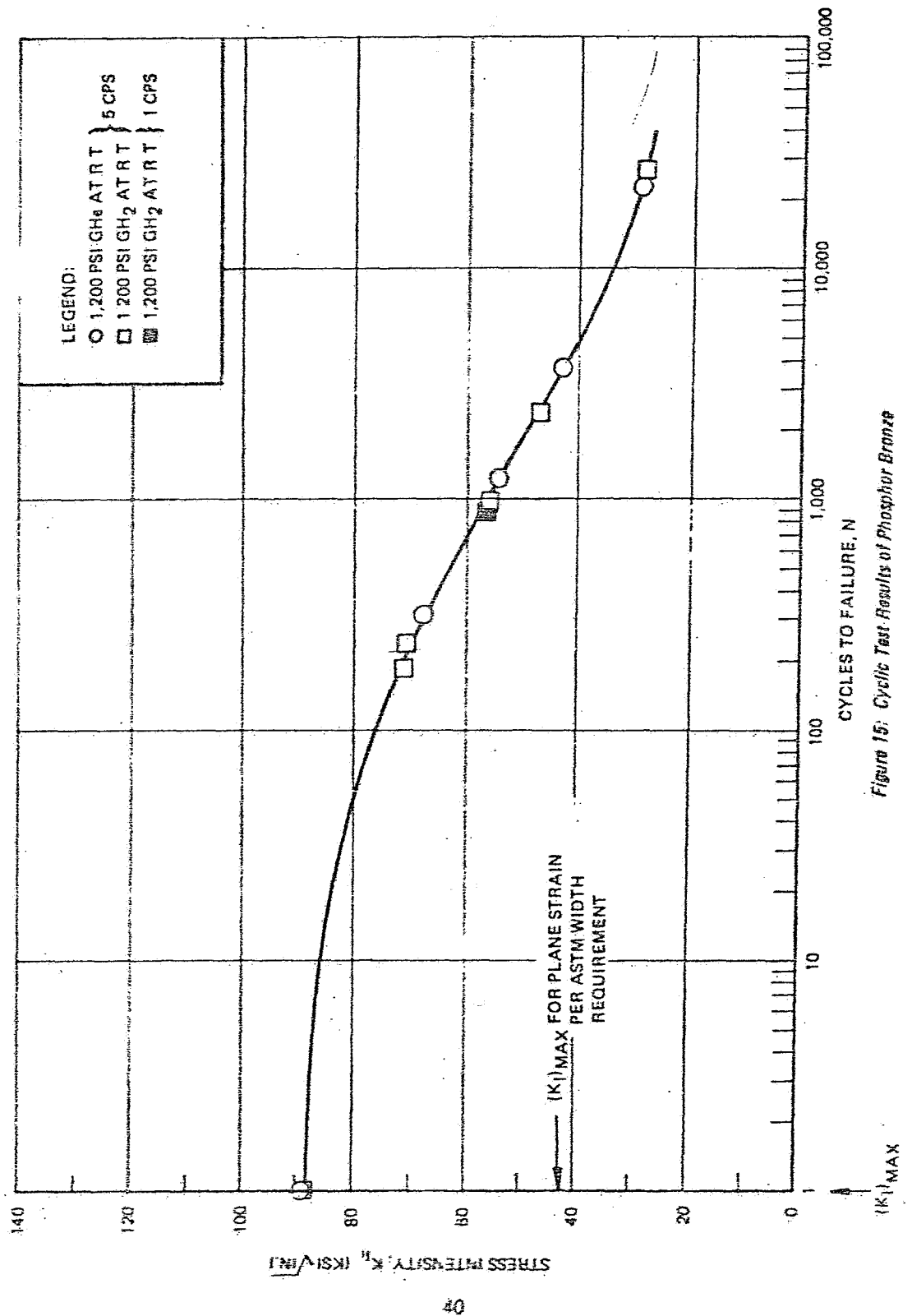


Figure 15: Cyclic Test Results of Phosphor Bronze

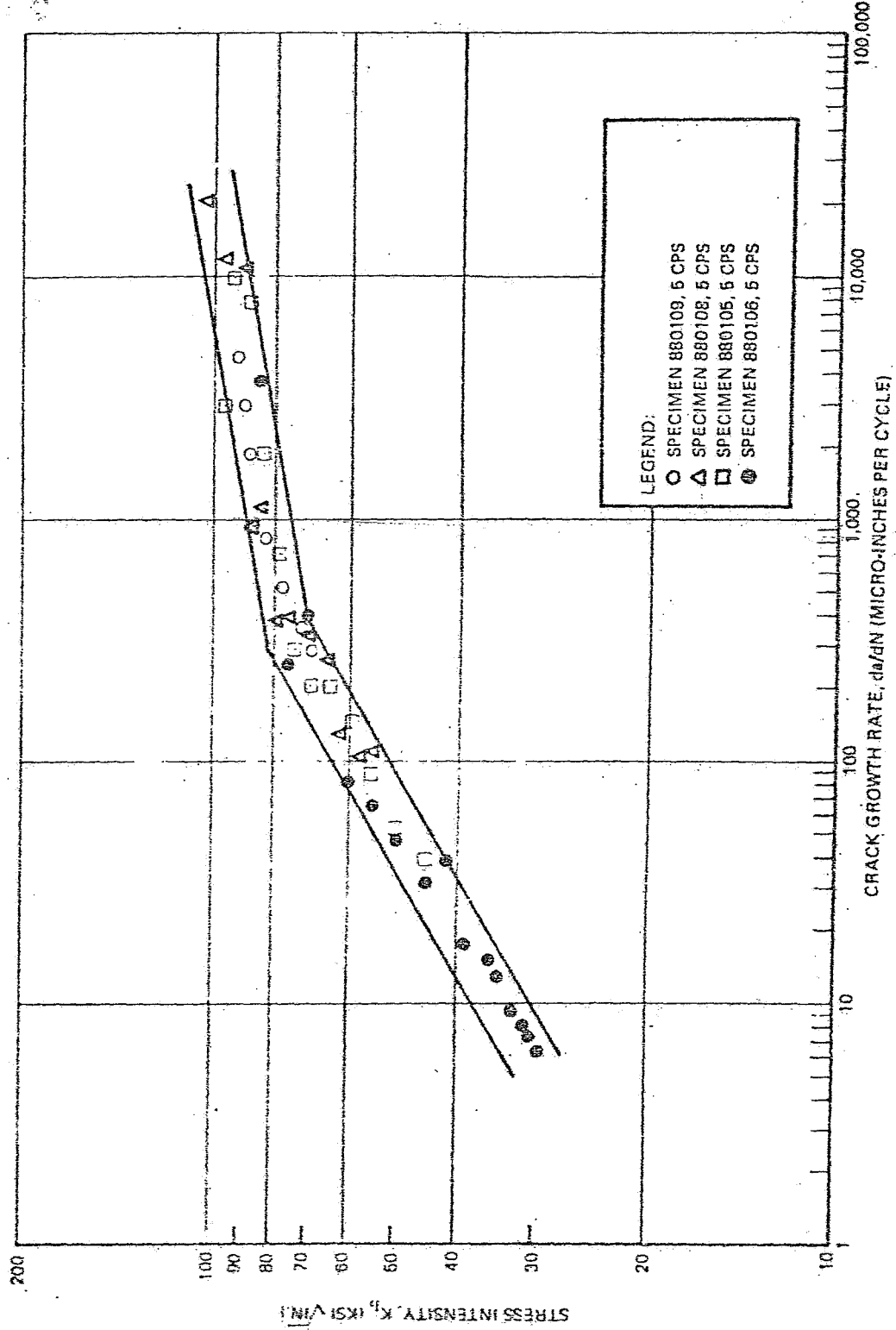


Figure 16 : Growth Rate Results of Phosphor Bronze in 1200 psig Gaseous Helium at Room Temperature

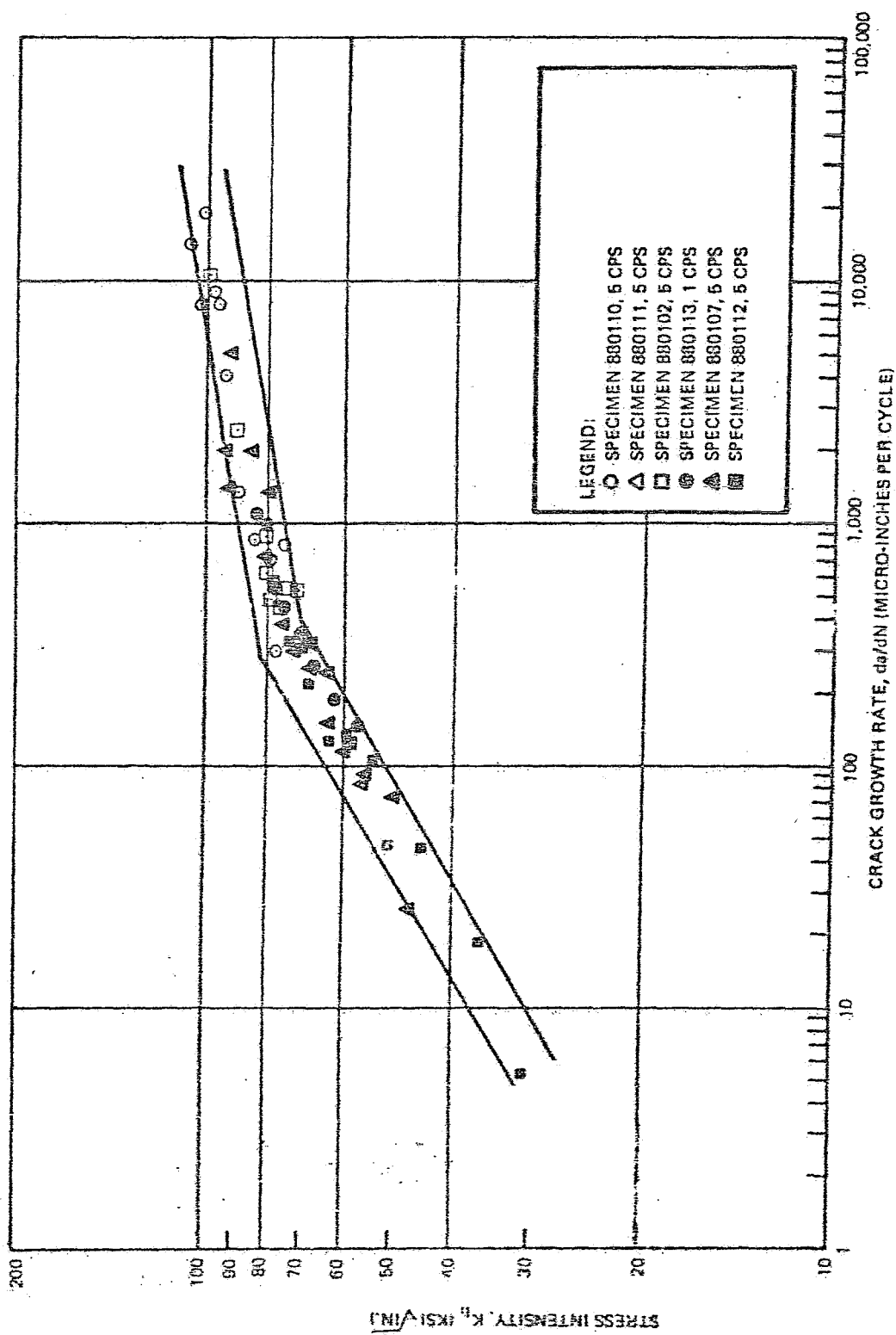


Figure 17: Growth Rate Results of Phosphor Bronze in 1200 psig Gaseous Hydrogen at Room Temperature

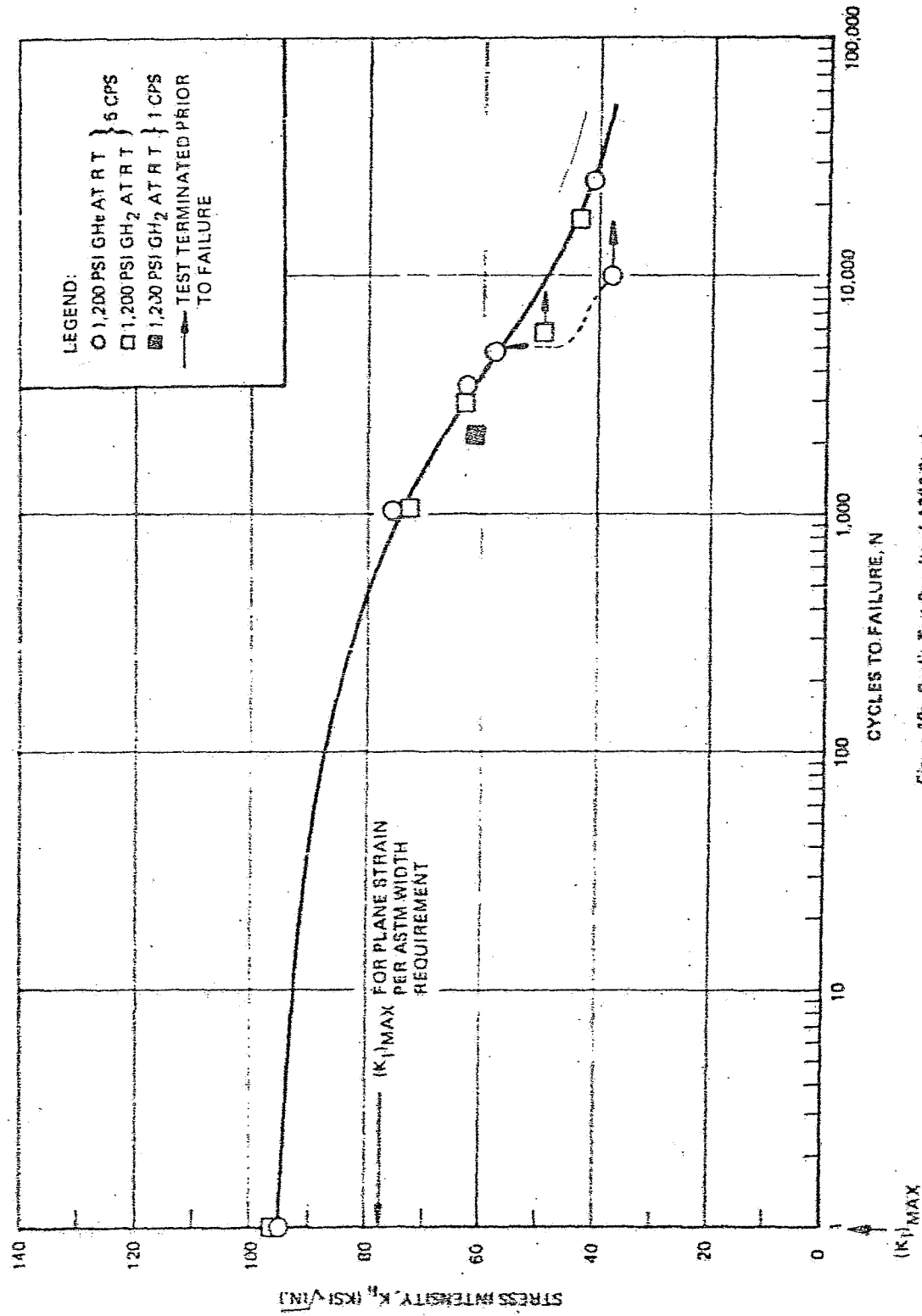


Figure 18: Cyclic Test Results of A295 Steel

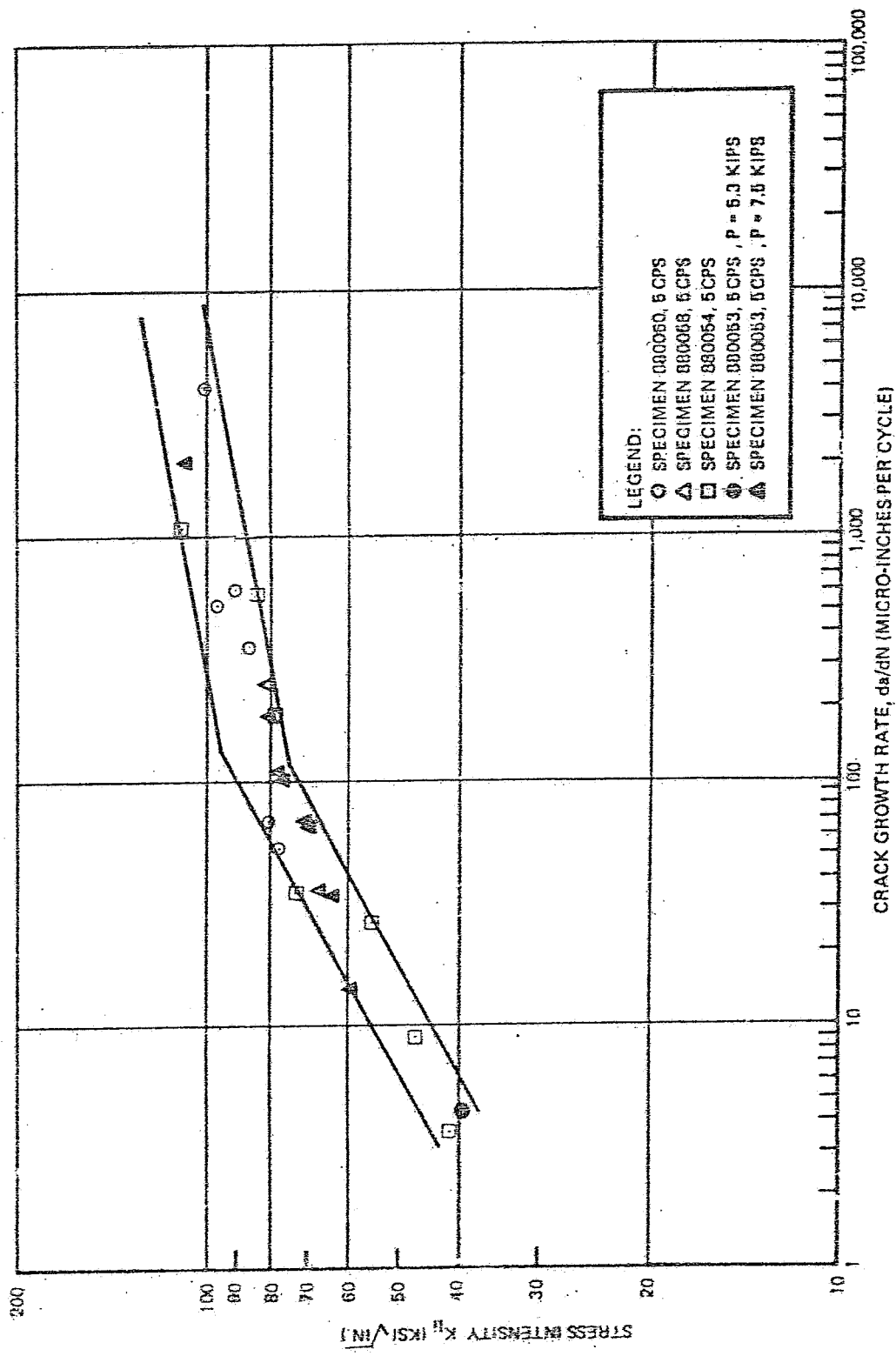


Figure 19 : Growth Rate Results of A286 Steel in 1200 psig Gaseous Helium at Room Temperature

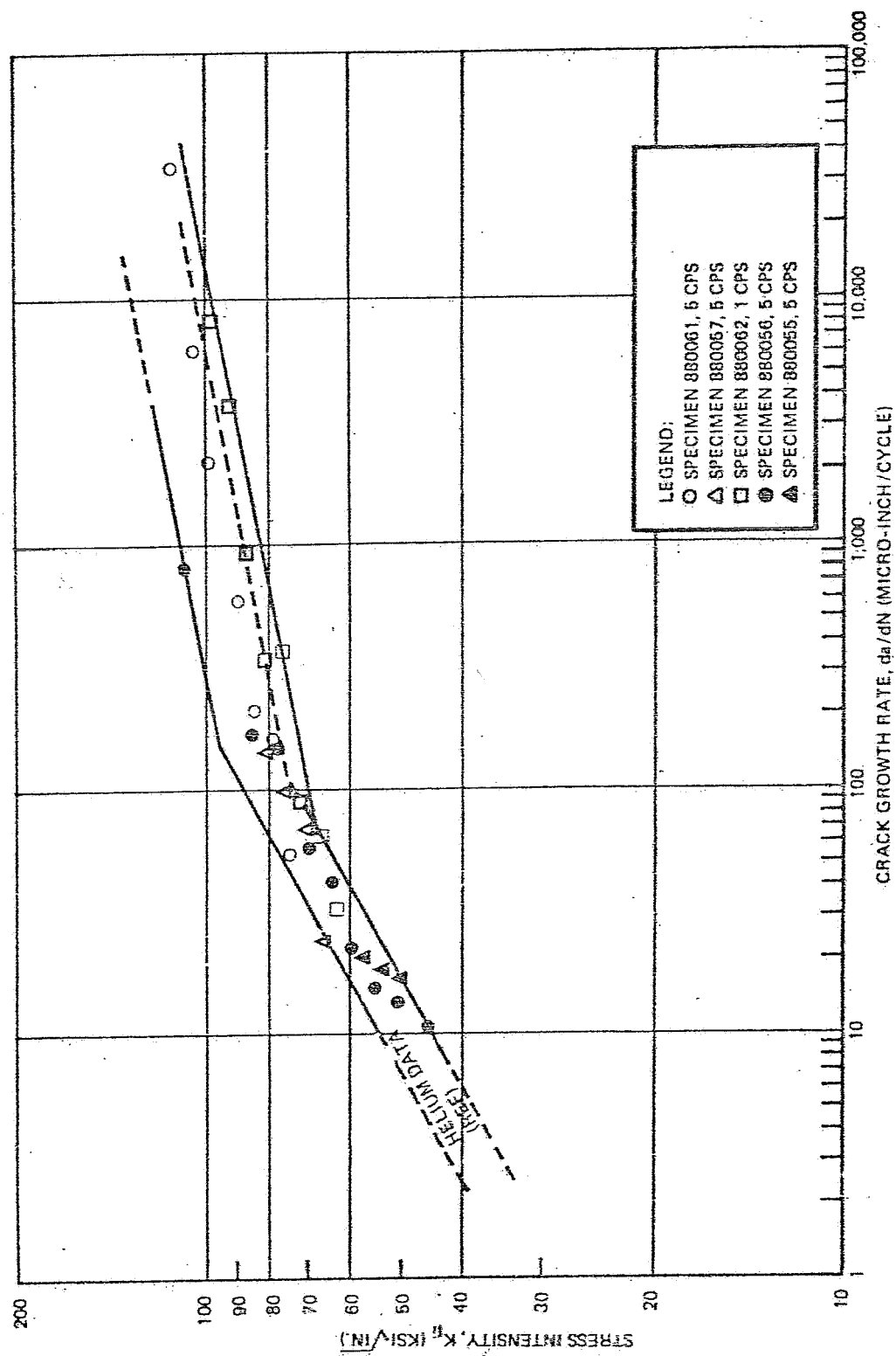


Figure 20 : Growth Rate Results of A285 Steel in 1200 psig Gaseous Hydrogen at Room Temperature

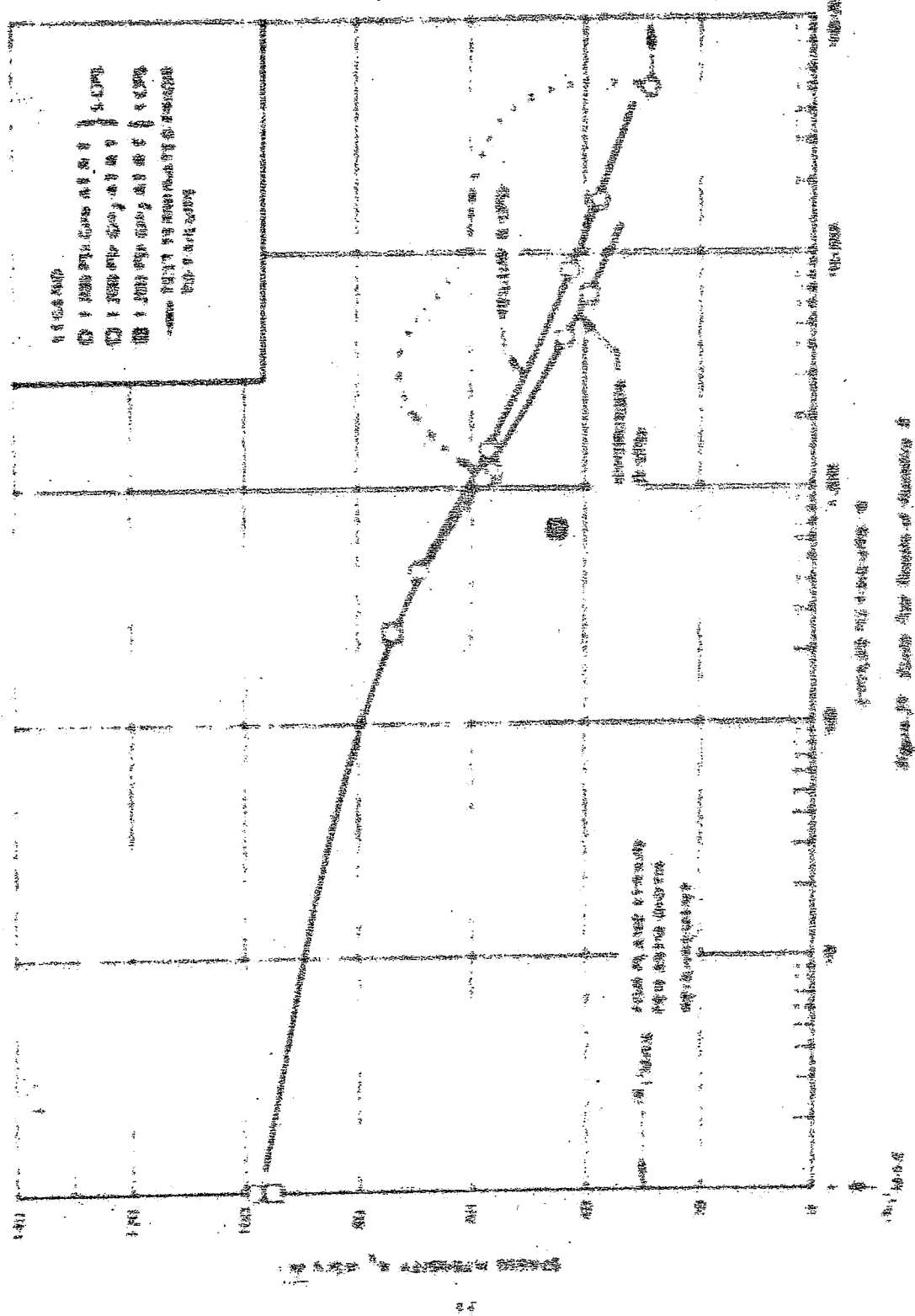
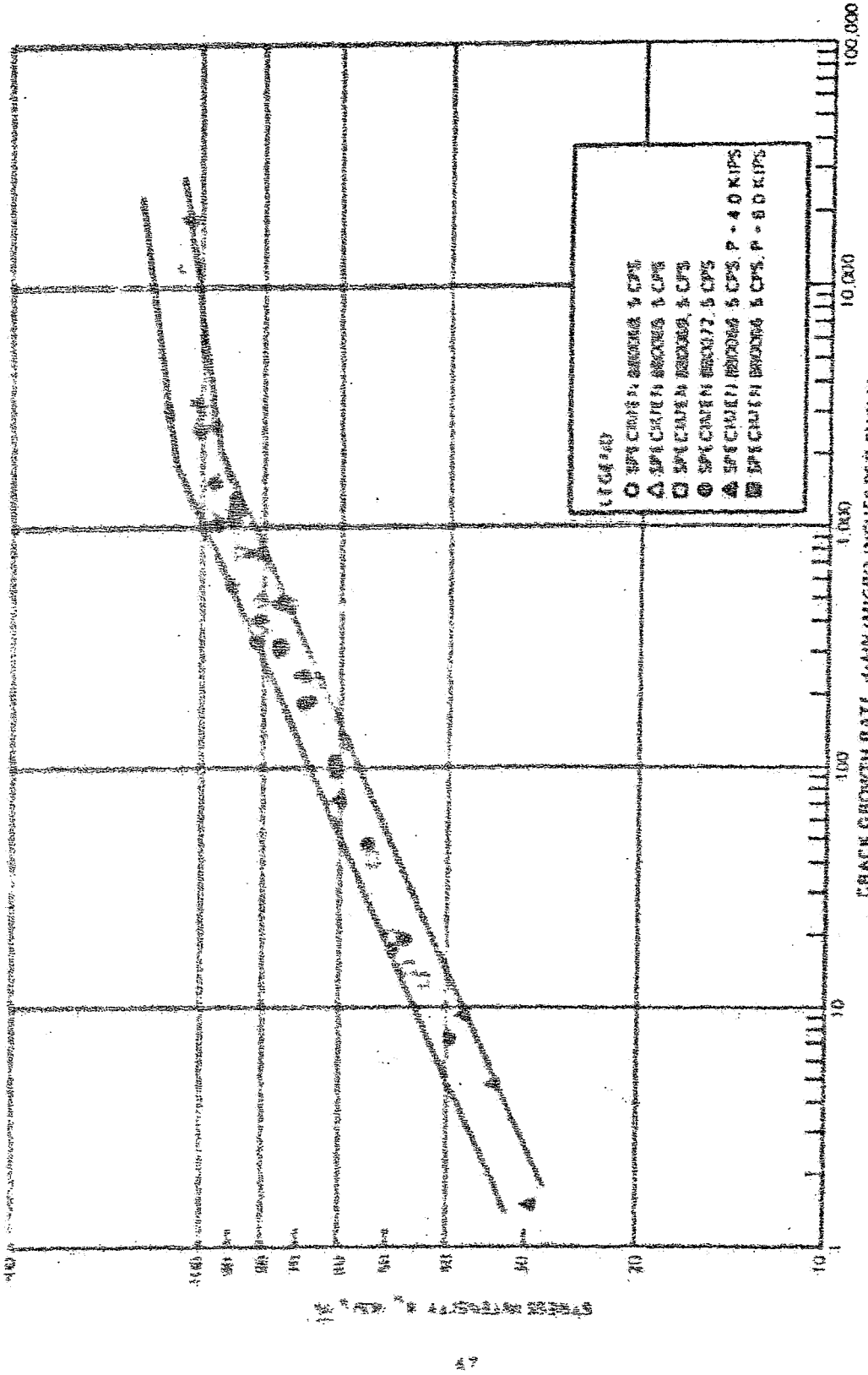


Figure 24 - Computed Stress Ratios of Matthey X at 1200 deg Fahrenheit at Room Temperature



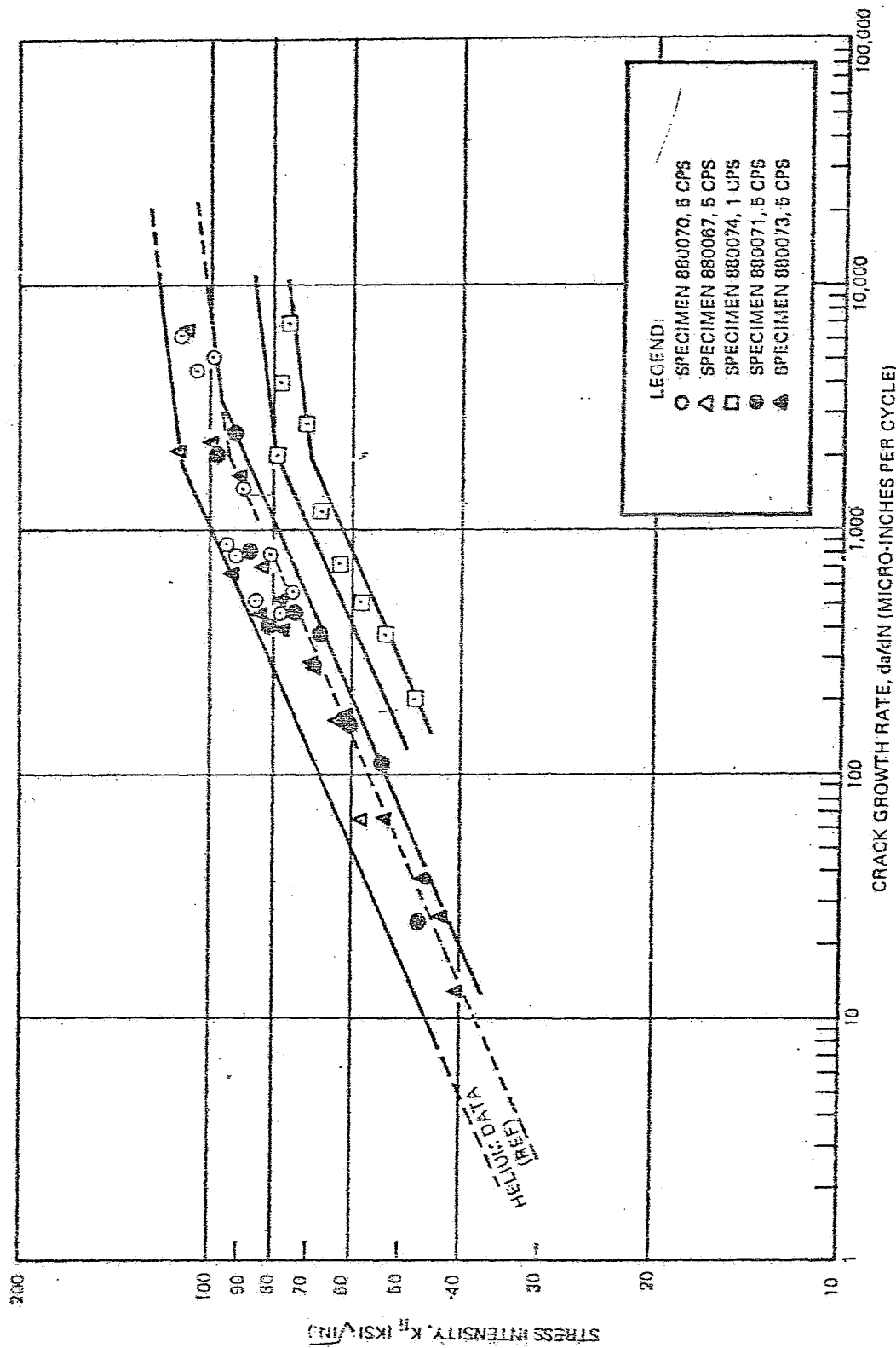


Figure 23: Growth Rate Results of Hastelloy X in 1200 psig Gaseous Hydrogen at Room Temperature

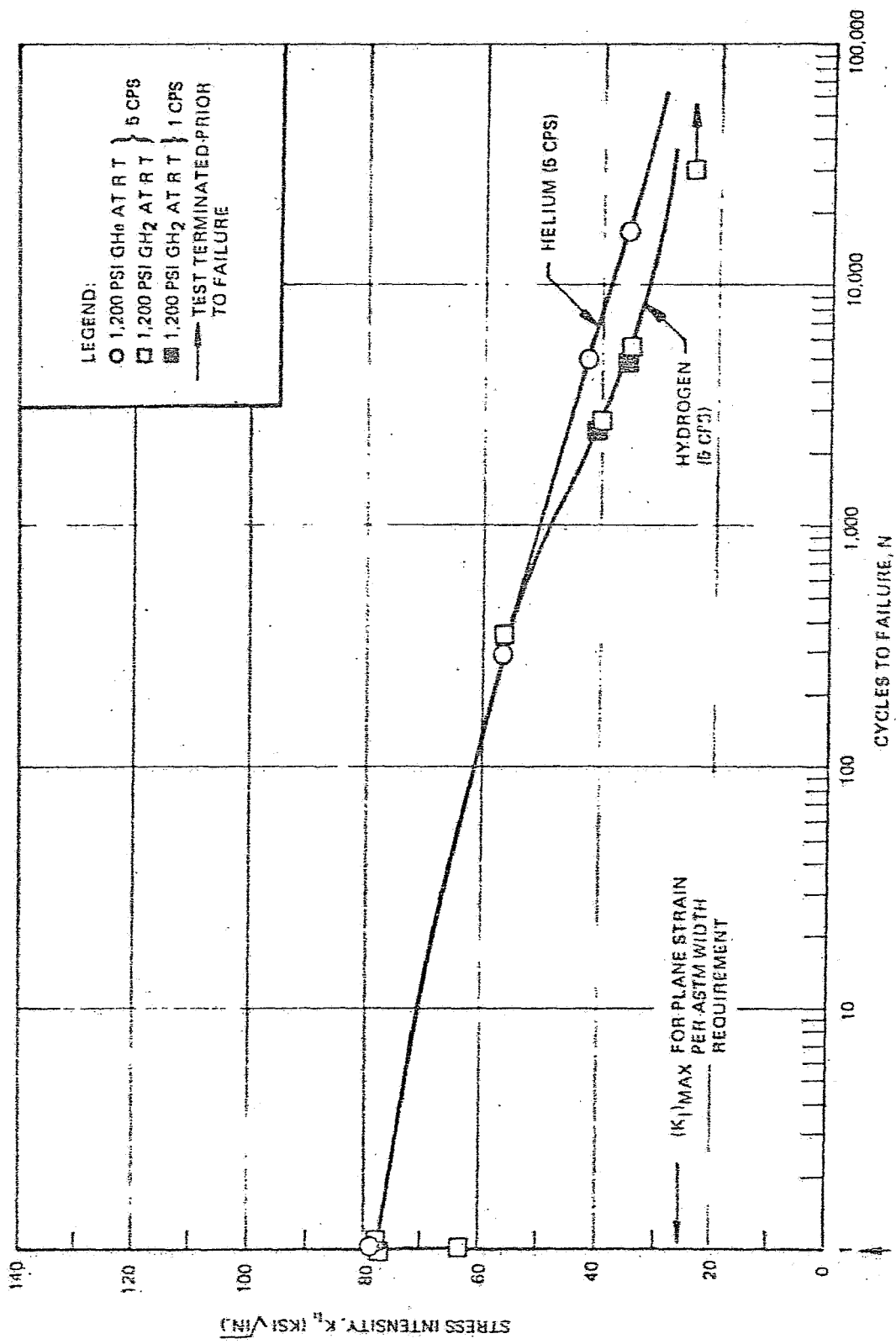


Figure 24: Cyclic Test Results of 347 Stainless Steel

$|K|_{\text{MAX}}$

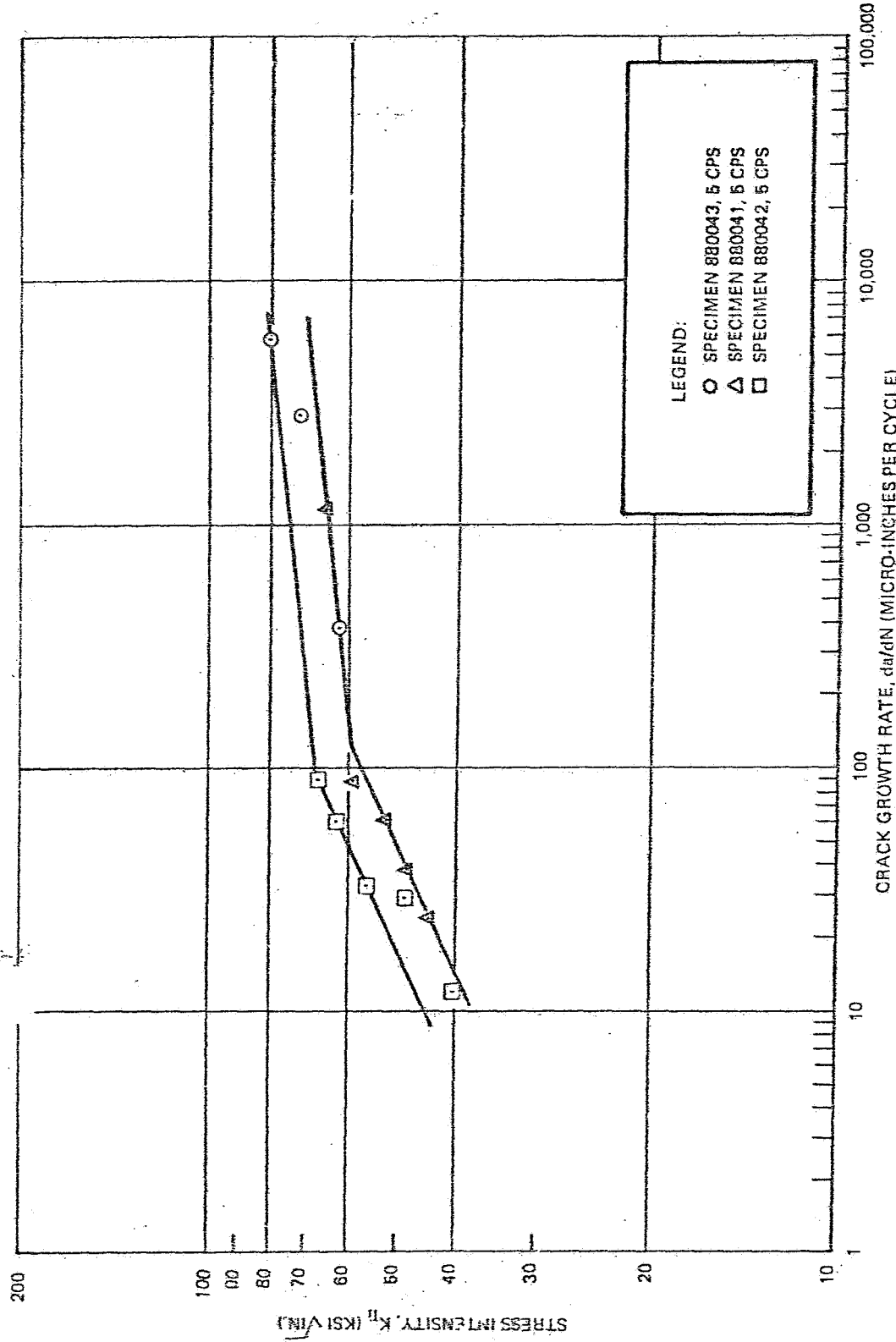


Figure 25. : Growth Rate Results of 347 Stainless Steel in 1200 psig Gaseous Helium at Room Temperature

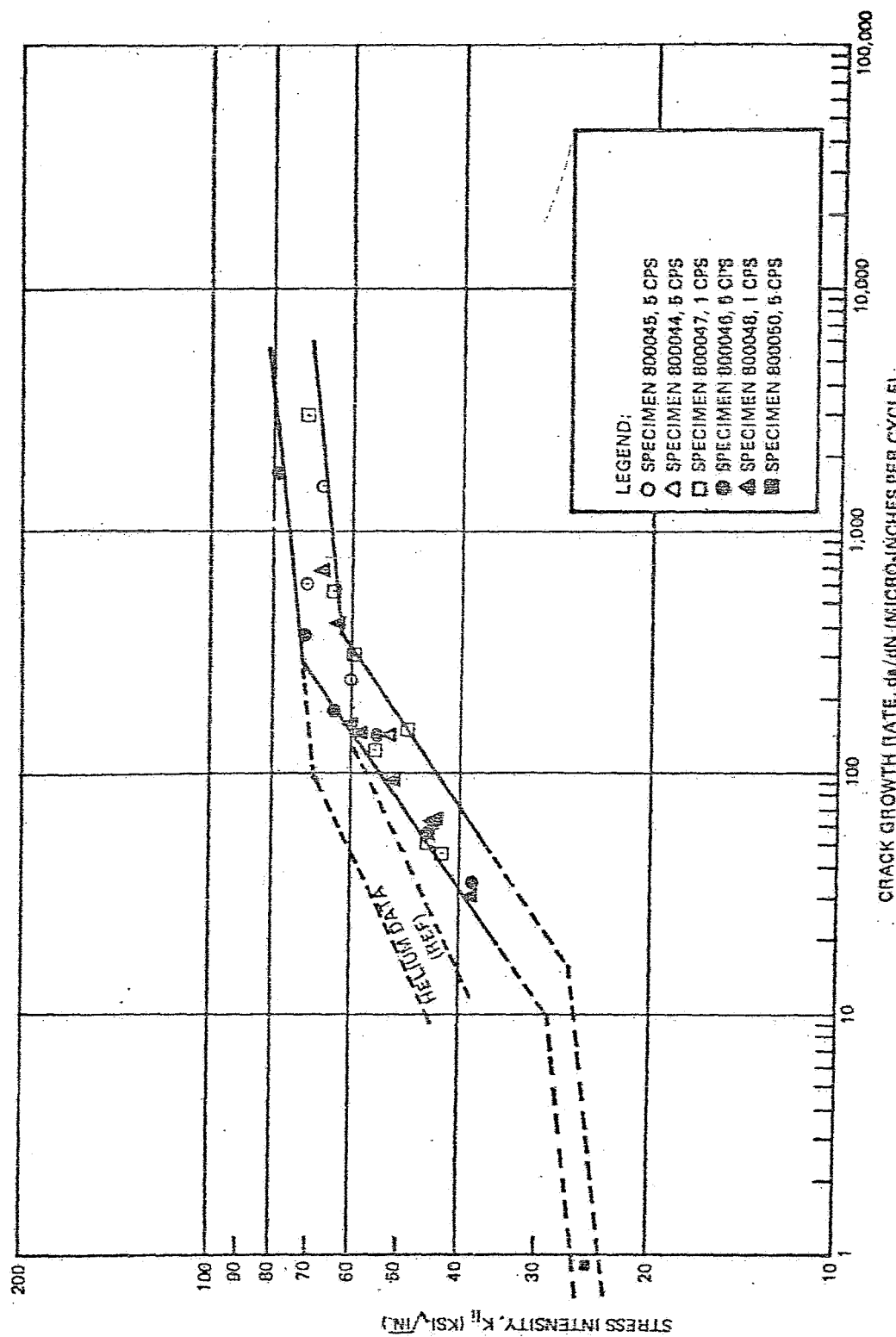


Figure 26 : Growth Rate Results of 347 Stainless Steel in 1200 psig Gaseous Hydrogen at Room Temperature

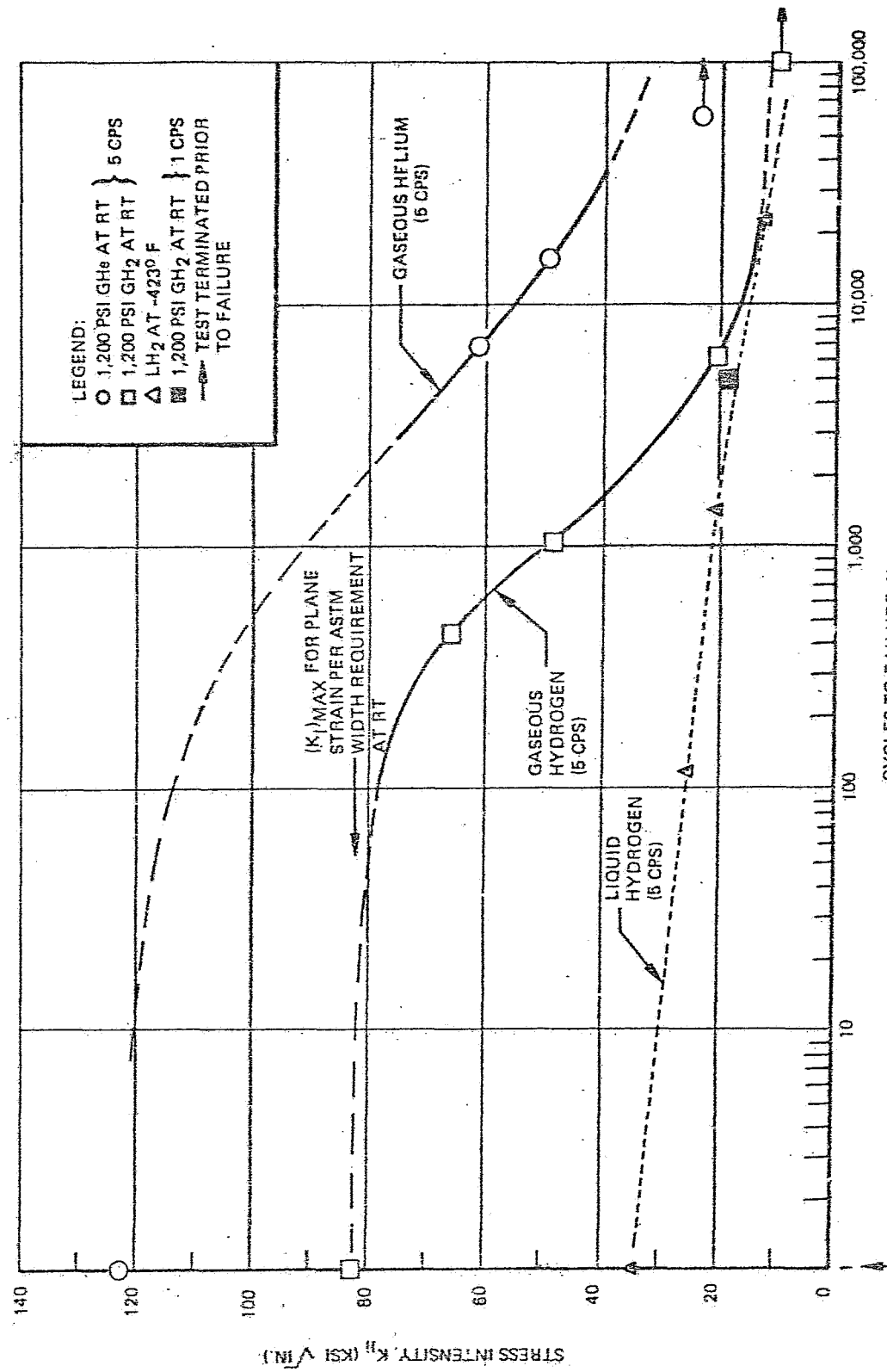


Figure 27: Cyclic Test Results of 310G Carbonized Steel

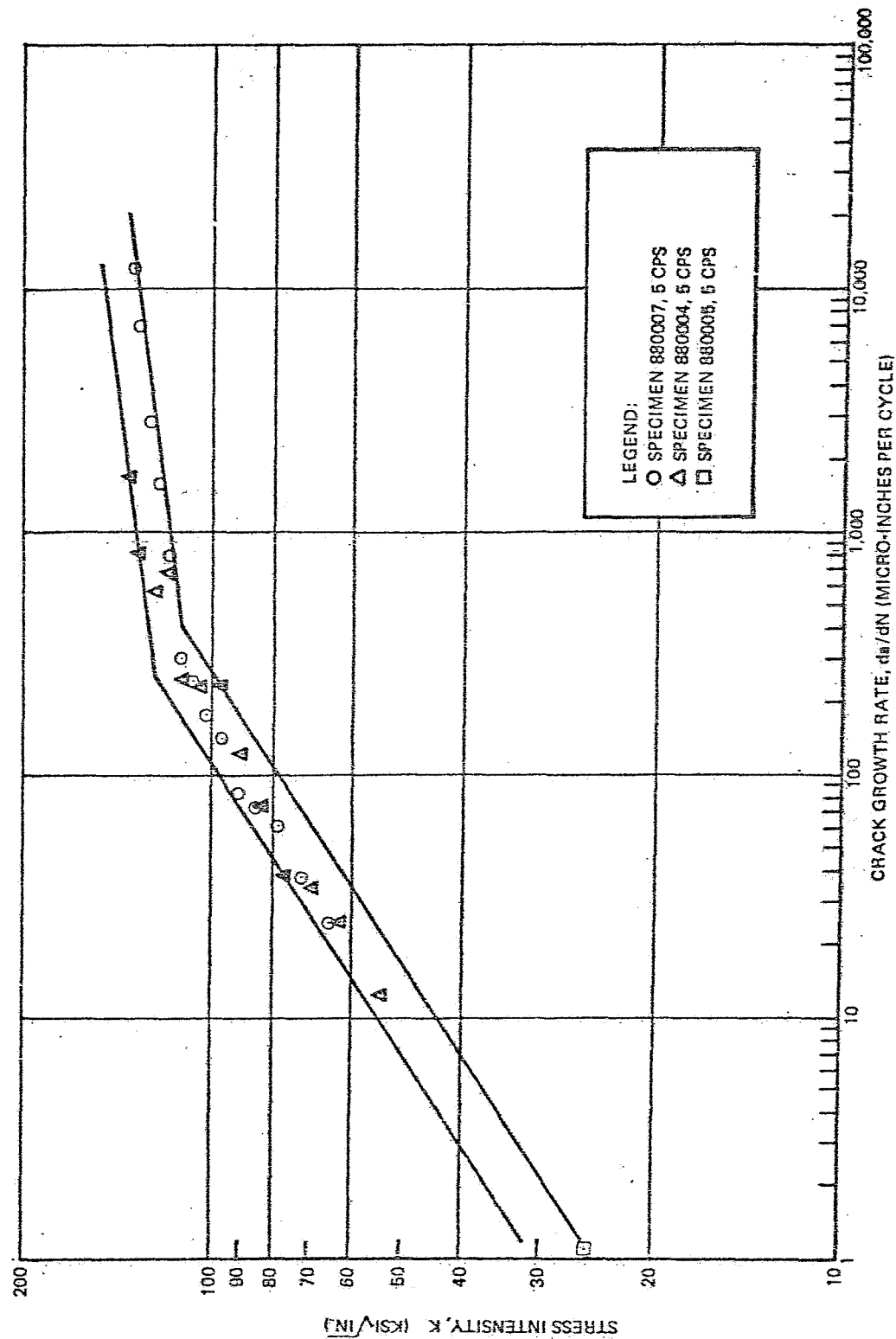


Figure 2B: Growth Rate Results of 93/10 Carbide Steel In 1200 psig Gaseous Helium at Room Temperature

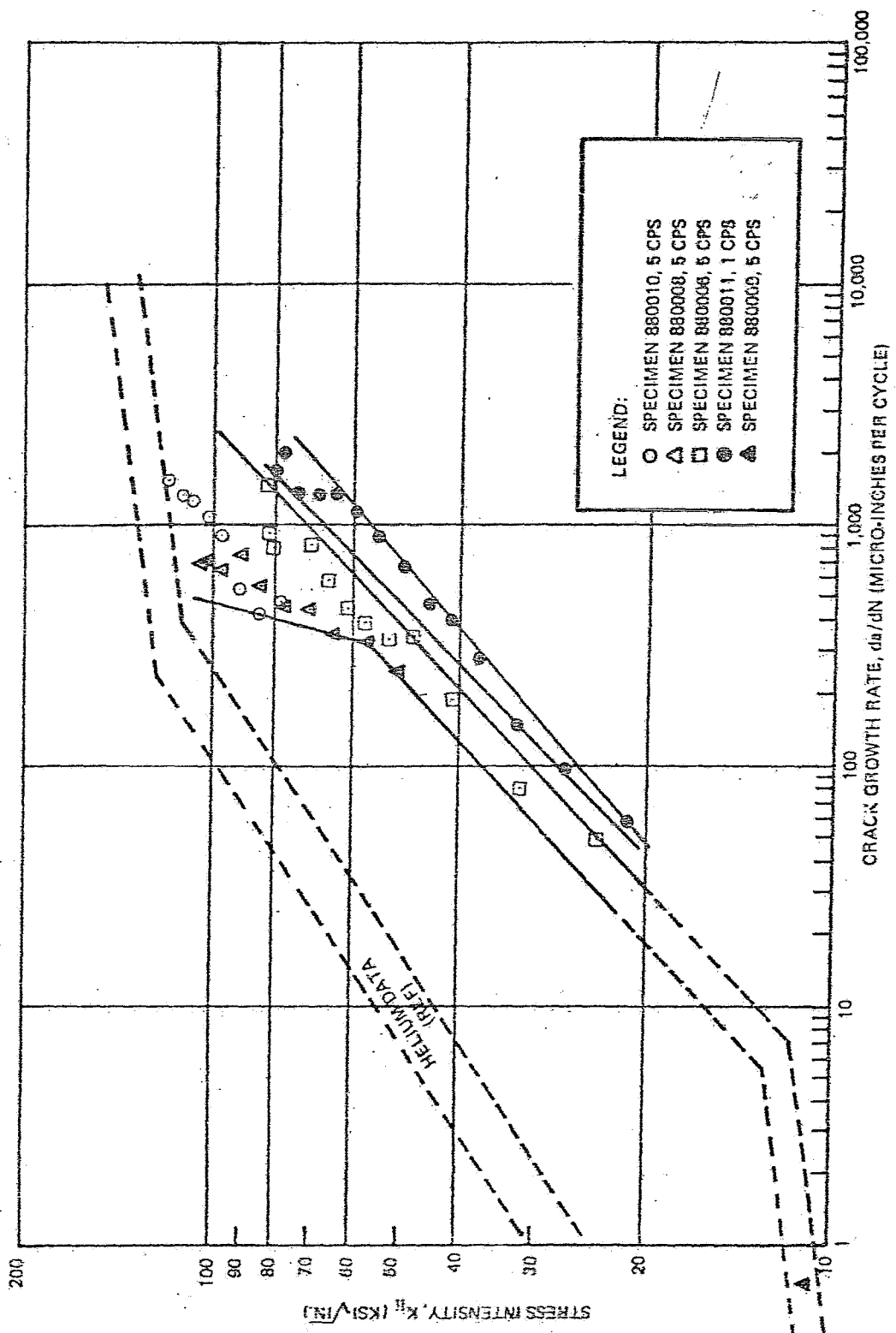


Figure 29: Growth Rate Results of 9310 Carborized Steel in 1200 psig Gaseous Hydrogen at Room Temperature

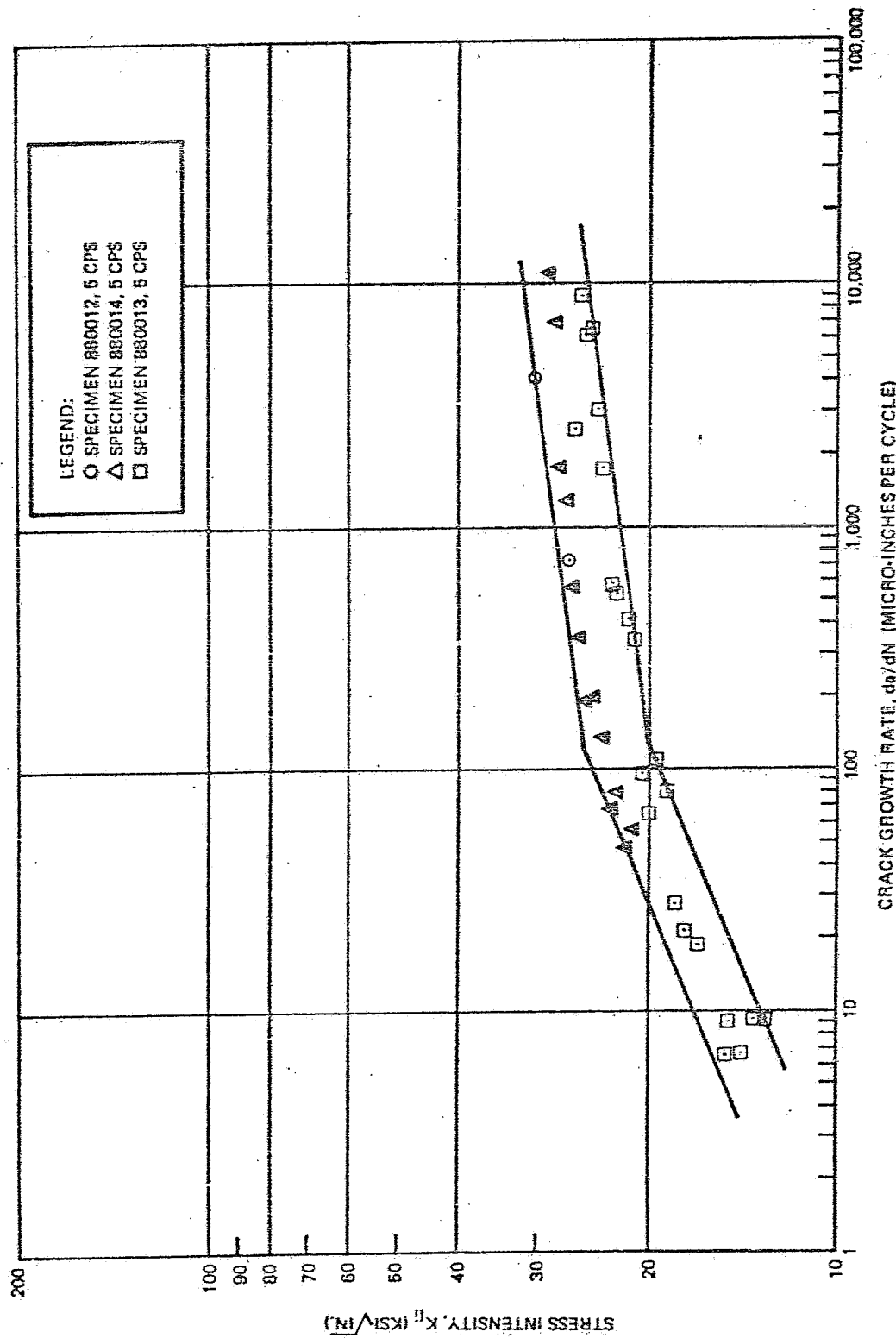


Figure 30: Growth Rate Results of 9310 Carbonized Steel in Liquid Hydrogen at -423°F

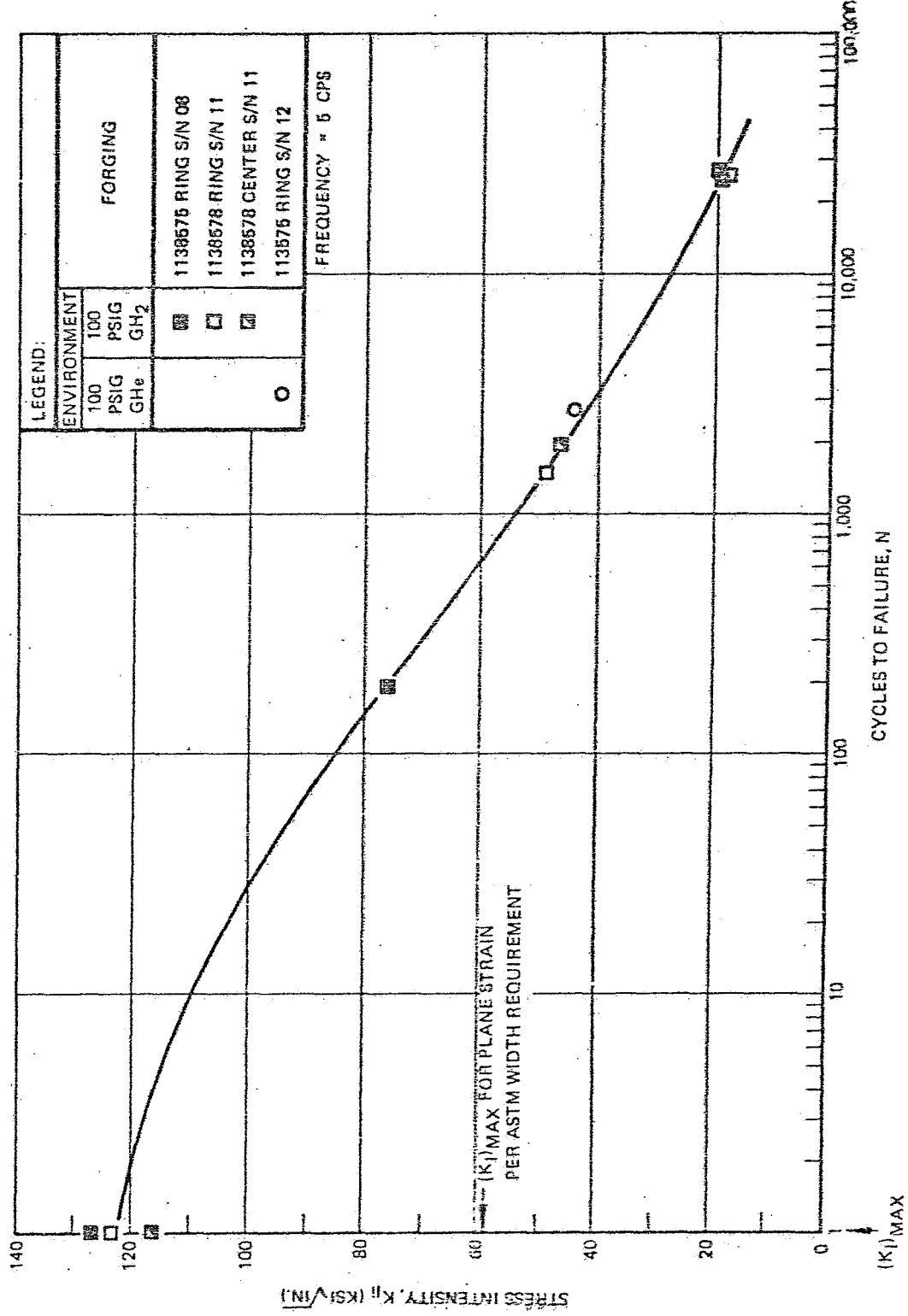


Figure 31: Cyclic Test Results of Ti-6Al-2.5Sn (EL1) Titanium at Room Temperature

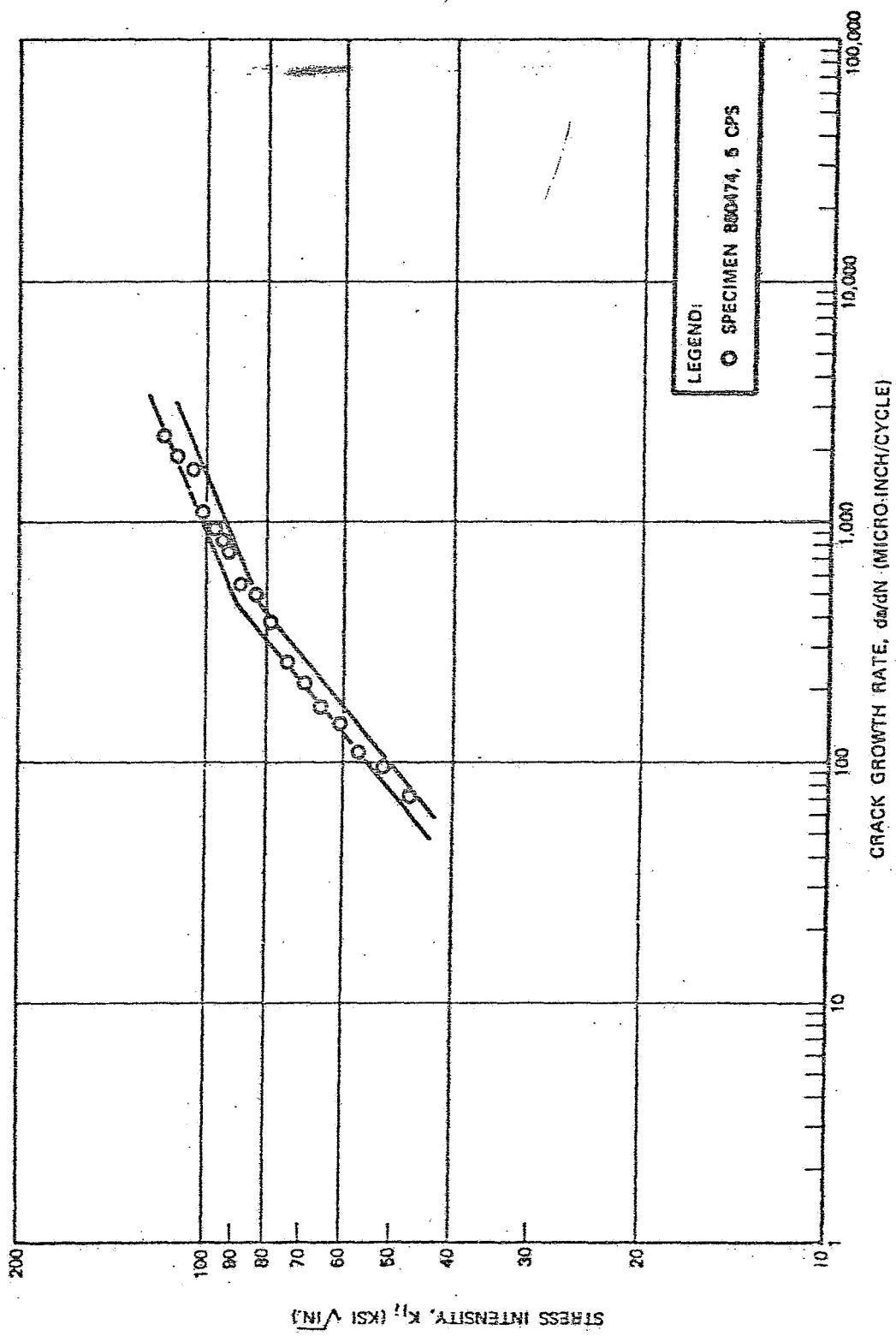


Figure 32: Growth Rate Results of 5Al-2.5 Sn (EL1) Titanium in 100 psig Gaseous Helium at Room Temperature

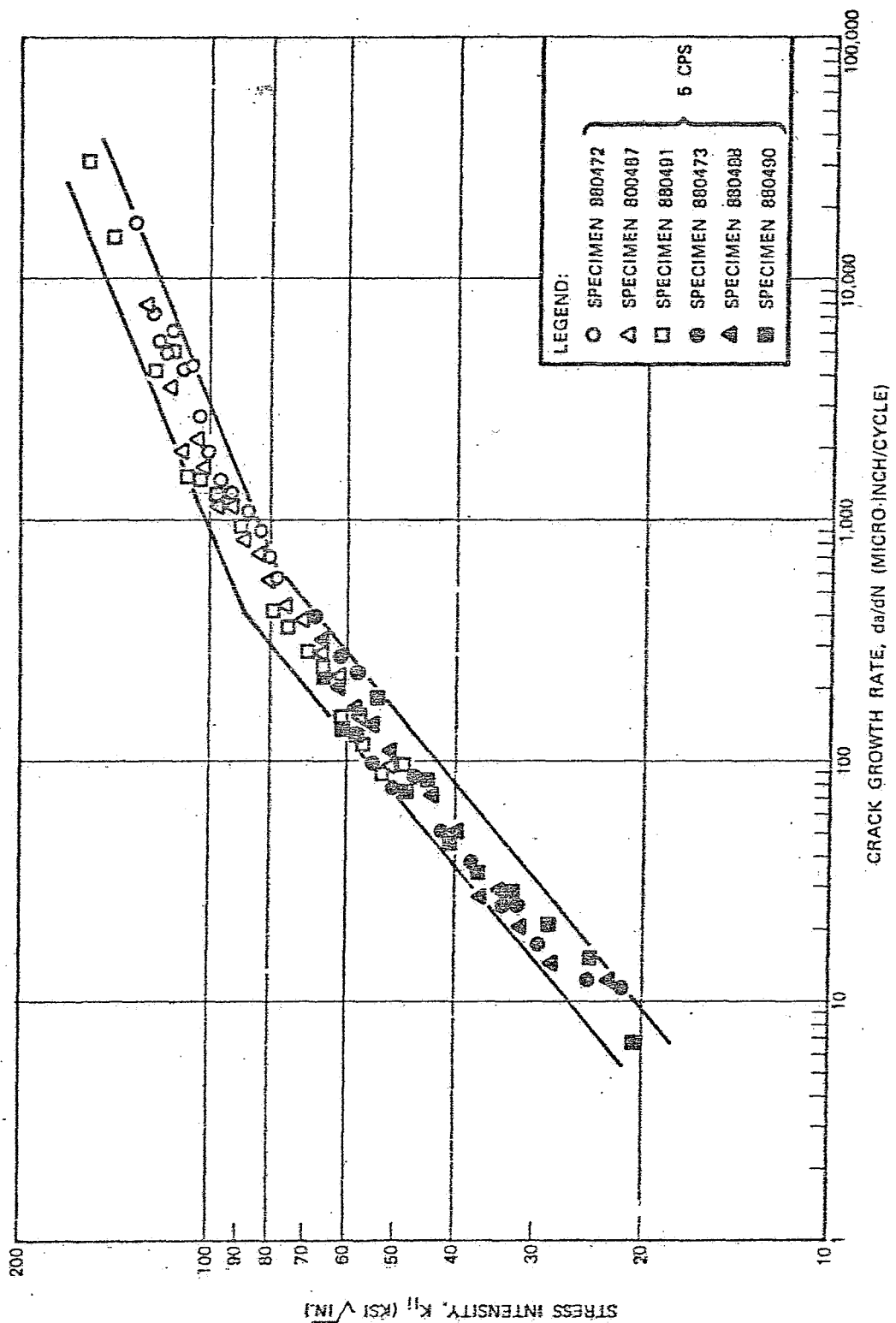


Figure 33: Growth Rate Results of 5Al-2.5 Sn (ELI) Titanium In 100 Psi Gaseous Hydrogen at Room Temperature

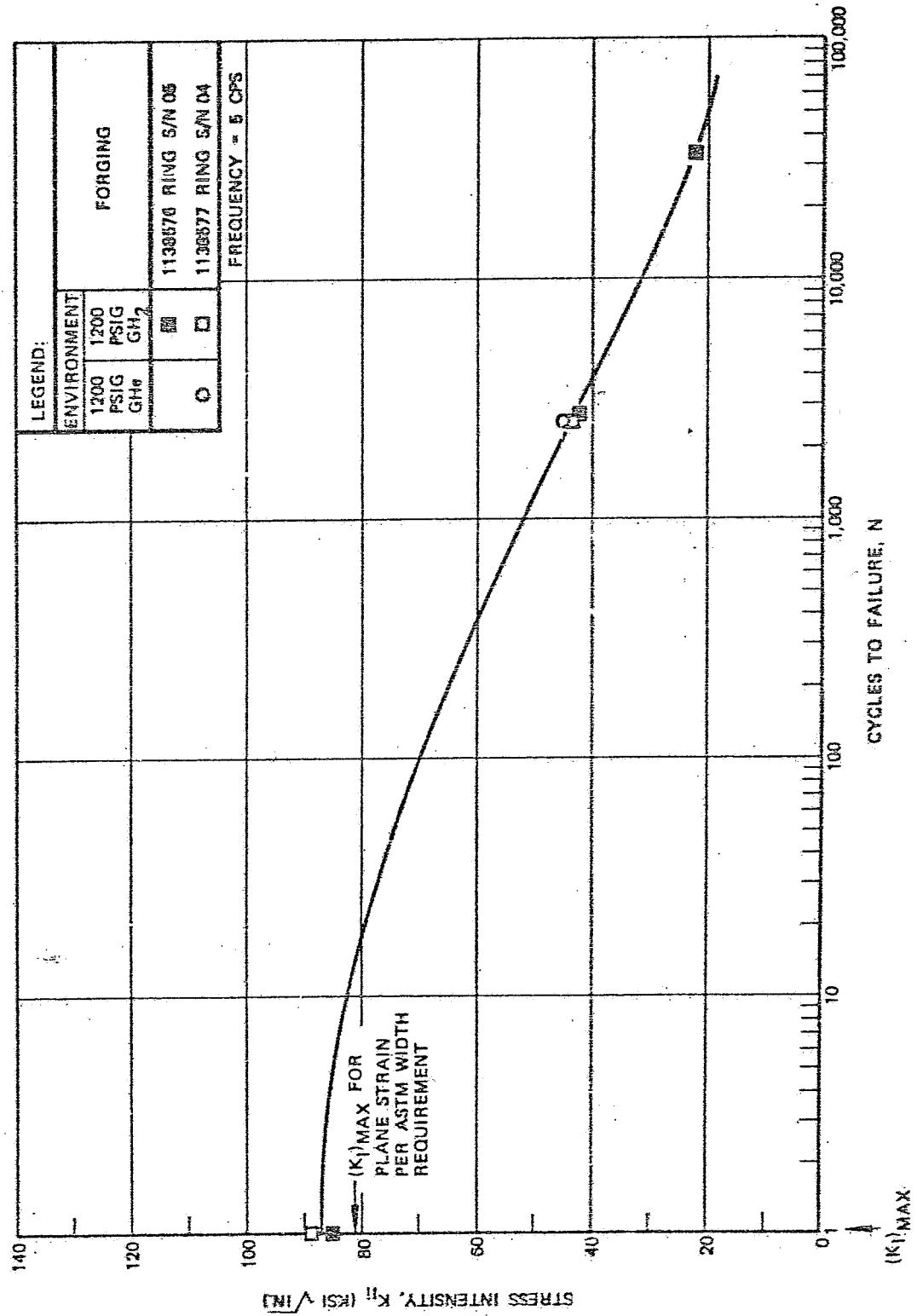


Figure 34: Cyclic Test Results of 5Al-2.5 Sn (ELI) Titanium at 160°F

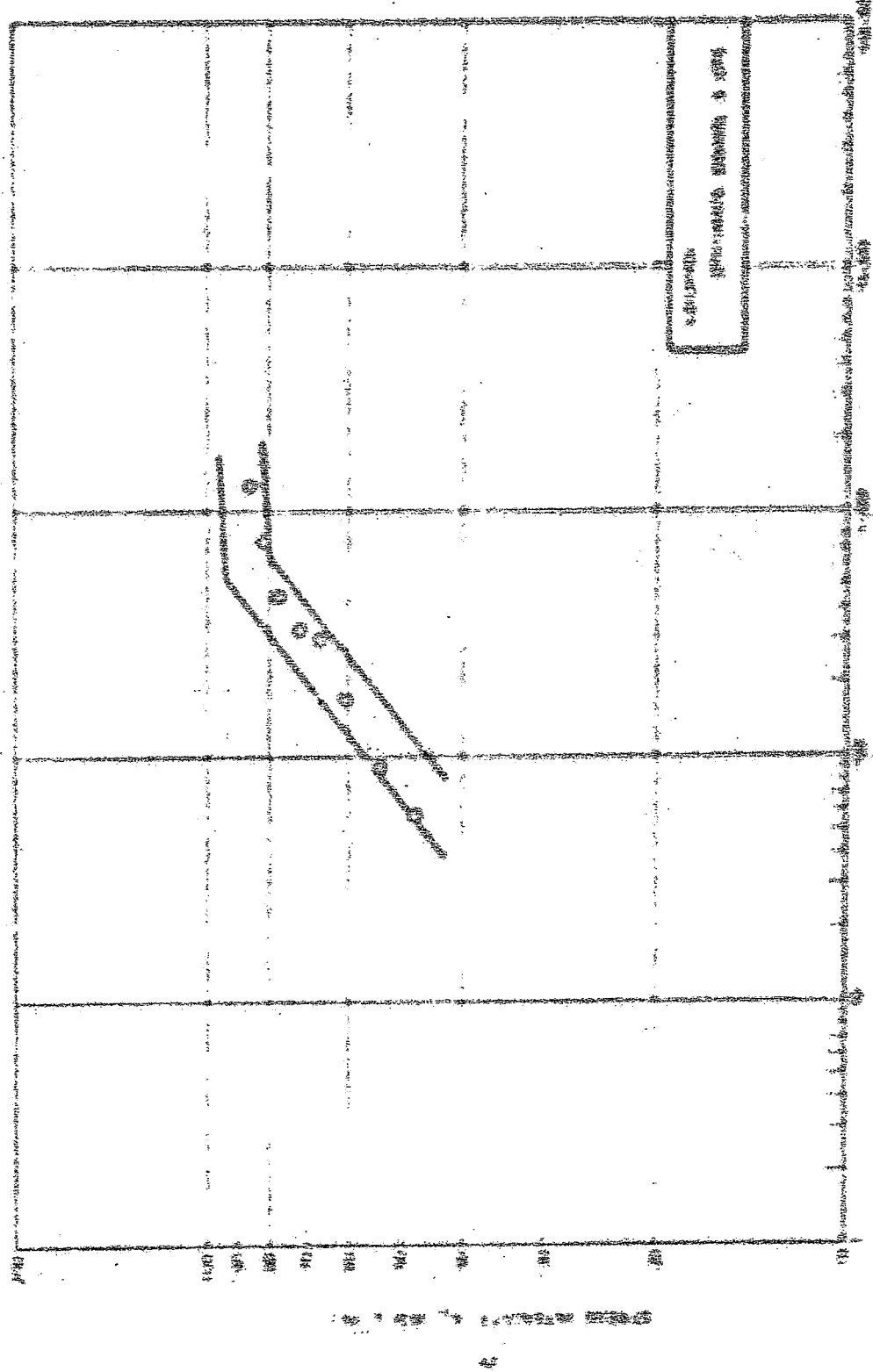


图 2.2 二分图的邻接矩阵。图中显示了图 2.1 所示的二分图的邻接矩阵，矩阵中的元素表示了图中各边的权值。

CRACK GROWTH RATE, IN 10<sup>-6</sup> MICRONS/HOUR



100  
80  
60  
40  
20  
0

10 20 30 40 50 60 70 80 90 100

CRACK GROWTH RATE, IN  $10^6$  MICRONS/HOUR

0 2 4 6 8 10

100  
80  
60  
40  
20  
0

10 20 30 40 50 60 70 80 90 100

CRACK GROWTH RATE, IN  $10^6$  MICRONS/HOUR

0 2 4 6 8 10

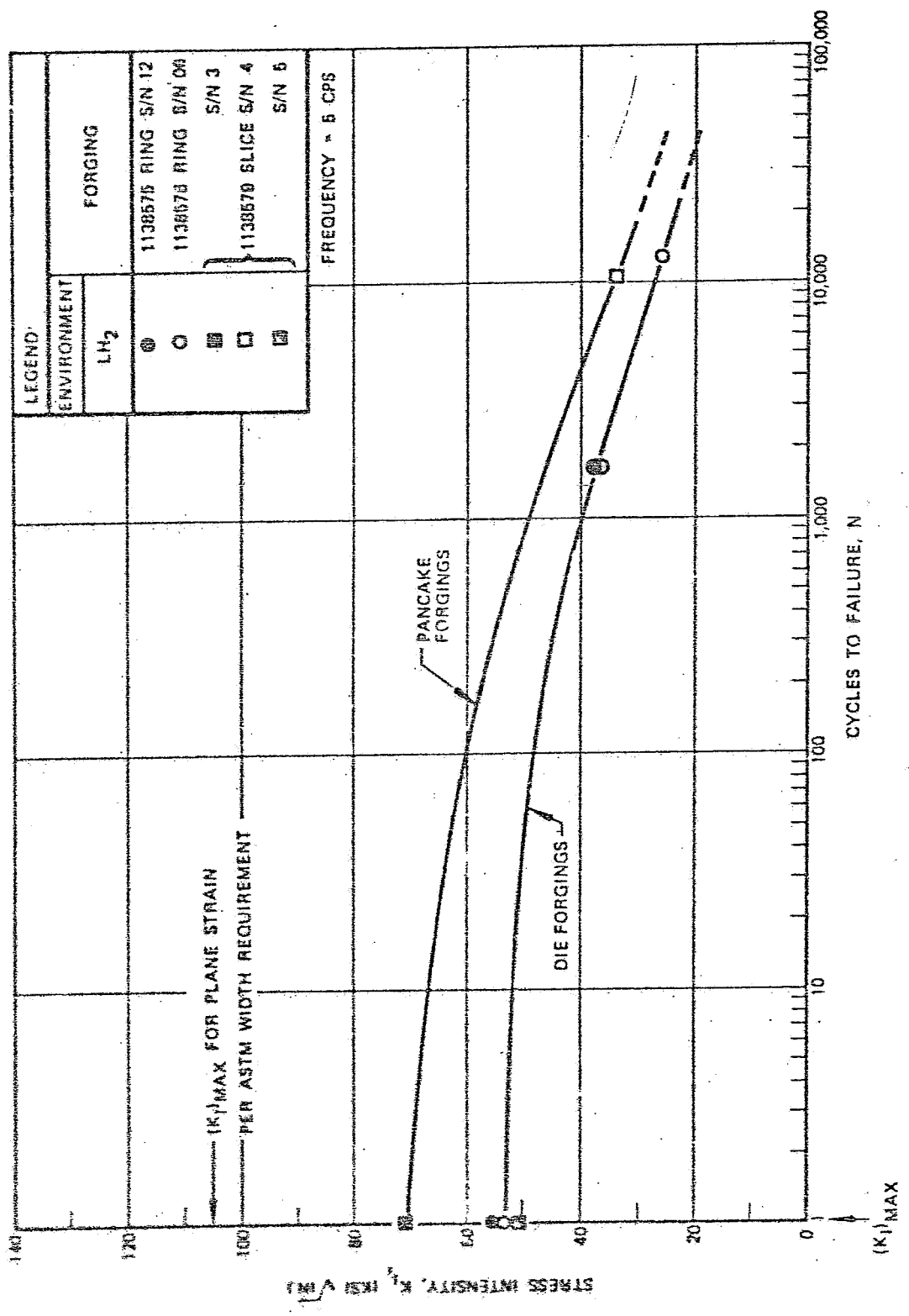


Figure 37: Cyclic Test Results of SAI-2.5 Sn (ELI) Titanium In Liquid Hydrogen at 423°F ~

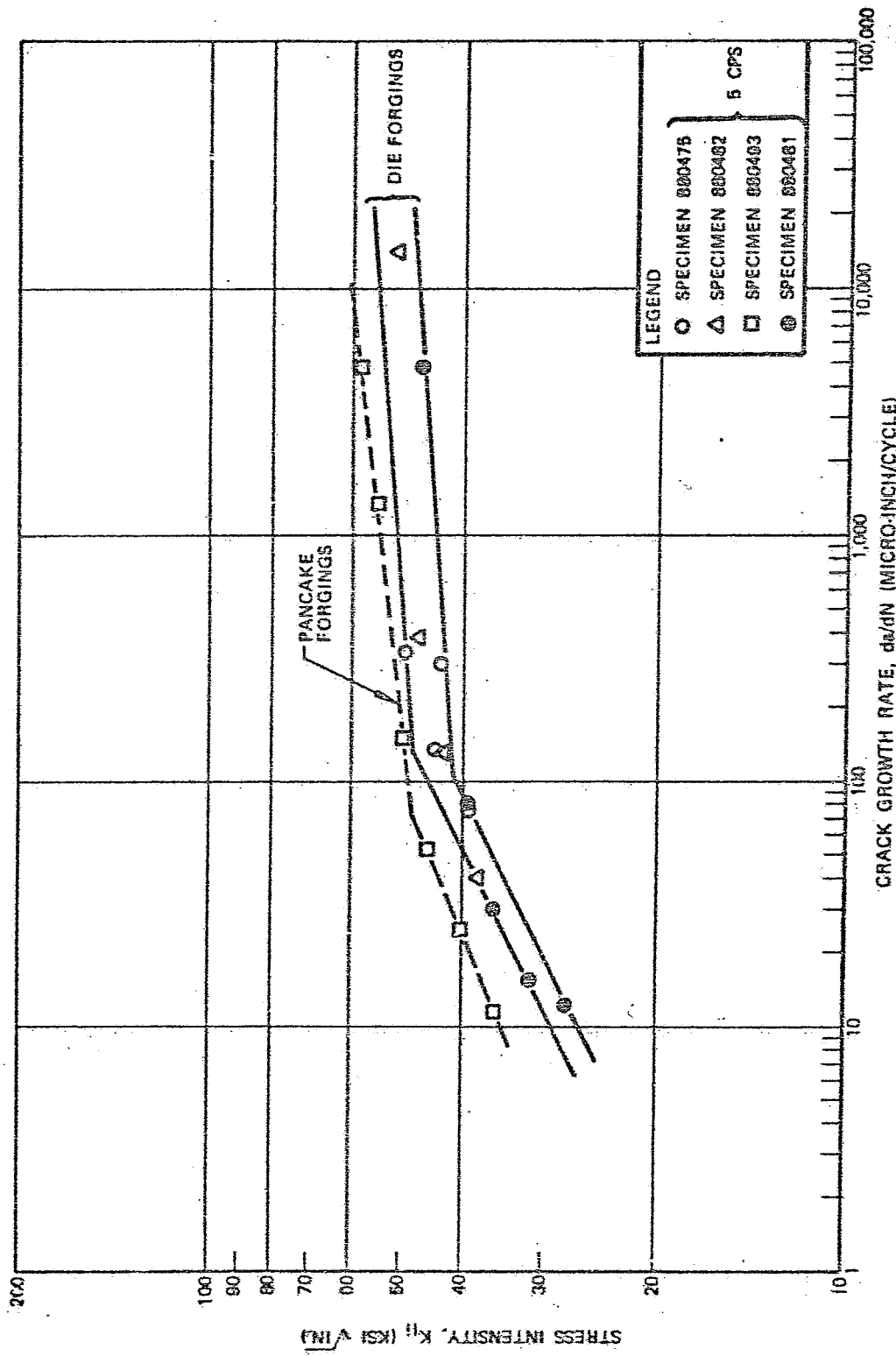


Figure 39: Growth Rate Results of AA12.5 Sn (ELI) Titanium in Liquid Hydrogen at 423°F

Table 1: Analysis of High Purity Gaseous Hydrogen

ITEM	NSFC SPEC 35A TABLE IA LIMITS ▶	RESULTS OF GAS ANALYSIS ▶				
		SAMPLE NO. 1	SAMPLE NO. 2	SAMPLE NO. 3	SAMPLE NO. 4	SAMPLE NO. 5
Total Purity	99.995%	>99.998%	>99.999%	>99.998%	>99.999%	>99.999%
Nitrogen Water Vol. Hydro Carbons	9 ppm	<8.05 ppm	<3.71 ppm	<4.51 ppm	<2.35 ppm	<4.51 ppm
Oxygen Argon	1 ppm	0.52 ppm	0.5 ppm	0.8 ppm	0.15 ppm	0.4 ppm
Helium	39 ppm	<10 ppm	<10 ppm	<10 ppm	<10 ppm	<10 ppm
Carbon Monoxide and Dioxide	1 ppm	<0.01 ppm	<0.01 ppm	<0.01 ppm	<0.01 ppm	<0.01 ppm
Total Impurities	50 ppm	<18.59 ppm	<14.22 ppm	<15.32 ppm	<12.51 ppm	<14.92 ppm

▶ By volume

▷ Obtained from Union Carbide - Linde Div.

*Table 2: 5Al-2.5 Sn (ELI) Titanium Specimen/Forging Correlation*

FORGING IDENTIFICATION			FRACTURE SPECIMEN IDENTIFICATION
PART NUMBER	ARCTURUS DIE NUMBER	SERIAL NUMBER	
1138575 (Ring Segment)	2915	08	1138365-104D/2915/08 S/N 880471
			1138365-104D/2915/08 S/N 880472
			1138365-104D/2915/08 S/N 880473
		12	1138365-104D/2915/12 S/N 880474
			1138365-104D/2915/12 S/N 880475
			1138365-104D/2915/12 S/N 880476
1138576 (Ring Segment)	2916	05	1138365-104D/2916/05 S/N 880477
			1138365-104D/2916/05 S/N 880478
			1138365-104D/2916/05 S/N 880479
		06	1138365-104D/2916/06 S/N 880480
			1138365-104D/2916/06 S/N 880481
			1138365-104D/2916/06 S/N 880482
1138577 (Ring Segment)	2917	04	1138365-104D/2917/04 S/N 880483
			1138365-104D/2917/04 S/N 880484
			1138365-104D/2917/04 S/N 880485
1138578 (Ring Segment)	2918	11	1138365-104D/2918/11 S/N 880486
			1138365-104D/2918/11 S/N 880487
			1138365-104D/2918/11 S/N 880488
1138578 (Whole Forging)	2918	11	1138365-104D/2918/11F S/N 880489
			1138365-104D/2918/11F S/N 880490
			1138365-104D/2918/11F S/N 880491
1138579 (Half Forging)	X292	3	1138365-104D/X292/3 S/N 880492
		4	1138365-104D/X292/4 S/N 880493
		5	1138365-104D/X292/5 S/N 880494

Table 3: Static Fracture Tests of ARMCO 22-13-5 at Room Temperature

SPECIMEN S/N	TEST PARAMETERS AT	CRACK LENGTH (INCHES)				MAX % "W" DEVIATION	A/W	P <sub>U</sub> (KIPS)	$\Delta \sigma_{\text{eff}} / \Delta \sigma_0$	TEST ENVIRONMENT	Y	$K_I$ (KSI $\sqrt{\text{IN}}$ )	REMARKS
		$a_1$	$a_2$	$a_3$	$a_{avg}$								
880075	5% OFFSET SLOPE	0.992	1.007	1.022	1.007	-1.5	0.50	9.30	0.2	1200 PSIG	13.9	62.9	No Prior Test History
	P <sub>MAX</sub>	0.992	1.007	1.022	1.007	-1.5	0.50	17.30	-	GHE	13.9	124.3	
880078	5% OFFSET SLOPE	1.012	1.010	1.012	1.011	+0.1	0.51	8.40	0.3	1200 PSI	14.0	58.1	No Prior Test History
	P <sub>MAX</sub>	1.012	1.010	1.012	1.011	+0.1	0.51	18.75	-	GHE	14.0	117.8	

Table 4: Cyclic Tests of ARMCO 22-13-5 at Room Temperature in Gaseous Helium

SPECIMEN S/N	TEST PARAMETERS AT	CRACK LENGTH (INCHES)				MAX % "W" DEVIATION	A/W	P <sub>MAX</sub> (KIPS)	FIELD (KIPS)	TEST ENVIRONMENT	TEST DURATION (CYCLES)	Y	$K_I$ (KSI $\sqrt{\text{IN}}$ )	REMARKS	
		$a_1$	$a_2$	$a_3$	$a_{avg}$										
880082	INITIATION	0.972	0.977	0.982	0.979	-0.3	0.49	12.0	5	1200 PSIG	0.016	13.4	78.1	Test Terminated Just Prior to Failure Varying from Normal	
	TERMINATION	1.160	1.147	1.152	1.152	+0.5	0.56	-	30.0	GHE	0.039	16.8	109.4		
880080	INITIATION	0.976	0.977	0.972	0.976	-0.3	0.49	30.0	5	1200 PSIG	0.016	13.6	66.4	Test Terminated Just Prior to Failure	
	TERMINATION	1.227	1.227	1.222	1.229	+0.2	0.61	-	30.0	GHE	0.026	12.9	104.8		
880078	INITIATION	0.967	0.986	1.000	0.984	-0.7	0.60	7.0	5	1200 PSIG	>0.351	0.010	13.7	47.9	Test Terminated Just Prior to Failure Reached $\Delta$ Limit on Test Fixture
	TERMINATION	1.540	1.510	1.510	1.520	+1.3	0.78	-	7.0	GHE	>0.030	34.8	148.7		
880027	INITIATION	0.992	0.992	0.990	0.991	-0.1	0.60	-	5	1200 PSIG	0.006	13.7	30.7	Specimen Cycled for 10,001 Cycles Three Load Increased to 9 Kips and Test Continued. Terminated Just Prior to Failure - Reached $\Delta$ Limit on Test Fixture	
	TERMINATION	1.018	1.019	1.012	1.016	+0.4	0.61	-	5	GHE	0.008	14.0	31.7		
880027	INITIATION	1.015	1.018	1.017	1.016	+0.4	0.61	-	5	2,584 PSIG	0.014	14.1	63.7	Test Continued. Terminated Just Prior to Failure - Reached $\Delta$ Limit on Test Fixture	
	TERMINATION	1.550	1.400	1.560	1.503	+6.3	0.75	-	5	GHE	>0.032	32.9	181.8		

\*EXCEEDED RECORDER DISPLACEMENT FULL SCALE

Table 5: Cyclic Tests of ARMCO 22-13-5 at Room Temperature in Gaseous Hydrogen

SPECIMEN S/N	TEST PARAMETERS AT	CRACK LENGTH (INCHES)				MAX % " " DEVIATION	S/N	P <sub>MAX</sub> (KIPS)	FREQ (CPS)	TEST ENVIRONMENT	TEST DURATION (CYCLES)	PEAK TO PEAK FLAW OPENING (INCHES)	Y	$K_I \sqrt{IN}$	REMARKS
		$\bar{x}_1$	$\bar{x}_2$	$\bar{x}_3$	$\bar{x}_{avg}$										
890083	INITIATION	0.995	0.992	0.977	0.988	-1.1	0.68	12.0	5	1200 PSIG GH <sub>2</sub>	563 $>0.549$	0.220	13.6	81.1	Test Terminated Just Prior to Failure. Vented and Marked.
	TERMINATION	1.420	1.410	1.400	1.410	+2.7	0.71						25.5	128.5	
890081	INITIATION	0.972	0.982	0.987	0.980	-0.3	0.69	10.0	5	1200 PSIG GH <sub>2</sub>	1,008 $>0.046$	0.276	13.6	61.5	Test Terminated Just Prior to Failure. Vented and Marked.
	TERMINATION	1.357	1.362	1.357	1.357	+2.4	0.68						21.8	128.3	
890086	INITIATION	0.990	0.984	0.972	0.982	-1.5	0.69	10.0	1	1200 PSIG GH <sub>2</sub>	6315 1,442	0.215	13.6	67.1	Test Terminated Just Prior to Failure. Vented and Marked.
	TERMINATION	1.342	1.360	1.362	1.358	+1.5	0.69						23.0	138.7	
890084	INITIATION	0.955	0.972	0.976	0.971	-0.5	0.69	7.0	5	1200 PSIG GH <sub>2</sub>	8,286 0.579	0.210	13.4	49.2	Specimen Cycled with $\Delta = 0.010$ . Vented and Marked.
	TERMINATION	1.229	1.235	1.224	1.229	+0.5	0.61						22.9	73.2	
890079	INITIATION	0.974	0.977	0.982	0.975	+0.4	0.69	7.0	5	1200 PSIG GH <sub>2</sub>	10,241 0.243	0.209	12.5	40.7	Test Terminated Just Prior to Failure.
	TERMINATION	1.420	1.462	1.427	1.436	+2.5	0.72						23.1	117.5	
890088	INITIATION	0.962	0.972	0.972	0.968	-0.8	0.68	9.0	5	1200 PSIG GH <sub>2</sub>	2,805 0.226	0.212	12.4	68.1	Specimen Cycled back $\Delta = 0.030$ . Then Load Increased to 12.0 Kips and Specimen Went to Test Fixture Under in 2 Cycles.
	TERMINATION	1.222	1.257	1.242	1.244	+1.0	0.62						19.3	129.3	
	INITIATION	1.237	1.257	1.242	1.244	+0.0	0.62	12.0	2				—	—	
	TERMINATION	1.520	1.470	1.570	1.573	+3.5	—						—	—	

\*EXCEEDED RECORDER DISPLACEMENT FULL SCALE

Table 6: Static Fracture Tests of Phosphor Bronze at Room Temperature

SPECIMEN S/N	TEST PARAMETERS AT	CRACK LENGTH (INCHES)				MAX % " " DEVIATION	S/N	P (KIPS)	$\Delta_0 \delta P / \Delta P$	TEST ENVIRONMENT	Y	$K_I \sqrt{IN}$	REMARKS
		$\bar{x}_1$	$\bar{x}_2$	$\bar{x}_3$	$\bar{x}_{avg}$								
890104	5% OFFSET SLOPE	1.012	1.050	1.042	1.036	-2.2	0.052	7.60	0.0	1200 PSIG GH <sub>2</sub>	14.4	57.9	No Prior Test History
	P <sub>MAX</sub>	1.012	1.050	1.042	1.036	-2.2	0.052	12.15	—			89.0	
890103	5% OFFSET SLOPE	1.007	1.047	1.050	1.036	-2.7	0.052	8.80	0.0	1200 PSIG GH <sub>2</sub>	14.4	64.4	No Prior Test History
	P <sub>MAX</sub>	1.007	1.047	1.050	1.036	-2.7	0.052	12.10	—			98.6	

Table 7: Cyclic Tests of Phosphor Bronze at Room Temperature in Gaseous Helium

SPECIMEN S/N	TEST PARAMETERS AT	CRACK LENGTH (INCHES)				MAX % Δ DEVIATION	d/w	P-MAX (KIPS)	F-LOAD (CPH)	TEST ENVIRONMENT	TEST DURATION (CYCLES)	PEAK TO PEAK FLAW OPENING (INCHES)	Y	K <sub>I</sub> (KSI √IN)	REMARKS
		a <sub>1</sub>	a <sub>2</sub>	a <sub>3</sub>	a <sub>avg</sub>										
880109	INITIATION	1.000	0.998	0.997	0.998	-2.1	0.49	10.0	B	PSIG	1200	0.021	13.9	67.8	Test Terminated Just Prior to Failure, Vented then Marked.
	TERMINATION	1.178	1.193	1.192	1.193	-2.9	0.68					0.041	12.2	92.6	
880108	INITIATION	0.880	0.997	0.976	0.986	-1.8	0.49	8.5	B	PSIG	1200	0.020	13.8	54.0	Test Terminated Just Prior to Failure, Vented then Marked.
	TERMINATION	1.372	1.432	1.267	1.367	-6.1	0.68					0.043	24.3	113.4	
880106	INITIATION	1.022	1.037	1.072	1.027	5.1.1	0.51	6.0	B	PSIG	1200	0.025	14.2	42.6	Test Terminated Just Prior to Failure, Vented then Marked.
	TERMINATION	1.410	1.480	1.382	1.473	-4.6	0.71					0.043	26.9	99.2	
880108	INITIATION	1.047	1.047	0.987	1.030	-3.2	0.52	4.0	B	PSIG	1200	0.029	14.3	29.1	Test Terminated Just Prior to Failure, Vented then Marked.
	TERMINATION	1.500	1.580	1.480	1.527	-4.1	0.78					0.037	39.1	60.0	

\*EXCEEDED RECORDER DISPLACEMENT FULL SCALE

Table 8: Cyclic Tests of Phosphor Bronze at Room Temperature in Gaseous Hydrogen

SPECIMEN S/N	TEST PARAMETERS AT	CRACK LENGTH (INCHES)				MAX % Δ DEVIATION	d/w	P-MAX (KIPS)	F-LOAD (CPH)	TEST ENVIRONMENT	TEST DURATION (CYCLES)	PEAK TO PEAK FLAW OPENING (INCHES)	Y	K <sub>I</sub> (KSI √IN)	REMARKS
		a <sub>1</sub>	a <sub>2</sub>	a <sub>3</sub>	a <sub>avg</sub>										
880110	INITIATION	0.970	1.010	1.042	1.020	-4.4	0.50	10.0	B	PSIG	1200	0.028	14.0	70.1	Specimen Cycled Until $\Delta = -0.031^+$ , Marked and Reversed, Terminated Just Prior to Failure, Vented then Marked.
	TERMINATION	1.047	1.072	1.100	1.071	-2.7	0.54					0.031	16.1	77.9	
880111	INITIATION	1.047	1.077	1.105	1.078	-2.7	0.56	8.0	B	PSIG	1200	0.023	16.1	78.5	Specimen Cycled Until $\Delta = -0.031^-$ , Marked and Reversed, Terminated Just Prior to Failure, Vented then Marked.
	TERMINATION	1.147	1.327	1.287	1.247	-8.0	0.62					0.061	19.4	103.4	
880111	INITIATION	0.990	1.067	1.082	1.050	-0.8	0.60	8.0	B	PSIG	1200	0.030	13.8	65.2	Specimen Cycled Until $\Delta = -0.030^-$ , Marked and Reversed, Terminated Just Prior to Failure, Vented then Marked.
	TERMINATION	1.207	1.227	1.222	1.219	-1.0	0.61					0.035	18.5	82.0	
880102	INITIATION	1.217	1.237	1.223	1.229	-1.0	0.61	8.0	B	PSIG	1200	0.026	18.9	83.7	Specimen Cycled Until $\Delta = -0.030^-$ , Marked and Reversed, Terminated Just Prior to Failure, Vented then Marked.
	TERMINATION	1.430	1.525	1.486	1.510	-7.3	0.76					0.044	23.6	168.0	
880113	INITIATION	1.202	1.160	1.062	1.243	-6.9	0.57	8.0	B	PSIG	1200	0.025	18.5	70.7	Test Terminated Just Prior to Failure, Vented then Marked.
	TERMINATION	1.473	1.450	1.322	1.431	-6.9	0.72					0.048	27.3	133.0	
880117	INITIATION	1.032	1.008	0.977	1.001	+2.6	0.50	8.0	B	PSIG	1200	0.026	13.8	56.0	Test Terminated Just Prior to Failure, Vented then Marked.
	TERMINATION	1.252	1.252	1.207	1.226	-2.6	0.62					0.036	19.2	65.4	
880117	INITIATION	1.002	1.080	1.082	1.058	+1.1	0.53	6.0	B	PSIG	1200	0.017	15.0	46.5	Specimen Cycled Until $\Delta = -0.027^+$ , Marked and Reversed, Terminated Just Prior to Failure, Vented then Marked.
	TERMINATION	1.247	1.264	1.242	1.251	-1.0	0.63					0.027	19.8	65.6	
880112	INITIATION	1.250	1.267	1.245	1.254	-1.0	0.53	4.0	B	PSIG	1200	0.028	18.6	66.0	Specimen Cycled Until $\Delta = -0.027^-$ , Marked and Reversed, Terminated Just Prior to Failure, Vented then Marked.
	TERMINATION	1.377	1.482	1.362	1.406	+6.3	0.70					0.056	34.3	93.4	
880112	INITIATION	1.032	1.040	0.983	1.006	-7.6	0.50	4.0	B	PSIG	1200	0.020	13.3	28.0	Specimen Cycled Until $\Delta = -0.028^-$ , Marked and Reversed, Terminated Just Prior to Failure, Vented then Marked.
	TERMINATION	1.324	1.320	1.300	1.321	-1.8	0.68					0.039	22.0	60.3	
880112	INITIATION	1.234	1.300	1.290	1.271	-1.6	0.58	4.0	B	PSIG	1,100	0.020	22.7	50.3	Specimen Cycled Until $\Delta = -0.028^+$ , Marked and Reversed, Terminated Just Prior to Failure, Vented then Marked.
	TERMINATION	1.522	1.526	1.472	1.505	-4.7	0.75					0.036	33.1	81.2	

EXCEEDED RECORDER DISPLACEMENT FULL SCALE

APPROXIMATELY

Table 9: Static Fracture Test of A286 Steel at Room Temperature

SPECIMEN S/N	TEST PARAM- ETERS AT	CRACK LENGTH (INCHES)				MAX % DEVIATION	N/W	P (KIPS)	$\Delta P_{\text{eff}}/\Delta P$	TEST ENVIRONMENT	Y	$K_I$ (ksi/√in)	REMARKS
		$a_1$	$a_2$	$a_3$	$a_{avg}$								
B20051	5% OFFSET SLOPE	1.022	1.021	1.077	1.050	3.6	0.53	5.30	0.0	1200 PSIG	14.8	40.5	No Prior Test History
	P <sub>MAX</sub>	1.022	1.021	1.077	1.050	3.6	0.53	12.45	-	GHE	14.8	86.1	
B20052	5% OFFSET SLOPE	1.064	1.057	1.010	1.042	3.1	0.52	5.50	0.0	1200 PSIG	14.5	40.7	No Prior Test History
	P <sub>MAX</sub>	1.064	1.052	1.010	1.042	3.1	0.52	12.95	-	GHE	14.5	95.8	

Table 10: Cyclic Tests of A286 Steel at Room Temperature in Gaseous Helium

SPECIMEN S/N	TEST PARAM- ETERS AT	CRACK LENGTH (INCHES)				MAX % DEVIATION	N/W	P <sub>MAX</sub> (KIPS)	FREQ (CPS)	TEST ENVIRONMENT	TEST CYCLES (CYCLES)	PEAK TO TEAR FLAW OPENING (INCHES)	$K_I$ (ksi/√in)	REMARKS
		$a_1$	$a_2$	$a_3$	$a_{avg}$									
B20053	INITIATION	1.060	1.068	1.237	1.165	-1.7	0.53	10.8	6	1200 PSIG	6,018	14.7	75.7	Test Terminated Just Prior to Failure.
	TERMINATION	-	-	-	1.218	-	0.57	-	-	GHE	2,232	18.8	502.3	
B20054	INITIATION	1.057	1.068	1.072	1.072	+1.5	0.54	8.8	6	1200 PSIG	6,215	16.1	62.4	Test Terminated Just Prior to Failure.
	TERMINATION	1.279	1.280	1.260	1.267	+1.3	0.62	-	-	GHE	2,233	20.1	30.5	
B20055	INITIATION	1.023	0.967	0.948	0.953	+5.1	0.49	6.8	6	1200 PSIG	6,058	13.8	40.3	Test Terminated Just Prior to Failure. Reached $\Delta$ Limit on Test stress.
	TERMINATION	1.130	1.650	1.557	1.536	+13.4	0.37	-	-	GHE	2,223	36.8	133.8	
B20053	INITIATION	1.024	1.037	0.987	1.013	-2.2	0.51	3.0	-	10,025 PSIG	0.003	14.1	27.4	Specimen Cycled For 10,025 Cycles. Then Increased Load to 9.3 Kips and Cycled For 10,027 Cycles and Then Increased Load to 7.5 Kips. Test Terminated Just Prior to Failure - Reached $\Delta$ Limit on Test Failure.
	TERMINATION	1.024	1.037	0.987	1.013	-2.2	0.51	-	-	GHE	0.003	14.1	27.4	
	INITIATION	1.024	1.037	0.987	1.019	-2.2	0.51	6.3	6	1200 PSIG	0.003	14.1	37.8	
	TERMINATION	1.070	1.080	1.029	1.063	-2.3	0.53	-	-	GHE	0.008	14.3	40.7	
B20054	INITIATION	1.070	1.080	1.039	1.063	-2.3	0.53	7.5	-	14,800 PSIG	0.013	14.9	57.5	Specimen Cycled For 10,027 Cycles and Then Increased Load to 7.5 Kips. Test Terminated Just Prior to Failure - Reached $\Delta$ Limit on Test Failure.
	TERMINATION	1.120	1.500	1.480	1.450	+22.7	0.71	-	-	GHE	0.022	29.7	134.8	

\*EXCEEDED RECORDER DISPLACEMENT FULL SCALE

\*\*APPROXIMATELY

Table 11: Cyclic Tests of A285 Steel at Room Temperature in Gaseous Hydrogen

SPECIMEN S/N	TEST PARAM- ETERS AT	CRACK LENGTH INCHES)				MAX % DEVIATION	$\delta/\nu$	P <sub>MAX</sub> (KIPSI)	K <sub>REQ</sub> (KPSI)	TEST ENVIRONMENT	CYCLES	PEAK TO PEAK FLAW OPENING (INCHES)	Y	$K_1$	$K_1 \times Y$ (KCI <sub>1</sub> /TH)	REMARKS
		$\delta_1$	$\delta_2$	$\delta_3$	$\delta_{avg}$											
88051	INITIATION	1.000	1.042	1.068	1.030	-2.5	0.52	10.0	-	1200	P5G	1.062	2518	14.2	72.5	Test Terminated Just Prior to Failure Vertical Flaw Wanted.
	TERMINATION	1.267	1.350	1.240	1.286	+5.0	0.64	-	GH <sub>2</sub>	>0.007	70.8	117.7				
88057	INITIATION	1.064	1.085	1.070	1.073	+1.1	0.54	8.6	-	1200	P5G	2.914	8213	16.1	62.5	Test Terminated Just Prior to Failure
	TERMINATION	1.252	1.317	1.307	1.294	-2.9	0.66	-	GH <sub>2</sub>	>0.007	21.5	55.7				
88062	INITIATION	1.053	1.087	1.037	1.065	+1.3	0.53	8.6	-	1200	P5G	2.169	2514	14.2	62.5	Test Terminated Just Prior to Failure Vertical and Wanted.
	TERMINATION	1.242	1.327	1.260	1.306	+6.0	0.65	-	GH <sub>2</sub>	2.033	21.5	56.2				
88068	INITIATION	1.052	1.028	1.034	1.019	-1.2	0.51	8.0	-	1200	P5G	1.009	16.1	42.9		Test Terminated Just Prior to Failure Vertical & Limit on Test Flaws.
	TERMINATION	1.572	1.550	1.480	1.527	-4.4	0.78	-	GH <sub>2</sub>	>0.025	36.1	100.2				
88069	INITIATOR	1.280	1.104	1.114	1.069	-2.9	0.64	-	1200	P5G	1.010	16.1	42.2		Test Terminated in $\Delta = 0.014$	
	TERMINATOR	1.172	1.207	1.201	1.186	+1.2	0.60	8.6	GH <sub>2</sub>	1.014	17.8	53.8				

\*EXCEEDED RECORDER DISPLACEMENT FULL SCALE

Table 12: Static Fracture Tests of Hastelloy X at Room Temperature

SPECIMEN S/N	TEST PARAM- ETERS AT	CRACK LENGTH INCHES)				MAX % DEVIATION	$\delta/\nu$	P <sub>MAX</sub> (KIPSI)	$\Delta \sigma_p / \Delta p$	TEST ENVIRONMENT	Y	$K_1$	$K_1 \times Y$ (KCI <sub>1</sub> /TH)	REMARKS	
		$\delta_1$	$\delta_2$	$\delta_3$	$\delta_{avg}$										
88064	5% OFFSET SLOPE	1.037	1.047	1.002	1.029	+2.6	0.51	5.40	0.0	1200	P5G	14.29	46.4		No Prior Test History
	P <sub>MAX</sub>	1.037	1.047	1.002	1.029	+2.6	0.51	13.60	-	GH <sub>2</sub>	14.29	95.5			
88063	5% OFFSET SLOPE	1.022	1.042	1.020	1.026	+1.4	0.51	5.20	0.0	1200	P5G	14.28	46.9		No Prior Test History
	P <sub>MAX</sub>	1.022	1.042	1.020	1.026	+1.4	0.51	13.29	-	GH <sub>2</sub>	14.28	95.5			

**Table 13: Cyclic Tests of Hastelloy X at Room Temperature in Gaseous Helium**

SPECIMEN S/N	TEST PARAM- ETERS AT	CRACK LENGTH (INCHES)				MAX % IN DEVIATION	K/N	P <sub>MAX</sub> (KIPS)	FREQ (cps)	TEST ENVIRONMENT	TEST DURATION (CYCLES)	PEAK TO PEAK FLAW OPENING (INCHES)	>	$K_I$ (ksi $\sqrt{\text{Hz}}$ )	REMARKS
		$a_1$	$a_2$	$a_3$	$a_{avg}$										
68006	INITIATION	0.694	1.610	0.670	1.031	+0.9	0.63	15.0	6	PBG GHE	400	0.019	12.5	62.1	Test Terminated Just Prior to Failure, Vertical Shear Marked.
	TERMINATION	1.394	1.392	1.272	1.270	+2.9	0.64					0.023	15.4	61.3	
68009	INITIATION	1.913	1.032	1.024	1.019	+1.9	0.61	6.0	6	PBG GHE	1,070	0.013	14.1	58.7	Test Terminated Just Prior to Failure, Vertical Shear Marked.
	TERMINATION	1.392	1.392	1.392	1.390	+1.3	0.67					0.023	21.2	58.5	
68009	INITIATION	1.579	1.527	1.567	1.575	-1.1	0.51	6.0	6	PBG GHE	8,000	0.009	14.1	48.7	Test Terminated Just Prior to Failure, Vertical Shear Marked.
	TERMINATION	1.462	1.468	1.462	1.461	-1.3	0.72					0.023	21.0	52.3	
680072	INITIATION	1.159	1.697	1.167	1.589	-1.3	0.62	6.0	6	PBG GHE	1200	0.003	14.5	37.3	Test Terminated Just Prior to Failure, Vertical Shear Marked.
	TERMINATION	1.480	1.020	1.029	1.028	-1.1	0.74					0.023	21.5	36.3	
68009	INITIATION	1.019	1.022	1.612	1.029	+1.2	0.68	4.0	6	PBG	1200	0.013	14.1	25.8	
	TERMINATION	1.189	1.189	1.183	1.183	+0.8	0.69					0.023	17.2	25.2	Test Terminated After 6,000 Cycles
	INITIATION	1.169	1.169	1.169	1.168	+0.8	0.69	6.0		GHE	1,121	0.013	17.3	51.5	Just Prior to Failure, No Crack Initiated
	TERMINATION	1.432	1.432	1.475	1.433	+1.3	0.67					0.023	27.5	51.5	

**Table 14: Cyclic Tests of Hastelloy X at Room Temperature in Gaseous Hydrogen**

SPECIMEN S/N	TEST PARAM- ETERS AT	CRACK LENGTH (INCHES)				MAX % IN DEVIATION	K/N	P <sub>MAX</sub> (KIPS)	FREQ (cps)	TEST ENVIRONMENT	TEST DURATION (CYCLES)	PEAK TO PEAK FLAW OPENING (INCHES)	>	$K_I$ (ksi $\sqrt{\text{Hz}}$ )	REMARKS	
		$a_1$	$a_2$	$a_3$	$a_{avg}$											
680070	INITIATION	1.030	1.048	1.022	1.031	+0.9	0.62	15.0	6	PBG GHE	1200	208	0.017	14.2	72.7	Specimen Cycled Until $\Delta a = 0.025"$ , Horizontal Shear, Restored, Terminated.
	TERMINATION	1.187	1.372	1.147	1.188	+1.8	0.68					0.023	17.0	56.0		
	INITIATION	1.150	1.182	1.152	1.184	+1.6	0.68					0.024	17.1	51.2	Just Prior to Failure, Vertical shear marked.	
	TERMINATION	1.250	1.257	1.250	1.250	+2.1	0.64					0.023	20.2	113.5		
680057	INITIATION	1.003	1.022	1.013	1.012	-1.2	0.61	8.0	6	PBG GHE	1200	1,071	0.012	14.0	56.4	Specimen Cycled Until $\Delta a = 0.025"$ , Horizontal Shear, Restored, Terminated.
	TERMINATION	1.227	1.232	1.247	1.242	+1.2	0.62					0.023	16.3	51.5		
	INITIATION	1.223	1.258	1.264	1.265	+1.3	0.65					0.024	17.1	51.2	Just Prior to Failure, Vertical shear marked.	
	TERMINATION	1.342	1.362	1.352	1.372	+2.2	0.69					>0.023	24.5	114.8		
680074	INITIATION	1.022	1.027	1.047	1.046	+2.7	0.52	6.0	6	PBG GHE	1200	630	0.012	14.0	44.7	Terminated Just Prior to Failure, Vertical Shear Marked.
	TERMINATION	1.312	1.337	1.347	1.328	+2.5	0.57					0.023	22.8	51.8		
680071	INITIATION	1.020	1.047	1.027	1.025	+1.4	0.52	8.0	6	PBG GHE	4,700	0.053	14.1	51.9	Specimen Cycled Until $\Delta a = 0.025"$ , Horizontal Shear, Restored, Terminated.	
	TERMINATION	1.332	1.337	1.400	1.321	+1.7	0.68					0.023	22.0	56.7		
	INITIATION	1.341	1.347	1.312	1.334	+1.6	0.57					0.024	22.7	56.7	Just Prior to Failure, Vertical shear marked.	
	TERMINATION	1.442	1.442	1.072	1.428	+1.8	0.71					0.023	22.7	53.2		
680073	INITIATION	1.070	1.090	1.070	1.077	+1.2	0.54	6.0	6	PBG GHE	1200	6,168	0.008	16.2	28.3	Specimen Cycled Until $\Delta a = 0.025"$ , Horizontal Shear, Restored, Terminated.
	TERMINATION	1.300	1.347	1.340	1.328	+2.2	0.68					0.015	22.8	54.0		
	INITIATION	1.300	1.347	1.340	1.328	+2.2	0.66					0.015	22.8	54.0	Just Prior to Failure, Vertical shear marked.	
	TERMINATION	1.470	1.500	1.484	1.485	+1.0	0.74					0.026	31.6	53.1		

\*EXCEEDED RECORDER DISPLACEMENT FOR U SCALE

Table 15: Static Fracture Tests of 347 Stainless Steel at Room Temperature

SPECIMEN S/N	TEST PARAM- ETERS AT	CRACK LENGTH INCHES				MAX % "n" DEVIATION	σ/W (KIPS)	ΔσP/ΔP (KSI)	TEST ENVIRONMENT	Y	K <sub>I</sub> (KSI $\sqrt{\text{IN}}$ )	REMARKS
		$\delta_1$	$\delta_2$	$\delta_3$	$\delta_{avg}$							
S80040	5% OFFSET SLOPE	1.000	1.020	1.004	1.008	+1.2	0.50	14.10	0.0	1200 PSG	13.94	28.7
	PEAK	1.000	1.020	1.004	1.008	+1.2	0.50	14.10	-	GHE	13.94	79.1
S80039	5% OFFSET SLOPE	0.932	0.957	0.952	0.954	+0.3	0.50	14.50	0.0	1200 PSG	13.72	33.5
	MAX	0.932	0.957	0.952	0.954	+0.3	0.50	14.50	-	GHE	13.72	63.3
S80048	5% OFFSET SLOPE	0.907	0.940	0.940	0.929	-2.4	0.48	7.20 <sup>a</sup>	0.0	700 PSG	12.81	44.4
	MAX	0.907	0.940	0.940	0.929	-2.4	0.48	7.20 <sup>a</sup>	-	GHE	12.81	76.9
S80050	5% OFFSET SLOPE	0.929	0.973	0.935	0.946	+2.3	0.47	7.00 <sup>a</sup>	0.0	1200 PSG	13.04	44.4
	MAX	0.929	0.973	0.935	0.946	+2.3	0.47	7.00 <sup>a</sup>	-	GHE	13.04	79.7

<sup>a</sup> DURING SECOND SUSTAINED LOAD CYCLE

\*\* DURING LOAD TO FAILURE

Table 15: Cyclic Tests of 347 Stainless Steel at Room Temperature in Gaseous Helium

SPECIMEN S/N	TEST PARAM- ETERS AT	CRACK LENGTH INCHES				MAX % "n" DEVIATION	σ/W (KIPS)	P <sub>MAX</sub> (KIPS)	TEST ENVIRONMENT	TEST DURATION (IN CLS)	Y	K <sub>I</sub> (KSI $\sqrt{\text{IN}}$ )	REMARKS
		$\delta_1$	$\delta_2$	$\delta_3$	$\delta_{avg}$								
S80043	INITIATION	1.017	1.027	0.997	1.014	-1.7	0.51	8.2	8	1200 PSG	0.013	14.0	55.6
	TERMINATION	1.226	1.226	1.226	1.226	-	0.82	8.2	GHE	0.020	16.1	24.7	Test Terminated Just Prior to Failure and Marked.
S80047	INITIATION	1.002	1.030	1.003	1.013	+1.7	0.51	8.9	8	1200 PSG	0.009	14.0	42.3
	TERMINATION	1.270	1.270	1.270	1.270	-	0.54	8.9	GHE	0.017	22.7	68.3	Test Terminated Just Prior to Failure and Marked.
S80042	INITIATION	1.007	1.030	1.032	1.018	+1.4	0.51	8.9	8	1200 PSG	0.007	14.1	35.6
	TERMINATION	1.340	1.360	1.360	1.360	+0.7	0.60	8.9	GHE	0.019	23.4	68.0	Test Terminated Just Prior to Failure and Marked.

\*\* APPROXIMATELY

Table 17: Cyclic Tests of 347 Stainless Steel at Room Temperature in Gaseous Hydrogen

SPECIMEN S/N	TEST PARAM- ETERS AT	CRACK LENGTH (INCHES)				MAX % DEVIATION	A/W	P <sub>MAX</sub> (KIPS)	FREQ (CPS)	TEST ENVIRON- MENT	TEST DURATION (CYCLES)	PEAK TO PEAK FLAW OPENING (INCHES)	>	K <sub>1</sub> (KSI $\sqrt{\text{IN}}$ )	REMARKS
		a <sub>1</sub>	a <sub>2</sub>	a <sub>3</sub>	a <sub>avg</sub>										
380045	INITIATION	1.000	1.014	1.016	1.008	-0.6	0.50	8.0	5	1200 PSIG GH <sub>2</sub>	355	0.015	13.8	55.0	Test Terminated Just Prior to Failure. Welded and Machined.
	TERMINA-TION	1.130	1.180	1.157	1.149	+2.7	0.57					0.010	15.3	71.7	
380044	INITIATION	0.950	0.956	0.955	0.955	+1.6	0.48	6.5	5	1200 PSIG GH <sub>2</sub>	2329	0.005	12.3	38.0	Test Terminated Just Prior to Failure. Welded and Machined.
	TERMINA-TION	1.275	1.275	1.275	1.275	-	0.64					0.010	20.6	68.0	
380047	INITIATION	0.970	0.982	0.982	0.988	+1.5	0.49	6.5	7	1200 PSIG GH <sub>2</sub>	2573	0.003	13.8	40.0	Test Terminated Just Prior to Failure. Welded and Machined.
	TERMINA-TION	1.270	1.350	1.300	1.327	+3.3	0.65					0.010	21.1	71.0	
380046	INITIATION	0.957	1.000	0.954	0.957	+2.3	0.50	5.5	5	1200 PSIG GH <sub>2</sub>	8550	0.003	13.8	34.0	Test Terminated Just Prior to Failure. Welded and Machined.
	TERMINA-TION	1.420	1.460	1.380	1.420	+2.9	0.71					0.013	27.1	80.0	
380048	INITIATION	1.050	1.020	1.010	1.020	+1.0	0.51	5.0	1	1200 PSIG GH <sub>2</sub>	4284	0.003	14.1	35.0	Test Terminated Just Prior to Failure. Welded and Machined.
	TERMINA-TION	1.300	1.360	1.320	1.327	+2.5	0.68					0.014	22.4	64.5	
380050	INITIATION	0.907	0.937	0.917	0.919	+1.4	0.48	4.5	5	1200 PSIG GH <sub>2</sub>	10005	0.005	12.7	24.0	
	TERMINA-TION	0.926	0.973	0.926	0.946	+2.8	0.47					0.005	13.0	25.0	Specimen Cycled for 50,000 Cycles. Specimen Then Pulled to Failure.
	FAILURE	0.929	0.973	0.926	0.946	+2.5	0.47	12.6	-			-	-	13.0	78.2

\*\*APPROXIMATELY

Table 18: Static Fracture Tests of 9310 Carburized Steel at Room Temperature and -42°F

SPECIMEN S/N	TEST PARAM- ETERS AT	CRACK LENGTH (INCHES)				MAX % DEVIATION	A/W	P <sub>0.8 / ΔP</sub> (KIPS)	TEST ENVIRON- MENT	>	K <sub>1</sub> (KSI $\sqrt{\text{IN}}$ )	REMARKS	
		a <sub>1</sub>	a <sub>2</sub>	a <sub>3</sub>	a <sub>avg</sub>								
380001	% OFFSET SLOPE	1.005	0.994	0.990	0.995	+0.9	0.50	15.70	0.4	RT	13.74	107.7	No Prior Test History
	APPARENT POP-IN <sup>a</sup>	1.005	0.994	0.990	0.995	+0.9	0.50	17.26	-	1200 PSIG GH <sub>2</sub>	13.74	118.5	
	P <sub>MAX</sub>	1.005	0.994	0.990	0.995	+0.9	0.50	17.35	-		13.74	122.4	
380005	% OFFSET SLOPE	1.150	1.110	1.170	1.143	-2.9	0.57	72.00	0.2	1200 PSIG GH <sub>2</sub>	16.59	113.5	Prior Cyclic Load of 3 Kips for 80,000 Cycles in GH <sub>2</sub> at RT
	P <sub>MAX</sub>	1.150	1.110	1.170	1.143	-2.9	0.57	33.93	-		16.59	123.3	
380002	% OFFSET SLOPE	0.992	0.930	0.959	0.927	+2.3	0.47	7.20	0.3	RT	12.82	45.0	No Prior Test History
380004	P <sub>MAX</sub>	0.922	0.930	0.959	0.937	+2.3	0.47	-	-	PSIG	12.82	32.2	
380005	P <sub>MAX</sub> WITH EST <sup>b</sup>	1.160	1.160	1.160	1.160	0.0	0.58	-	-	GH <sub>2</sub>	17.60	120.4	
380008	% OFFSET SLOPE	1.307	1.272	1.282	1.287	+1.6	0.64	10.40	0.0	ZERO	21.78	122.7	Prior Cyclic Load of 10 Kips for 450 Cycles in GH <sub>2</sub> at RT
380008	P <sub>MAX</sub>	1.307	1.272	1.282	1.287	+1.6	0.64	10.75	-	PSIG	20.79	126.8	
380008	% OFFSET SLOPE	1.382	1.367	1.382	1.377	-0.7	0.63	7.55	0.0	ZERO	24.51	109.0	Assumes Pop-in at 5% Offset Slope Prior cyclic load of 7.0 Kips for 3419 cycles in GH <sub>2</sub> at RT
380013	P <sub>MAX</sub>	1.382	1.367	1.382	1.377	-0.7	0.63	7.86	-	PSIG	24.75	114.0	
380013	% OFFSET SLOPE	1.630	1.640	1.550	1.640	+0.6	>0.8	250	0.0	RT	-	-	Prior Cyclic Load of 3 Kips for 4500 Cycles in GH <sub>2</sub> at RT
380008	P <sub>MAX</sub>	1.630	1.640	1.550	1.640	+0.6	>0.8	255	-	PSIG	-	-	
380002	% OFFSET SLOPE	1.072	1.017	1.070	1.053	-3.4	0.53	13.25	0.0	ZERO	14.71	100.0	Prior Cyclic Load of 3 Kips for 120,000 Cycles in GH <sub>2</sub> at RT
380002	P <sub>MAX</sub>	1.072	1.017	1.070	1.053	-3.4	0.53	15.10	-	PSIG	14.71	113.5	
380002	% OFFSET SLOPE	0.947	0.847	0.870	0.955	+1.6	0.46	5.00	0.0	ZERO	13.17	32.2	No Prior Test History
380002	P <sub>MAX</sub>	0.947	0.847	0.870	0.955	+1.6	0.46	5.00	-	PSIG	13.17	34.1	

\*\* ESTIMATED FROM FLAW FRACTURE FACE

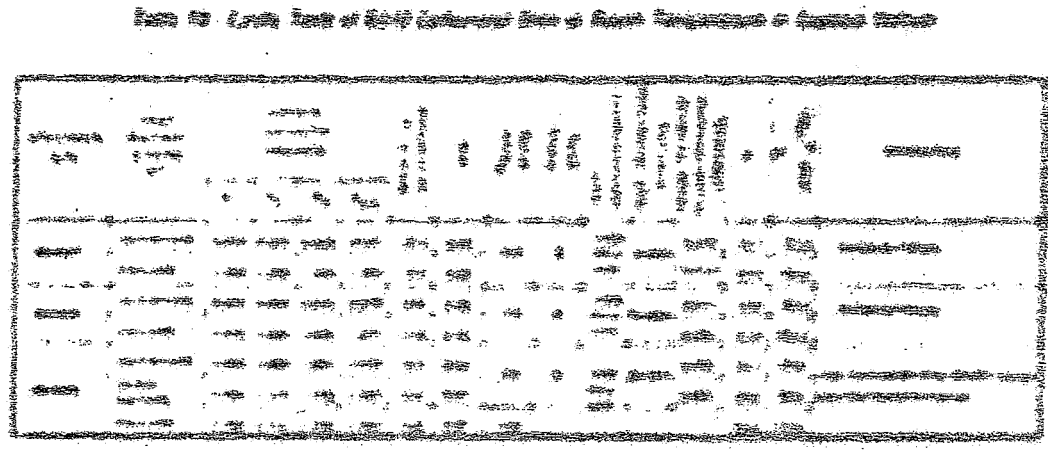
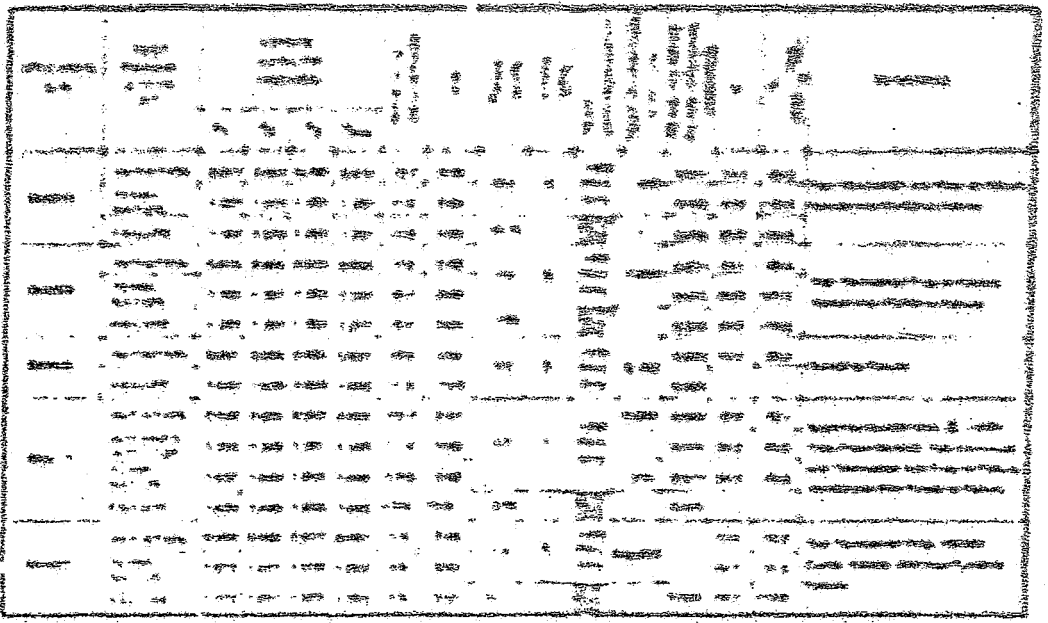
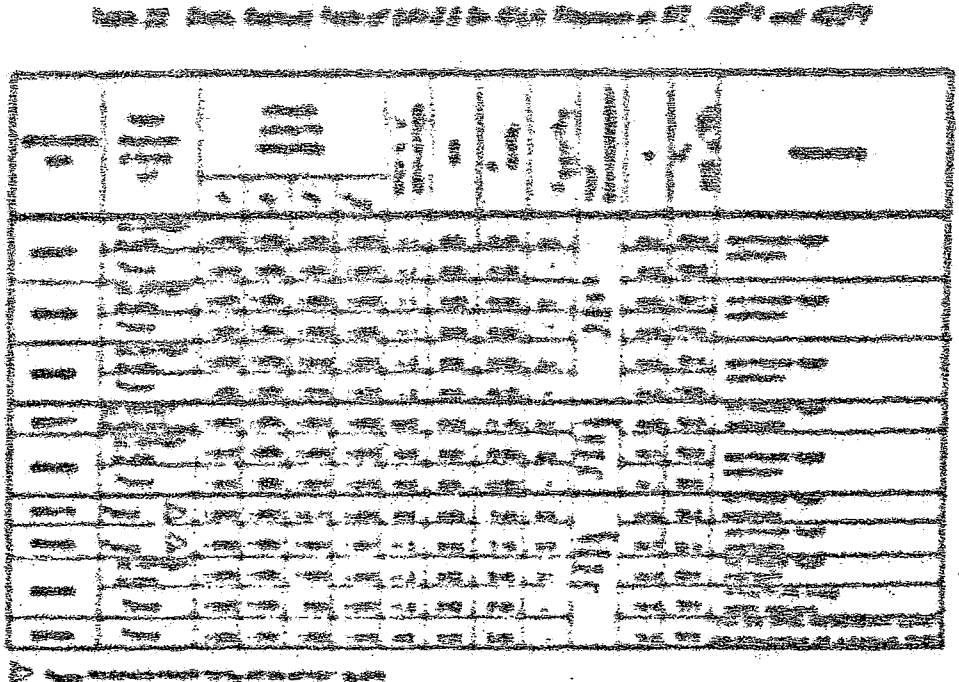
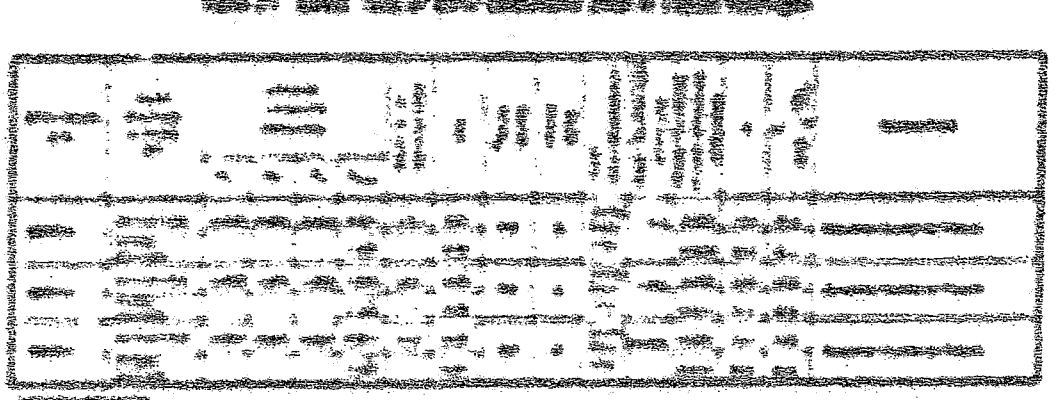
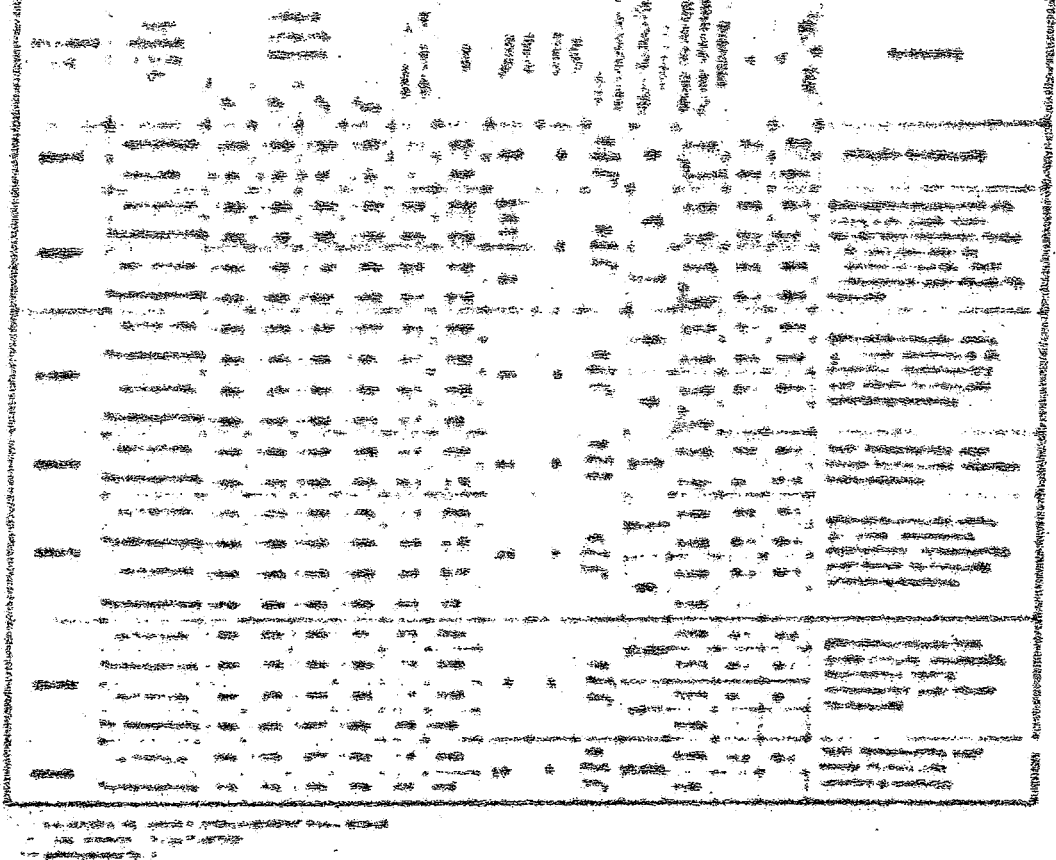


FIG. 22. *Cultus* (see Fig. 21)







**Table 3. Cost Rate of Service by Process**

	Process	Cost Rate (\$)	Cost Rate (%)
1	Initial Inventory	10000000	100%
2	Production	1000000	10%
3	Inventory holding	1000000	10%
4	Quality Control	1000000	10%
5	Delivery	1000000	10%
6	Total	3000000	30%

**Table 4. Cost Rate of Service by Process**

	Process	Cost Rate (\$)	Cost Rate (%)
1	Initial Inventory	10000000	100%
2	Production	1000000	10%
3	Inventory holding	1000000	10%
4	Quality Control	1000000	10%
5	Delivery	1000000	10%
6	Total	3000000	30%

**END**

**DATE FILMED**

**4 / 28 / 75**